In Situ and Modelled Soil Moisture Determination and Upscaling from Point-based to Field Scale

by

Emmanuel Rotimi Ojo

A Thesis
Submitted to the Faculty of Graduate Studies of
The University of Manitoba
in partial fulfillment of the requirements for the degree of

DOCTOR OF PHILOSOPHY

Department of Soil Science
University of Manitoba
Winnipeg, Manitoba

ABSTRACT

Ojo, Emmanuel Rotimi. Ph.D., The University of Manitoba, February, 2017. *In Situ* and Modelled Soil Moisture Determination and Upscaling from Point-based to Field Scale. Major Professor; Dr. Paul R. Bullock.

The relevance, value and multi-dimensional application of soil moisture in many areas such as hydrological, meteorological and agricultural sciences have increased the focus on this important part of the ecosystem. However, due to its spatial and temporal variability, accurate soil moisture determination is an ongoing challenge. In the fall of 2013 and spring of 2014, the accuracy of five soil moisture instruments was tested in heavy clay soils and the Root Mean Squared Error (RMSE) values of the default calibration ranged from 0.027 and 0.129 m^3 m^{-3}. However, after calibration, the range was improved to 0.014 – 0.040 m^3 m^{-3}. The need for calibration has led to the development of generic calibration procedures such as soil texture-based calibrations. As a result of the differences in soil minerology, especially in clay soils, the texture-based calibrations often yield very high RMSE. A novel approach that uses the Cation Exchange Capacity (CEC) grouping was independently tested at three sites and out of seven different calibration equations tested; the CEC-based calibration was the second best behind *in situ* derived calibration.

The high cost of installing and maintaining a network of soil moisture instruments to obtain measurements at limited points has influenced the development of models that can estimate soil moisture. The Versatile Soil Moisture Budget (VSMB) is one of such models and was used in this study. The comparison of the VSMB modelled output to the observed soil moisture data from a single, temporally continuous, in-field calibrated Hydra probe gave mean RMSE values of 0.052 m^3 m^{-3} at the eight site-years in coarse textured soils and 0.059 m^3 m^{-3} at the six site-years in fine textured soils. At field-scale level, the representativeness of an arbitrarily placed soil moisture station was compared to the mean of 48 data samples collected across the field. The single location underestimated soil moisture at 3 of 4 coarse textured fields with an average RMSE of 0.038 m^3 m^{-3} and at only one of the four fine textured sites monitored with an average RMSE of 0.059 m^3 m^{-3}.

This research provides valuable information that will not only assist in the choice of the best soil moisture instrument based on the nature of its applied use but also the magnitude of expected error associated with them. It also sheds light on the limitations of daily time-step models to accurately represent highly dynamic surface layers in coarse textured soils because of the significant variability that occurs in soil moisture content within a 24-hour period. This research showed that the installation of a single soil moisture instrument at one location on a field is a justifiable approach to upscaling. This is important for producers who use single data point from an arbitrary location to assess the field-average soil moisture condition.

ACKNOWLEDGEMENTS

I appreciate my parents from whose cistern I was taught great wisdom, not written with ink, but of things that pertains to life and godliness. To my siblings and in-laws, I appreciate your constant support and prayers. Special thanks to my lovely wife, Mary, for believing in me. Your words of wisdom are like the aurora that glows with inexpressible radiant beauty. To Joanne, the miracle of your birth and how strong and fast you are growing brings constant joy to my heart.

FOREWORD

This thesis has been prepared in the manuscript format in adherence with the guidelines established by the Department of Soil Science at the University of Manitoba.

Chapter 2 has been published:

Ojo, E.R., Bullock, P.R. and Fitzmaurice, J. 2015. Field performance of five soil moisture instruments in heavy clay soils. Soil Sci. Soc. Am. J. **79:** 20-29.

Chapter 3 has been published:

Ojo, E.R., Bullock, P.R., L'Heureux, J., Powers, J., McNairn, H. and Pacheco. A. 2015. Calibration and Evaluation of a Frequency Domain Reflectometry Sensor for Real-Time Soil Moisture Monitoring. Vadose Zone J. **14**: 1-12.

A version of Chapters 4 and 5 will be submitted for publication in the near future.

Mention of trade or manufacturer names is made for information only and does not imply an endorsement, recommendation or exclusion.

TABLE OF CONTENTS

LIST OF TABLES

LIST OF FIGURES

Figure   **Page**

1.   INTRODUCTION

Soil moisture is at the nexus of almost all environmentally-related activities. The partitioning of precipitation into infiltration, ground water percolation, runoff and evapotranspiration as well as the partitioning of incoming solar radiation into sensible and latent heat fluxes are influenced by soil moisture. Readily available surface soil moisture drives the preferential partitioning of solar radiation into latent heat flux which results in increased humidity of the surrounding area. In hydrology, surface runoff and groundwater leaching are largely influenced by the antecedent soil moisture content as well as the water holding capacity of the soil. Thus, soil water content is a significant factor in the risk for surface flooding. Models simulating watershed discharge had greater accuracy when soil moisture spatial data were included (Pauwels et al., 2001). Meteorologists can use information on soil moisture to determine the initiation of severe weather patterns (Hanesiak et al., 2004). In pedology, soil formation factors such as eluviation and mottling are dependent on the soil moisture content of the profile. Eluviation is the movement of suspended or dissolved materials with soil water within a soil profile and mottling occurs in soils that are frequently saturated, usually from a high water table.

Soil moisture also influences the population, biodiversity and activities of soil microbes. Brockett et al. (2012) studied the function and structure of microbial

1

community in seven types of forest to determine the influence of various factors such as soil chemistry, temperature, tree species and soil moisture. The authors discovered that soil moisture was the major factor that determined the enzyme activities of the microbial communities. In Manitoba, available soil moisture in the spring and additional growing season precipitation do not often meet crop water demand. When conditions are favourable, early planting dates have been associated with higher yields (O'Donovan et al., 2012; Tsimba et al., 2013) which may be due to greater utilization of spring moisture and less pest pressure during critical phase of crop growth. However, early access to the field can be limited, especially in heavy clay soils, when surface soil moisture is saturated.

1.1   Advances in Monitoring Soil Moisture

Accurate soil moisture determination has been a concern because of its spatial and temporal variation. The thermogravimetric procedure remains the standard method for determining soil moisture content. It involves oven-drying a known volume of moist soil for 24-48 hours. The change in mass due to evaporation loss is multiplied by the soil's bulk density and divided by the density of water to yield the volumetric water content (Topp et al. 2008). This procedure has several limitations such as non-repetitiveness of the sampled location because the process involves taking soil *ex situ*. In addition, it is a slow, labour intensive and practically daunting procedure if several root-zone samples are required. Despite these limitations, the thermogravimetric procedure is used as the

standard to which other indirect methods are calibrated because of its high accuracy (Robinson et al., 2008; Walker et al., 2004).

Soil moisture determination has evolved over the decades with the neutron probe being among the early successful instruments used extensively to determine soil moisture in field studies (Haverkamp et al., 1984). Fast moving neutrons produced by a radioactive source from the probe are released into the soil. As the neutrons collide with the hydrogen atoms present in soil water, they are thermalized. An accurate result is obtained because the amount of thermalized neutrons is proportional to the soil moisture since the main source of hydrogen variation in most soils is the change in water content. The need for certification to use a radioactive material, non-automation and the loss of non-thermalized neutrons to the atmosphere when used close to the soil surface are some of the major drawbacks of the neutron probe (Falleiros et al., 1993; Muñoz-Carpena et al., 2004).

Similar to the neutron probe, several indirect methods relate a property of soil, such as its thermal or dielectric property to its moisture content. Many instruments used to monitor soil moisture, including electromagnetic and remote sensing devices, explore the soil's dielectric property. The unique arrangement of hydrogen atoms relative to the oxygen atom in water gives rise to the displacement of positive and negative molecular charges. Thus, water has a dielectric constant of about 80 at room temperature due to its large permanent dipole moment (Robinson et al., 2008). This value is much higher than the dielectric constant of air which is 1 and the value of most dry mineral soils, which ranges from 2-5. The dielectric constant that is measured in soil is primarily due to the

volumetric water content of the soil. Thus, soil dielectric constant increases with increasing volumetric water content of the soil (Seyfried and Murdock, 2004).

Over the last two decades, dielectric sensors, such as Time Domain Reflectometry (TDR) and Frequency Domain Reflectometry (FDR) probes, have largely replaced the neutron probes because of the automation capability of the former. Many of the dielectric probes operate between 50 and 250 MHz and require calibration to achieve acceptable absolute accuracy of soil moisture measurements (Ojo et al., 2015). Using dataloggers, these probes can be installed to track soil moisture at very high temporal frequencies. The TDR measures the propagation time for an electromagnetic pulse along a waveguide, usually metal rods and the FDR monitors changes in circuit operating frequency when a capacitor connected to an oscillator forms an electric circuit (Muñoz-Carpena et al., 2004).

All five instruments compared in the second chapter of this thesis explore the soil's dielectric property to determine the soil water content. The study analysed the accuracy of both pre and post calibration equations of various soil moisture sensors in heavy clay soils. The focus on clay soils was as a result of several publications that highlighted concerns with the accuracy of soil moisture devices in clay soils due to their mineralogy and the amount of bound water present in the soil (Campbell, 1990; Saarenketo, 1998; Fares et al., 2004; Logsdon, 2005; Schwartz et al., 2009). A major disadvantage of point instruments, including all the sensors used in chapter 2, is their limited sensing volume which is often less than 10^{-4} m^3. In chapter 3, the accuracy was tested for several calibration equations developed for the sensor with the best post calibration result reported in chapter 2. This study reports on the use of one general

calibration equation developed for each of three cation exchange capacity CEC categories.

1.2   Scale Issues in Soil Moisture

The high spatial variability of soil moisture on a field scale has led to the development of several experimental and statistical procedures to characterize the variability. A widely used experimental procedure involves placing several point-based sensors in the field to determine the area-average soil moisture of those measurements. This approach is common for calibrating remotely sensed soil moisture (Macelloni et al., 2003; Bosch et al., 2006; Adams et al., 2013; McNairn et al., 2015). Instead of conducting intensive sampling every time the spatial average of a field is required, the time stability concept is being used to determine the single, most representative location on the field whose soil moisture values are consistently comparable to the field average (Grayson and Western, 1998; Jacobs et al., 2004; Martínez-Fernández and Ceballos, 2005)

Instruments that have been used for field-scale soil moisture determination include ground penetrating radar (GPR) and more recently, COsmic-ray Soil Moisture Observing System (COSMOS). These devices provide measurements at intermediate spatial scales which are a valuable link between point measurements and regional scale soil moisture. GPRs determine the soil dielectric permittivity by transmitting and reflecting high frequency electromagnetic waves and relating it to volumetric soil

moisture. It is a non-destructive sampling technique that can monitor sub-surface soil moisture. The unit can be deployed on a vehicle and soil moisture measurements taken as the vehicle travels over the soil surface (Huisman et al., 2003; Robinson et al., 2008; Dobriyal et al., 2012).

Shuttleworth et al. (2010) and Franz et al. (2013) discussed the use of COSMOS in determining intermediate scale soil moisture measurements. This relatively new instrument explores the fact that the fast neutron density above ground is due to cosmic rays interaction with the soil. The neutron density is less sensitive to soil type and is related to the mean soil moisture content at a horizontal scale of approximately 700 m. However, COSMOS's sensing depth is non-linearly related from about 76 cm in dry soils to about 12 cm in saturated soils (Zreda et al. 2008). Similar to GPRs, COSMOS units can be placed on a vehicle to map the soil moisture of an area. Dong et al. (2014) validated the use of a COSMOS rover for surface soil moisture determination and reported a root mean squared difference of 0.03 cm^3 cm^{-3} when compared to impedance probes. However, Hornbuckle et al. (2012) showed that it is important to account for the vegetation water content of actively growing vegetation for improved measurement accuracy.

Satellite-borne remote sensing is used for regional, national or global scale soil moisture monitoring. Passive remote sensing uses a radiometer to measure the naturally emitted electromagnetic radiation from the soil which is influenced by the soil's dielectric property as well as the surface roughness (Njoku and Entekhabi, 1996). Soil moisture measurements from radiometers result in a brightness temperature at coarse spatial resolution in the order of tens of kilometers and have been retrieved from platforms such

as the Advanced Microwave Scanning Radiometer for the Earth Observing System (AMSR-E) aboard a NASA satellite (Njoku et al., 2003). Active remote sensors, often called radars, measure the ratio of backscatter electromagnetic wave to the amount it emitted. Radars can provide high spatial resolution in the order of meters but are more sensitive to surface roughness and angle of incidence (Robinson et al., 2008). Canada's RADARSAT-2 is an example of space-borne platform that has been used for soil moisture retrieval (McNairn et al., 2011).

Field campaigns are conducted to validate the retrieval algorithms used for converting brightness temperature (for radiometer) and backscatter (for radar) to soil moisture while delineating potential sources of error such as vegetation and surface roughness. One such campaign was the SMAPVEX12 which provided the dataset used in chapter five of this thesis. The campaign involved intensive, in-field soil moisture sampling to coincide with the time of flight overpass with a radiometer and/or radar. The intensive field sampling allowed for the comparison of the field averaged-soil moisture to observations from a single location as well as modelled soil moisture.

Regardless of which instrument is used to determine soil moisture at various spatial scales, calibration is an important procedure. Soil moisture derived from satellite-borne radar or radiometer to determine soil moisture at large spatial scales (e.g. watershed) can be calibrated using field scale instruments such as the GPR or COSMOS. Both GPR and COSMOS can be calibrated using several point data collected by FDRs or TDRs which are, in turn, thermo-gravimetrically calibrated. These different layers of calibration have the potential of introducing bias.

Due to the cost and intensive labour associated with monitoring soil moisture, models are often used to overcome these limitations and to provide spatial soil estimates. The Versatile Soil Moisture Budget (VSMB), discussed in chapters 4 and 5, is one such model and was selected due to its wide use on the Canadian Prairies (Akinremi et al., 1996; Chipanshi et al., 2013). Results from the model were compared to observations made in the field to determine the model's accuracy.

1.3   Thesis Organization

Following this general introduction are four data chapters prepared in a manuscript format and presented separately as a major section. Each data chapter contains an abstract that provides a synopsis of the chapter; an introduction outlining the knowledge gap and the objective(s) of the chapter; a materials and methods section which describes the detailed process involved in data gathering; results and discussion that explains the findings observed in the chapter in relation to other similar studies; a conclusion section which highlights critical findings in the chapter and a list of references used in the chapter. The final chapter, following the four data chapters, presents the overall synthesis of this thesis. It provides an overarching integration of the individual manuscripts and presents practical implications of the research conducted and recommendations for future study.

1.4   References

Adams, J. R., Berg, A. A. and McNairn, H. 2013. Field Level Soil Moisture Variability at 6- and 3-cm Sampling Depths: Implications for Microwave Sensor Validation. Vadose Zone J., **12**:1–12.

Akinremi, O. O., McGinn, S. M. and Barr, A. G. 1996. Simulation of soil moisture and other components of the hydrological cycle using a water budget approach. Can. J. Soil Sci., **76**:133–142.

Bosch, D. D., Lakshmi, V., Jackson, T. J., Choi, M. and Jacobs, J. M. 2006. Large scale measurements of soil moisture for validation of remotely sensed data: Georgia soil moisture experiment of 2003. J. Hydrol., **323**:120–137.

Brockett, B. F. T., Prescott, C. E. and Grayston, S. J. 2012. Soil moisture is the major factor influencing microbial community structure and enzyme activities across seven biogeoclimatic zones in western Canada. Soil Biol. Biochem., **44**:9–20.

Campbell, J. E. 1990. Dielectric properties and influence of conductivity in soils at one to fifty megahertz. Soil Sci. Soc. Am. J., **54**:332–341.

Chipanshi, A. C., Warren, R. T., L'Heureux, J., Waldner, D., McLean, H. and Qi, D. 2013. Use of the National Drought Model (NDM) in Monitoring Selected Agroclimatic Risks Across the Agricultural Landscape of Canada. Atmosphere-Ocean, **51**:471–488.

Dobriyal, P., Qureshi, A., Badola, R. and Hussain, S. A. 2012. A review of the methods available for estimating soil moisture and its implications for water resource management. J. Hydrol., **458**–**459**:110–117.

Dong, J., Ochsner, T. E., Zreda, M., Cosh, M. H. and Zou, C. B. 2014. Calibration and Validation of the COSMOS Rover for Surface Soil Moisture Measurement. Vadose Zone J., **13**:1–8.

Falleiros, M. C., Ravelo Sanchez, A., Souza, M., Bacchi, O. O. S., Pilotto, J. E. and Reichardt, K. 1993. Neutron probe measurement of soil water content close to soil surface. Sci. Agric., **50**:333–337.

Fares, A., Buss, P., Dalton, M., El-Kadi, A. I. and Parsons, L. R. 2004. Dual field calibration of capacitance and neutron soil water sensors in a shrinking–swelling clay soil. Vadose Zone J., **3**:1390–1399.

Franz, T. E., Zreda, M., Ferre, T. P. A. and Rosolem, R. 2013. An assessment of the effect of horizontal soil moisture heterogeneity on the area-average measurement of cosmic-ray neutrons. Water Resour. Res., **49**:6450–6458.

Grayson, R. B. and Western, A. W. 1998. Towards areal estimation of soil water content from point measurements: time and space stability of mean response. J. Hydrol., **207**:68–82.

Hanesiak, J. M., Raddatz, R. L. and Lobban, S. 2004. Local initiation of deep convection on the Canadian prairie provinces. Bound.-Layer Meteorol., **110**:455–470.

Haverkamp, R., Vauclin, M. and Vachaud, G. 1984. Error analysis in estimating soil water content from neutron probe measurements: 1. Local standpoint. Soil Sci., **137**:78–90.

Hornbuckle, B., Irvin, S., Franz, T., Rosolem, R. and Zweck, C. 2012. The potential of the COSMOS network to be a source of new soil moisture information for SMOS and SMAP. In 2012 IEEE International Geoscience and Remote Sensing Symposium (pp. 1243–1246). IEEE. Retrieved from http://ieeexplore.ieee.org/xpls/abs_all.jsp?arnumber=6351317

Huisman, J. A., Hubbard, S. S., Redman, J. D. and Annan, A. P. 2003. Measuring soil water content with ground penetrating radar. Vadose Zone J., **2**:476–491.

Jacobs, J. M., Mohanty, B. P., Hsu, E.-C. and Miller, D. 2004. SMEX02: Field scale variability, time stability and similarity of soil moisture. Remote Sens. Environ., **92**:436–446.

Logsdon, S. 2005. Time Domain Reflectometry Range of Accuracy for High Surface Area Soils. Vadose Zone J., **4**:1011–1019.

Macelloni, G., Paloscia, S., Pampaloni, P., Santi, E. and Tedesco, M. 2003. Microwave radiometric measurements of soil moisture in Italy. Hydrol. Earth Syst. Sci. Discuss., **7**:937–948.

Martínez-Fernández, J. and Ceballos, A. 2005. Mean soil moisture estimation using temporal stability analysis. J. Hydrol., **312**:28–38.

McNairn, H., Jackson, T. J., Wiseman, G., Béliar, S., Berg, A., Bullock, P., Colliander, A., Cosh, M. H., Kim, S.-B., Magagi, R., Moghaddam, M., Njoku, E. G., Adams, J. R., Saeid Homayouni, Ojo, E. R., Rowlandson, T., Shang, J., Goita, K. and Hossein, M. 2015. The Soil Moisture Active Passive Validation Experiment 2012 (SMAPVEX12): Pre-Launch Calibration and Validation of the SMAP Satellite. IEEE Trans. Geosci. Remote Sens., **53**:2784–2801.

McNairn, H., Merzouki, A. and Pacheco, A. 2011. Monitoring soil moisture to support risk reduction for the agriculture sector using RADARSAT-2 (pp. 3618–3621). Presented at the Geoscience and Remote Sensing Symposium (IGARSS 2011), Vancouver, BC, Canada: IEEE International.

Muñoz-Carpena, R., Shukla, S. and Morgan, K. 2004. Field devices for monitoring soil water content. University of Florida Cooperative Extension Service, Institute of Food

and Agricultural Sciences, EDIS. Retrieved from http://www.bae.ncsu.edu/topic/go_irrigation/docs/Field-devices-monitoring-.pdf

Njoku, E. G. and Entekhabi, D. 1996. Passive Microwave Remote Sensing of Soil Moisture. J. Hydrol., **184**:101–129.

Njoku, E. G., Jackson, T. J., Lakshmi, V., Chan, T. K. and Nghiem, S. V. 2003. Soil moisture retrieval from AMSR-E. IEEE Trans. Geosci. Remote Sens., **41**:215–229.

O'Donovan, J. T., Turkington, T. K., Edney, M. J., Juskiw, P. E., McKenzie, R. H., Harker, K. N., Clayton, G. W., Lafond, G. P., Grant, C. A., Brandt, S., Johnson, E. N., May, W. E. and Smith, E. 2012. Effect of seeding date and seeding rate on malting barley production in western Canada. Can. J. Plant Sci., **92**:321–330.

Ojo, E. R., Bullock, P. R. and Fitzmaurice, J. 2015. Field Performance of Five Soil Moisture Instruments in Heavy Clay Soils. Soil Sci. Soc. Am. J., **79**:20–29.

Pauwels, V. R., Hoeben, R., Verhoest, N. E. and De Troch, F. P. 2001. The importance of the spatial patterns of remotely sensed soil moisture in the improvement of discharge predictions for small-scale basins through data assimilation. J. Hydrol., **251**:88–102.

Robinson, D. A., Campbell, C. S., Hopmans, J. W., Hornbuckle, B. K., Jones, S. B., Knight, R., Ogden, F., Selker, J. and Wendroth, O. 2008. Soil Moisture Measurement for Ecological and Hydrological Watershed-Scale Observatories: A Review. Vadose Zone J., **7**:358–389.

Saarenketo, T. 1998. Electrical properties of water in clay and silty soils. J. Appl. Geophys., **40**:73–88.

Schwartz, R. C., Evett, S. R. and Bell, J. M. 2009. Complex permittivity model for time domain reflectometry soil water content sensing: II. Calibration. Soil Sci. Soc. Am. J., **73**:898–909.

Seyfried and Murdock 2004. Measurement of soil water content with a 50-MHz soil dielectric sensor. Soil Sci. Soc. Am. J. **68**: 394–403.

Shuttleworth, W. J., Zreda, M., Zeng, X., Zweck, C. and Ferré, T. P. 2010. The COsmic-ray Soil Moisture Observing System (COSMOS): a non-invasive, intermediate scale soil moisture measurement network. Br. Hydrol. Soc. Newctle., 1–7.

Topp, G.C., G.W. Parkin and T.P.A. Ferré. 2008. Soil water content. *In* Soil Sampling and Methods of Analysis (Carter, M.R. and E.G. Gregorich, eds.), CRC Press, Boca Raton, Fl. p. 939-961.

Tsimba, R., Edmeades, G. O., Millner, J. P. and Kemp, P. D. 2013. The effect of planting date on maize grain yields and yield components. Field Crops Res., **150**:135–144.

Walker, J. P., Willgoose, G. R. and Kalma, J. D. 2004. In situ measurement of soil moisture: a comparison of techniques. J. Hydrol., **293**:85–99.

Zreda, M., Desilets, D., Ferré, T. P. A., and Scott, R. L. 2008. Measuring soil moisture content non-invasively at intermediate spatial scale using cosmic-ray neutrons. *Geophys. Res. Lett*,, **35**:L21402-1 – L21402-5.

2. FIELD PERFORMANCE OF FIVE SOIL MOISTURE INSTRUMENTS IN HEAVY CLAY SOILS

2.1 Abstract

The increased use of soil moisture retrieval from satellites has heightened the need for improved accuracy of point measurements which are used to validate remotely sensed soil moisture products. A wide range of devices can be installed for operational monitoring of soil moisture. However, many of these devices have not been tested *in situ* in soils with very high reactive clay content. The objective of this study was to evaluate the accuracy in field performance of five soil moisture sensors: the EnviroSCAN ^{TM} Probe; the Diviner 2000 (both from Sentek Technologies); Hydra Probe® Soil Sensor (Stevens Water Monitoring Systems); ThetaProbe ML2x (Delta-T Devices) and ECHO EC5 (Decagon) in soils with clay content exceeding 70%. The instruments' default calibrations were tested against observed soil moisture from core samples using the thermogravimetric method. New calibration equations were developed for each device and these new equations were evaluated using an independent dataset. The ThetaProbe had the lowest root mean square error (RMSE) of 0.025 m^3 m^{-3} and mean bias error (MBE) of 0.002 m^3 m^{-3} in the pre-calibration analysis. Although the Hydra probe showed the highest pre-calibration errors, the instrument made the greatest improvement in post-calibration analysis with the RMSE value of 0.129 m^3 m^{-3} using the default equation

reduced to 0.014 m^3 m^{-3} using in-situ calibration and the 0.110 m^3 m^{-3} MBE was reduced to 0 after applying in-situ calibration.

2.2   Introduction

Water plays a very significant role in nearly all earth processes and one of the most anthropogenically-significant aspects of the water cycle is soil moisture. The variability of weather parameters, especially, precipitation is a major meteorological driver that influences soil-water dynamics. The location and timing of extreme weather events such as hailstorms and tornadoes have even been linked to variability in soil moisture (Hanesiak et al., 2004). Drought and flood risks are strongly impacted by variation in antecedent soil moisture. Crop yields in semi-arid regions are highly correlated to soil moisture levels (Walker, 1989; Raddatz et al., 1994). Likewise, crop disease and insect pressure are strongly impacted by soil moisture (Bom and Boland, 2000; Todd et al., 2002; Matheron and Porchas, 2005).

The complexity of land topography and heterogeneity of soil create significant spatial variability in soil moisture levels which is a challenge for determination of soil moisture on a large spatial scale. Point measurements of soil moisture with a high level of absolute accuracy are essential for developing meaningful measures of soil moisture at a broad scale. Many different devices can be installed for operational monitoring of soil moisture at specific points, including devices that monitor soil moisture temporal variability every few seconds. However, they do not measure soil moisture directly but

determine a soil property, e.g. soil dielectric, which can be related to the moisture content of the soil. The choice of soil moisture monitoring technique is dependent on the data application. Considerations such as long- or short-term; continuous or occasional; surface or soil profile monitoring as well as available resources in terms of cost, installation technicality, field accessibility, data collection frequency, sensor durability and ruggedness in field conditions like stoniness and salinity; adaptability under various weather conditions as well as the range of output parameters are important for designing any soil moisture monitoring network. Farmers may be more concerned about the cost of the device than the absolute soil moisture value. However, researchers tend to be more critical about the choice of device that will provide an accurate absolute value.

The behavior of water coupled with complex pore space geometry in clay soils often constitutes a major challenge that affects the electromagnetic property of the soil being sensed. Dielectric permittivity sensors operating at frequencies lower than 100 MHz tend to be sensitive to temperature and electrical conductivity due to the polarization effect (Chen and Or, 2006; Assouline et al., 2010). Studying the effect of temperature on the complex permittivity of 19 soils using a 50 MHz frequency Hydra probe, Seyfried and Grant (2007), observed a $\pm$ 0.028 m^3 m^{-3} change in volumetric water content as a result of the positive and negative effect of the real dielectric in a 40°C temperature change (from 5°C to 45°C). The imaginary component of the dielectric was found to be about six-times more sensitive to temperature change than the real component. Kelleners et al. (2005) observed that the overestimation of permittivity values was due to dielectric dispersion and ionic conductivity. They suggested that by increasing the operating frequency of sensors from less than 175 MHz to greater than 1

GHz, performance of reflectometers may be enhanced because at higher frequencies, sensors are less sensitive to dielectric dispersion and ionic conductivity.

Several studies have investigated the performance of soil moisture instruments. Huang et al. (2004) compared the performance of five water sensors including the ThetaProbe, Aqual-Tel, Profile Probe, Watermark and Aquaterr to determine if the factory calibrations of these devices can be used in the field. They observed that using the factory-recommended parameters, the Profile Probe (r^2 = 0.987, RMSE = 0.018 m^3 m^{-3}) and the ThetaProbe (r^2 = 0.983, RMSE = 0.037 m^3 m^{-3}) were more accurate than other soil moisture sensors when tested in the laboratory. However, when the Profile Probe laboratory derived calibration was evaluated under field conditions, it over-estimated soil moisture, especially at depth. This study and others such as Lukanu and Savage (2006), Logsdon (2009) and Ojo (2012) show that soil moisture instrument calibrations developed by the manufacturers using laboratory procedures are not always adaptable for use under field conditions. Field calibration of the sensors should be developed using different soil types. Paige and Keefer (2008) evaluated three soil moisture sensors installed in a shrub-covered, semi-arid watershed in Arizona and they reported that each sensor responded differently to precipitation events and soil variability. Chow et al. (2009) compared the field performance of nine soil moisture sensors in sandy loam in the maritime region of Canada. The authors observed that the sensor with the best factory calibration had a relative root mean square error of 15.78% with an r^2 of 0.75.

Most soil moisture sensor calibration and inter-sensor comparison studies are carried out on coarse and/or medium textured soils (Fares and Alva, 2000; McMichael and Lascano, 2003; Chandler et al., 2004; Geesing et al., 2004; Plauborg et al., 2005;

Polyakov et al., 2005; Evett et al., 2006; Lukanu and Savage, 2006; Paige and Keefer, 2008; Kelleners et al., 2009; Chow et al., 2009; Gabriel et al., 2010; Sakaki et al., 2011; Paraskevas et al., 2012; Mittelbach et al., 2012). None of the literature reviewed had reported an *in situ* calibration or inter-sensor comparison study in soils with > 65% clay content.

The thermogravimetric method is the standard method for quantifying soil moisture and it involves oven drying a known volume of moist soil and determining the weight loss to give gravimetric water content which can be multiplied by the bulk density of soil, divided by the density of water to obtain the volumetric water content (Topp et al. 2008). This method has significant limitations because it is a relatively slow process that requires intensive labour and the sampled soil cannot be used for repeated measurement. Despite these limitations, this method is very important for calibrating soil moisture sensors (Robock et al., 2000; Walker et al., 2004; Robinson et al., 2008). Robinson et al. (2008) and Dobriyal et al. (2012) published comprehensive reviews on the various soil physical properties and the corresponding soil sensing instrumentation used in determining soil moisture.

In this study, five widely used sensors were evaluated. These are: the EnviroSCAN [TM] Probe; the Diviner 2000 (both from Sentek technologies); Hydra Probe® Soil Sensor (Stevens Water Monitoring Systems); ThetaProbe ML2x (Delta-T Devices) and Decagon ECHO EC5. The objectives of this study were to evaluate the accuracy in field performance of five soil moisture instruments in heavy clay soil by comparing the soil moisture output from their factory default calibration to the volumetric

water content using the thermogravimetric method, and to assess the improvements in accuracy made from new *in situ* calibration equations developed for each sensor.

2.3   Materials and Methods

2.3.1   Site Description

The experiment was conducted at the Regional Operation Center of Agriculture and Agri-Food Canada (AAFC), Winnipeg Canada in the fall of 2013 and spring of 2014. The study area, being vertisolic, is characterized by heavy clay soil with the surface (0 – 15 cm) texture ranging from 67 to 76% clay and sand content ranging from 5 to 7% with 7.8% organic matter; the sub-surface texture (15 – 30 cm) contained 69 to 74% clay and 5 to 6% sand with 5.5% organic matter. The cation exchange capacity ranged between 36.3 - 45.1 and 42.9 – 47.8 meq/100g of soil surface and subsurface layers respectively. The site elevation is 233 m above sea level and lies within the Osborne soil series which is a poorly drained Rego Humic Gleysol developed on moderately to strongly calcareous, fine textured lacustrine deposits.

About 8% of the Canadian Prairie farmland is vertisolic soils with clayey (greater than 60% clay content) glacio-lacustrine parent materials and is characterized by high soil water holding capacity and low hydraulic conductivity. At low soil moisture contents, these soils shrink, which results in the formation of big cracks. At high soil moisture contents, the soil swells because of the dominance of smectite clay minerals (Anderson, 2010). Vertisolic soils occur in the Manitoba Red River Valley which is a highly

productive agricultural area. Due to its low hydraulic conductivity, this soil type contributes to seasonal spring flooding from snowmelt which sometimes results in delayed seeding. In-situ soil moisture monitoring networks have been established in this region by AAFC as well as Manitoba Agriculture Food and Rural Development (MAFRD) to assist in flood/drought monitoring and forecasting. The evaluation of the accuracy of various soil moisture instruments and their adaptability to the heavy clay soils in this region is critical to ensure the accuracy of the soil moisture measurements for many hydrologic and agronomic applications.

2.3.2   Soil Moisture Instruments

The EnviroSCAN probe and the Diviner 2000 are multi-depth instruments. Both devices require the installation of an access tube in the ground and the soil volume measured is mostly within a 10 cm diameter of the tube (Schwank et al., 2006; Sentek Technologies, 2011). The ECHO-EC5, Hydra Probe and ThetaProbe soil moisture devices are prong-based with tines protruding out of the probe head. Table 2.1 provides information on the frequency and output of the five soil moisture instruments as well as some literature that provides detailed sensor descriptions, calibration studies and research applications.

2.3.3   Data Collection

Three areas were established and categorized as "wet", "moist" and "dry". Each area had several sampling sites established. The wet area was flooded a few days before sampling and rain shelters were placed above the dry area a few weeks before sampling. The wet, moist and dry calibration areas were expected to contain > 0.40 m^3 m^{-3}, 0.30-0.40 m^3 m^{-3} and < 0.30 m^3 m^{-3} volumetric water content, respectively. The Sentek tubes

19

were installed to 60 cm depth; and, 15 cm and 35 cm were the depths from which the observed soil moisture was compared to the sensor readings. On the sampling days, soil moisture content was first determined using the multi-depth instruments. Immediately after taking the readings, three soil cores (7 cm length and 7.2 cm diameter) were taken very close to each tube at 11 cm – 18 cm to represent the 15 cm depth and at 31 cm – 38 cm for the 35 cm depth. Each core was assigned to one of the three pronged instruments- Hydra Probe, ThetaProbe or ECHO to determine the instruments' soil moisture reading before using the thermogravimetric method to determine the volumetric water content. The observed volumetric water content for each core with a specific instrument was used to calibrate that instrument. However, the mean value from all three cores was used in calibrating the EnviroSCAN and Diviner. Volumetric water content sensed by the instruments in a heterogeneous medium such as soil is influenced by soil properties like bulk density and environmental conditions like temperature (Evett at al., 2006; Fares et al., 2007). The effect of these factors on the instruments' soil moisture readings were not analyzed in this study because the data collection, using all five instruments, was carried out under same conditions (e.g. bulk density and temperature).

Table 2.1 Information on soil moisture instruments

Instrument	Operating Frequency	Default Calibration[†]	Sensor Output	Literature
EnviroSCAN	100 MHz[‡]	$\theta = (5.11SF - 0.1456)^{2.475}$	Scaled Frequency	Paltineanu and Starr (1997); Nachabe et al. (2004); Kelleners et al. (2004); Schwank et al. (2006); Starr and Rowland (2007); Holcomb et al. (2011)
Diviner 2000	100 MHz[‡]	$\theta = (3.642SF)^{3.0175}$	Scaled Frequency	Groves and Rose (2004); Evett et al. (2006); Ma et al. (2007); Egea et al. (2009, 2010); Sentek Technologies (2011); Paraskevas et al. (2012)
ECHO- EC5	70 MHz	$\theta = 0.00085RAW - 0.48$	Raw Count	Rosenbaum et al. (2010); Sakaki et al. (2011); Decagon Devices Inc. (2012); Durigon et al. (2012)
Hydra Probe	50 MHz	$\theta = 0.109\sqrt{\varepsilon} - 0.179$	Real Dielectric	Cosh et al. (2004); Seyfried et al. (2005); Bellingham, K. (2007); Logsdon et al. (2010); Rowlandson et al. (2013); Vaz et al. (2013)
ThetaProbe ML2x	100 MHz	$\theta = 0.524V - 0.06$	Voltage (mV)	Delta-T Devices Ltd. (1999); Koyama et al. (2010); Sakaki et al. (2011); Kulasekera et al. (2011); Adams et al. (2013)

[†] Default calibration equations showing relationship between volumetric water content and sensor output.
[‡] Frequency varies with the soil permittivity within a range of approximately 100 MHz in water to 150 MHz in air (Schwank et al., 2006)

2.3.4   Calibration and Statistical Analysis

Soil moisture instruments relate measureable soil properties such as changes in frequency or dielectric permittivity to the volumetric water contents. Table 2.1 shows the pre-set factory calibration equations used by the instruments. However, to achieve better accuracy, user-specific calibration that relates the instruments' raw output to observed soil moisture is important. The volumetric water contents from the soil cores were related to the raw data from the instruments to develop new coefficients. A general calibration equation was developed for each of the five instruments using the entire data collected and the generated calibration for the multi-depth instruments were compared to other published calibration equations. After this, the data were divided into two halves; one half was used to develop a new calibration equation and the other half was used to evaluate the newly-developed equation.

Statistical indicators (equations 2.1 through 2.3) such as coefficient of determination (r^2), root mean square error (RMSE), normalized root mean square error (NRMSE) and the mean bias error (MBE) were used to compare the devices' output (D_i) to the observed soil moisture (Obs_i). Part of the measurement requirements of some missions such as Soil Moisture Active Passive (SMAP) and Soil Moisture and Ocean Salinity (SMOS) was to obtain volumetric soil moisture with an accuracy within 0.04 m^3 m^{-3} (Entekhabi et al., 2010; Kerr et al., 2010). The NRMSE gives the relative difference between the default and the observed values. If the NRMSE is < 10%, the default value can be considered excellent, good if between 10 – 20%, fair if within the 20 – 30% range but poor if > 30% (Raes et al., 2012).

$$RMSE = \left(\frac{\Sigma(D_i - Obs_i)^2}{n}\right)^{0.5} \qquad\qquad [2.1]$$

$$NRMSE = \frac{1}{Obs}\sqrt{\frac{\Sigma(D_i - Obs_i)^2}{n}}\,100 \qquad\qquad [2.2]$$

$$MBE = \frac{1}{n}\left[\Sigma_{i=1}^{N}(D_i - Obs_i)\right] \qquad\qquad [2.3]$$

2.4   Results and Discussion

2.4.1   Instrument Default Volumetric Water Content vs Thermogravimetric

The outputs of all five instruments using their default settings were compared to the volumetric water content from thermogravimetric analysis. Observed soil moisture ranged from near permanent wilting point at 0.20 m^3 m^{-3} to slightly above field capacity at 0.46 m^3 m^{-3} and this range covers most of the soil moisture conditions expected during the growing season. The volumetric water contents in the moist category (as described in the *Data Collection* section) were observed to be close to, or within the wet category in 45% of the cases. Thus, there were more data points close to field capacity than to permanent wilting point. Data analysis (not shown) did not indicate any observable difference in the instruments' sensing of the soil moisture at the two depths considered- 15 cm and 35 cm. Therefore, all of the data collected was analyzed together and no depth-related comparison is reported.

The results in Table 2.2 showed that the two multi-depth instruments (EnviroSCAN and Diviner) had lower R^2 of 0.80 and 0.62, respectively, when compared to the three pronged sensors with R^2 values ranging from 0.89 - 0.95. This may be due to

the presence of cracks within the soil sensing volume of the multi-depth instruments leading to greater underestimation at low soil moisture content (Fig 2.1, a-b). During core sampling, these cracks were avoided. Thus, the observed moisture content from core samples may not be entirely representative of the soil volume for calibrating the multi-depth instruments at low moisture content. In smectite clays, the shrinking of the soil at low moisture content creates cracks with water molecules adhering to the soil matrix and potentially creating an air pocket, with a very low dielectric constant in contact with the probe. Campbell (1990) observed that the degree of bonding of water molecules to soil particles influences the dielectric permittivity of the medium (cf. Schwartz et al., 2009). The underestimation at low soil moisture contents is less in the three pronged sensors because cracks were avoided in the core samples used in calibrating these sensors.

Table 2.2 Accuracy of soil moisture output from each sensor using their respective default calibration equations.

Instrument	n	R^2	RMSE $m^3 m^{-3}$	NRMSE %	MBE $m^3 m^{-3}$
EnviroSCAN	43	0.80	0.100	26.3	0.047
Diviner	44	0.62	0.075	19.7	-0.008
ECHO	50	0.89	0.058	15.1	0.014
Hydra	50	0.95	0.131	36.6	0.108
Theta	48	0.91	0.025	6.5	0.002

n = number of samples; R^2 = coefficient of determination; RMSE = Root Mean Square Error; NRMSE= Normalized Root Mean Square Error and MBE = Mean Bias Error.
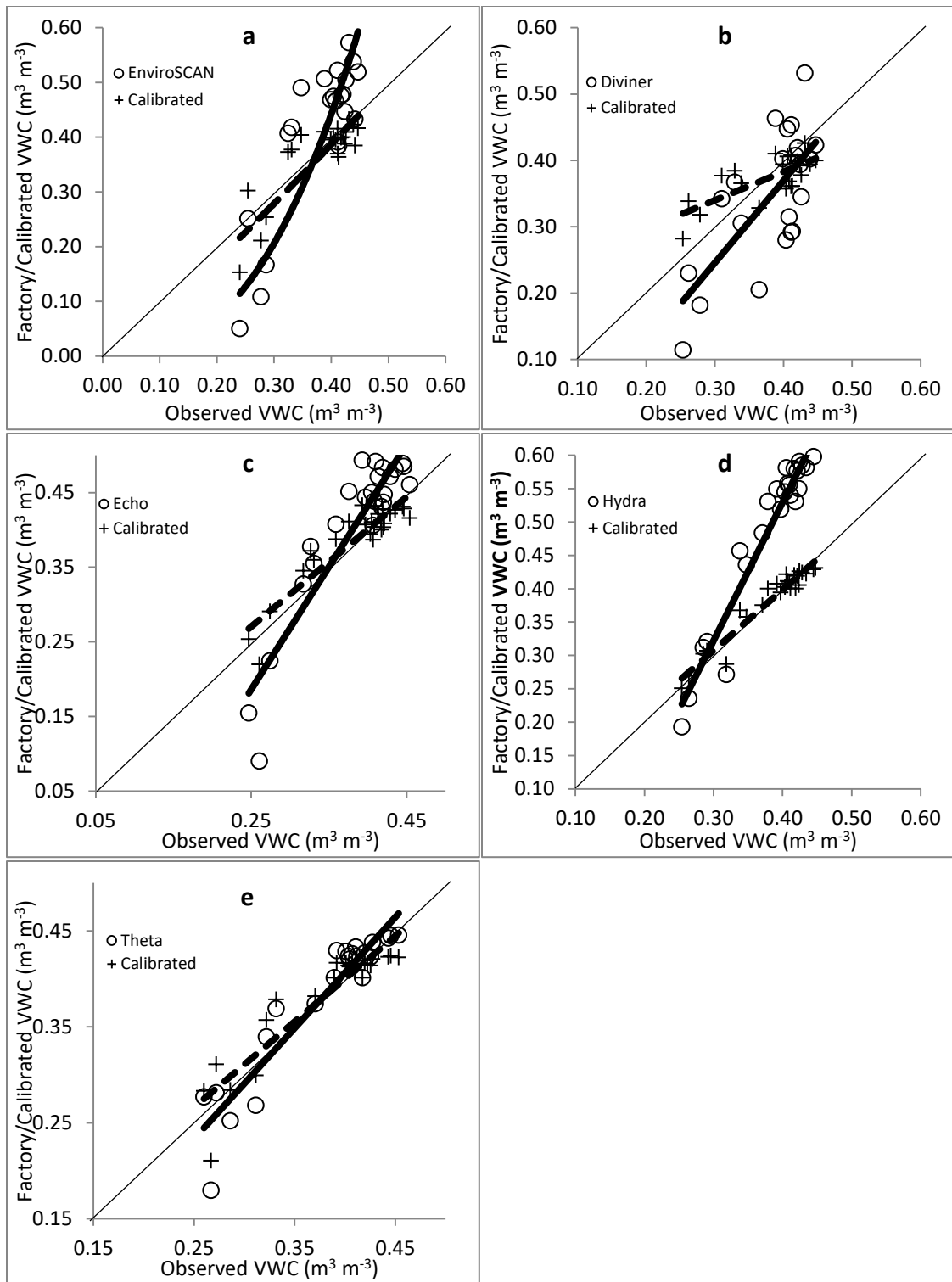
Figure 2.1   Comparison of observed moisture content with the factory-derived moisture content (o) and calibrated VWC (+) for (a) EnviroSCAN; (b) Diviner; (c) ECHO; (d) Hydra Probe and (e) ThetaProbe. The thin solid line is the 1:1 line, thick solid line is the factory-derived trend line and the thick dashed line is the calibration equation trend line.

The Hydra probe had the highest R^2 of 0.95. However, despite having the best R^2, the performance of the Hydra probe using the default setting was generally poor with RMSE, NRMSE and MBE of 0.131 m^3 m^{-3}, 36.6% and 0.108 m^3 m^{-3}, respectively. The sensor grossly overestimated soil moisture content near field capacity. This is consistent with studies such as Seyfried and Murdock (2004) who observed that the Hydra probe clay calibration equation gave unrealistic readings at high water contents. Logsdon and Hornbuckle (2006) compared three sensors and reported that the Hydra probe had the highest RMSE and suggested that this may be due to its lower operating frequency which is sensitive to electrical conductivity. Of all the instruments compared in this study, the Hydra Probe has the lowest operating frequency (Table 2.1). The Diviner showed a slightly negative mean bias error, but a positive bias was observed in all other sensors. Overall, the default setting of the ThetaProbe had the best performance with an RMSE of 0.025 m^3 m^{-3} and 0.2% bias. At low soil moisture content, all the instruments underestimated soil moisture (Figure 2.1). At the high end, however, EnviroSCAN, ECHO and Hydra Probe overestimated soil moisture. This result reinforces the need to calibrate the sensors to local conditions to enhance the accuracy of the output.
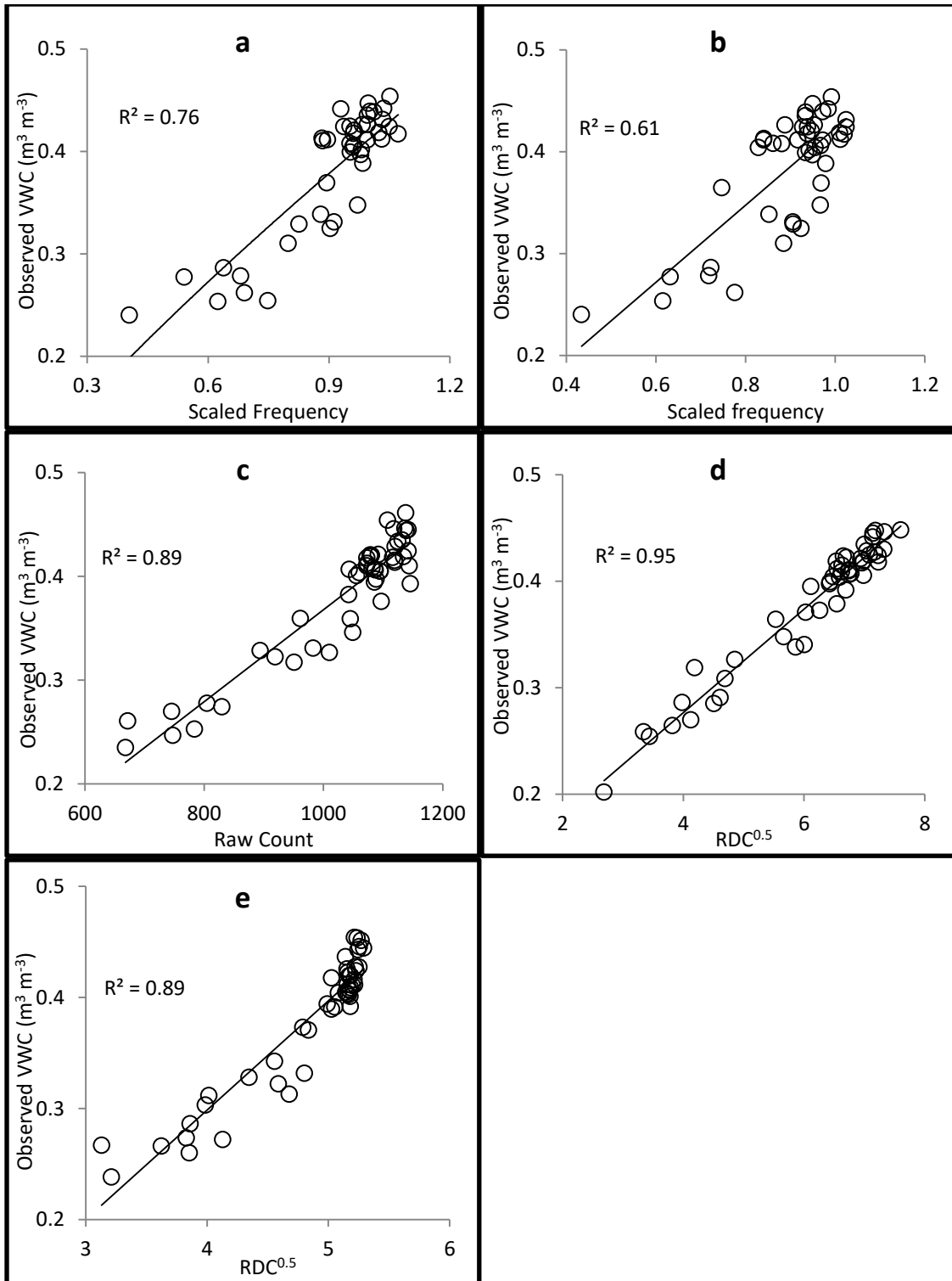
Figure 2. 2   General field calibration for (a) EnviroSCAN; (b) Diviner; (c) ECHO; (d) Hydra Probe and (e) ThetaProbe. VWC = Volumetric Water Content, RDC = Real Dielectric Constant.

2.4.2 Calibration Results

Table 2.3 shows the field calibration equations that were developed by relating the raw output from the sensors to observed volumetric water content from soil cores using all the data collected. The two multi-depth sensors showed lower R^2 values of 0.76 and 0.61 for the EnviroSCAN and Diviner, respectively, compared to the prong-based sensors with R^2 values of 0.89, 0.95 and 0.89 for the ECHO, Hydra Probe and ThetaProbe, respectively (Figure 2.2). Evett et al., (2006) compared the factory calibration of several soil moisture sensors, including the EnviroSCAN and Diviner, to observed soil moisture in silty clay loam, clay and clay loam soils. The calibration equations developed in the laboratory for the silty clay loam and clay had R^2 values of 0.993 and 0.992 for the EnviroSCAN and Diviner, respectively. Similarly, Groves and Rose (2004) obtained an R^2 value of 0.93 for laboratory calibration of the Diviner in clay soil. The R^2 values obtained by these authors are higher than the values obtained in our study. This can be explained by the controlled environment the laboratory provided in their study compared to field calibration.

Table 2.3 Field calibration equations developed for each sensor using all data points.

Instrument	n	R²	Equation[†]	x- input
EnviroSCAN	43	0.76	$\theta = 0.4121x^{0.8088}$	Scaled Frequency
Diviner	44	0.61	$\theta = 0.3781x + 0.0452$	Scaled Frequency
ECHO	50	0.89	$\theta = 0.0004x - 0.0752$	Raw Count
Hydra	50	0.95	$\theta = 0.0487x + 0.0816$	Real Dielectric$^{0.5}$
Theta	48	0.89	$\theta = 0.0985x - 0.0956$	Real Dielectric$^{0.5}$

[†] θ is volumetric soil moisture content.

Sentek Technologies (2011) conducted EnviroSCAN field calibration experiments in cracking clay soils at various sites in Australia and reported an R^2 of 0.58. In contrast, Fares et al., (2004), observed an R^2 value of 0.89 at a shrink-swell clay soil (35 – 100 cm depth) in South Australia using the EnviroSCAN. It should be noted that the manufacturer of these multi-depth devices, Sentek Technologies (2011), used power functions for the default calibration but reported many studies that have found and used linear functions. The equations developed in this study depict soil moisture (y-axis) as a function of the instruments' output- in this case, scaled frequency (x-axis). This is different from the suggested equation format which depicts scaled frequency as a function of soil moisture.

The calibration equations developed for the three pronged sensors had R^2 values of 0.89, 0.95 and 0.89 for the ECHO, Hydra Probe and ThetaProbe, respectively. The ThetaProbe with R^2 of 0.89 is higher than the R^2 value of 0.77 observed by Kaleita et al. (2005) who used the ThetaProbe for field calibration of soils with clay contents ranging from 16% - 26% . The ECHO probe R^2 value of 0.89 is slightly higher than the R^2 of 0.87 found by Odubanjo et al. (2013). Overall, the Hydra probe had the best R^2 of 0.95. This value is higher than the field calibration R^2 value of 0.81 obtained by Rowlandson et al. (2013) for > 40% the surface layer of clay soils across twenty-five fields in Manitoba, Canada.

Table 2.4 Comparison of published multi-depth sensors calibration equations.

Instrument	Texture (%) Clay - Silt	Equation	RMSE m^3 m^{-3}
EnviroSCAN			
This Study	71 - 24	$\theta = 0.4121SF^{0.8088}$	0.030
Evett et al.[†]	39 - 46	$\theta = 0.605SF^{3.812} + 0.024$	0.178
Sentek	Cracking Clay	$100\theta = (0.073 + SF)/0.0254$	0.029
Fares et al.[‡]	62 – 11	$\theta = 1.605SF^{0.552} - 1.186$	0.072
Diviner			
This Study	71 - 24	$\theta = 0.3781SF + 0.0452$	0.036
Evett et al.	39 - 46	$\theta = 0.457SF^{5.421} + 0.034$	0.116
Sentek[§]	Cracking Clay	$100\theta = (0.073 + SF)/0.0254$	0.036
Groves&Rose	44 - 19	$100\theta = (SF/0.3107)^{3.3715}$	0.090

θ = Volumetric water content (m^3 m^{-3}); SF = Scaled Frequency; RMSE = Root Mean Square Error

[†] Single calibration equation developed from silty clay loam with 30% clay and 53% silt; and clay soil with 48% clay and 39% silt (Evett et al., 2006).

[‡] Calibration equation and texture represents lower soil profile of 35-100 cm depth (Fares et al., 2004).

[§] Clay calibration equation derived using the EnviroSCAN but applied for use under the Diviner for comparison. 0.073 is the average of the "C" constant for the top 30 cm depth (Sentek Technologies, 2011).

2.4.3 Multi-depth Instruments' Calibration Comparisons

Calibration equations derived for the multi-depth sensors in this study were compared to several published calibrations conducted in clay soil (Table 2.4). Although there are quite a number of published calibrations for the multi-depth instruments, very few of these calibrations have been conducted in soils with > 35% clay. Groves and Rose (2004), and Evett et al. (2006) developed calibration equations in the laboratory for clay soils using the multi-depth instruments. Fares et al., (2004), Sentek Technologies (2011) and our study developed field-based calibration in clay soils. Figure 2.3 shows the comparison of the equations using both the Diviner and the EnviroSCAN. The two

laboratory-derived equations, using the Diviner, had almost the same air-dry and saturation points but different trajectories. Groves and Rose (2004) calibration equation showed higher volumetric water content than Evett et al. (2006) at the same scaled frequency. The Evett et al. (2006) laboratory-derived calibration using the EnviroSCAN was higher than the two laboratory-derived calibrations using the Diviner. A similar trend was observed between the laboratory-derived equations and Fares et al., (2004) clay calibration.at < 0.40 m^3 m^{-3} volumetric water content.
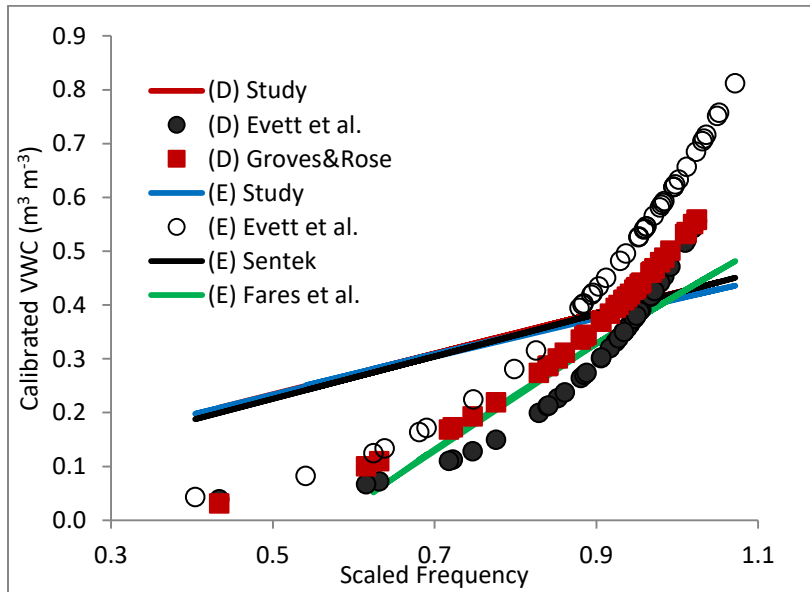
Figure 2.3   The comparison of several calibration equations. (D) and (E) represent Diviner and EnviroSCAN respectively. The lines are field-based calibrations and symbols are laboratory-based calibrations.

The field-derived calibration from Sentek Technologies (2011) using the EnviroSCAN was perfectly aligned with the Diviner calibration derived from this study. This perfect alignment is reflected in the RMSE of both calibrations which yielded 0.036 m^3 m^{-3} (Table 2.4). The EnviroSCAN calibration equation derived in this study showed slightly higher volumetric water contents at low scaled frequencies and slightly lower

water contents at high scaled frequencies than the Diviner calibration equation. These two equations derived in our study for the two multi-depth instruments were not significantly different from each other ($p = 0.48$) within the observed soil moisture range and this could be as a result of both devices operating at similar frequencies. At volumetric water contents less than 0.40 m^3 m^{-3}, the laboratory-derived calibrations and Fares et al., (2004) had lower soil moisture compared to the calibration equation from this study. Haberland et al. (2014) conducted both laboratory and field calibrations using the Diviner in clay loam and clay soils. The authors observed that the manufacturer's default equation showed satisfactory results in the laboratory but underestimated water content in both soils under field conditions.

2.4.4 Evaluation Results

The dataset was divided in half and new field calibration equations were developed for each device using one-half of the data. This was done to assess the improvements made over the default equation using independent datasets (the other half) that were not included in developing the calibration equations. Kaleita et al. (2005) conducted a ThetaProbe field calibration study of different medium textured soils in Iowa and showed that about 20 sample points were recommended for developing a valid field calibration equation. Both the calibration and evaluation datasets consist of more than 20 sample points. Table 2.5 shows that all the sensors had improved RMSE, NRMSE and MBE with the *in situ* calibration equations compared to the default in the evaluation dataset. The two multi-depth sensors had slight negative biases and the three pronged sensors were almost bias-neutral.

Table 2.5 Impact of *field* calibration on the accuracy of soil moisture measurement by each sensor.

Instrument		n	R^2	RMSE $m^3 m^{-3}$	NRMSE %	MBE $m^3 m^{-3}$
EnviroSCAN	Default	22	0.71	0.096	25.3	0.033
	Calibrated			0.040	10.5	-0.012
Diviner	Default	22	0.51	0.080	21.0	-0.035
	Calibrated			0.040	10.6	-0.006
ECHO	Default	25	0.84	0.060	15.6	0.023
	Calibrated			0.023	6.0	0.003
Hydra	Default	25	0.94	0.129	33.9	0.110
	Calibrated			0.014	3.8	0.000
Theta	Default	24	0.88	0.027	7.1	0.003
	Calibrated			0.023	6.0	0.002

n = number of samples; R^2 = coefficient of determination; RMSE = Root Mean Square Error; NRMSE= Normalized Root Mean Square Error and MBE = Mean Bias Error

Figure 2.1a showed that the EnviroSCAN calibration equation line was very close to the 1:1 line. At low soil moisture contents, it had slight underestimation but this gap was smaller at high moisture contents. Although a power function was used in the calibration, the line behaved like a linear regression line within the range of observed moisture content. The NRMSE was reduced from 25.3% to 10.5%. Figure 2.1b showed that the default equation for the Diviner consistently underestimated soil moisture. On the other hand, the calibration trend-line crossed the 1:1 trend-line at about 0.37 m^3 m^{-3} and showed overestimation at low soil moisture content and underestimation at high soil moisture content. Thus, depending on the evaluation dataset, the developed calibration equation for the Diviner may result in very minimal improvement over the default equation. The calibration analysis of both the ECHO and ThetaProbe showed that the calibrated soil moisture data had a slight overestimation at low soil moisture contents and this disappeared as the moisture content increased (Fig 2.1 c and e). As discussed earlier,

the ThetaProbe gave the best result during the pre-calibration analysis and this is observed in the close fit of the default trend-line to the 1:1 line. Calibration resulted in minimal improvements.

Of all the sensors compared, the Hydra probe showed greatest improvement with field calibration. The RMSE of 0.129 m^3 m^{-3} using the default equation was reduced to 0.014 m^3 m^{-3} using the *in situ* calibration. The 11% overestimation bias was non-existent using the calibration equation, i.e., on the average, no overestimation or underestimation occurred. Figure 2.1d showed that the Hydra probe calibration trend line (dashed line) almost perfectly aligned with the 1:1 line. Thus, using the square root of the Hydra probe's real dielectric constant, we observed a nearly perfect absolute accuracy with observed volumetric water content and this showed the absolute necessity of *in situ* calibration before using the instrument in heavy clay soils.

The effect of soil temperature on volumetric water measurement by capacitance sensors have been well documented (Schwank and Green, 2007; Fares et al., 2007; Seyfried and Grant, 2007). Analysis conducted in this study did not include any correction for temperature. Data collection was carried out at soil temperatures between 10 – 20 °C and all the instruments were used under similar conditions. Therefore, temperature correction for the instruments used in this study is not expected to lead to a significant difference in the result of this instruments' performance study. It should be noted that beyond the soil texture and temperature, other factors such as salinity, cation exchange capacity, clay mineralogy and the amount of bound water can influence how soil moisture is sensed by the instruments (Schwartz et al., 2009). The calibration

equations developed in this study should be evaluated at other heavy clay sites to determine their adaptability.

2.5 Conclusions

The field performance of five instruments that monitor soil moisture was compared in heavy clay soil and *in situ* calibration equations were generated. Two of these instruments had simultaneous multi-depth sensing capability and the other three instruments were prong-based, single-depth sensors. Soil moisture was monitored at 15 and 35 cm depths and core samples were collected to calibrate the instruments. Regardless of the instrument used, *in situ* calibration improved the performance of the instruments. The Hydra probe had the greatest improvement resulting in reduced RMSE from 0.129 m^3 m^{-3} to 0.014 m^3 m^{-3} in the evaluation dataset and underscored the importance of developing *in situ* calibration before using the instrument, especially in heavy clay soils. This study showed that the ThetaProbe did not need to be calibrated because the improvement observed with calibration was minimal.

Linear regression was used to describe the relationship between the raw output from the instrument and the observed volumetric water content for all the sensors except the EnviroSCAN where a power function was used. The two multi-depth instruments showed similar post-calibration performance with RMSE of 0.04 m^3 m^{-3}. The calibration equations generated for the two instruments were not significantly different from each other. However, using the default calibration equation, the Diviner had a better

performance RMSE of 0.08 m^3 m^{-3} compared to RMSE of 0.096 m^3 m^{-3} for the EnviroSCAN. The performance of both multi-depth instruments was poorer than the three pronged instruments because the multi-depth instruments underestimated observed soil moisture at low moisture contents. This was likely due to the presence of some cracks within the sensing volume of the dry clay soil. These cracks were avoided in taking core samples used for calibration of the pronged sensors. Some might argue that the calibration procedure was not an accurate depiction of the soil matrix under dry conditions. However, it must be remembered that when these sensors are deployed in heavy clay soils, cracking is a normal occurrence.

2.6   Acknowledgments

2.7   References

Adams, J. R., Berg, A. A. and McNairn, H. 2013. Field Level Soil Moisture Variability at 6- and 3-cm Sampling Depths: Implications for Microwave Sensor Validation. Vadose Zone J., **12**:1–12.

Anderson, D. 2010. Vertisolic Soils of the Prairie Region. Prairie Soils Crops J., **3**:29–36.

Assouline, S., Narkis, K., Tyler, S. W., Lunati, I, Parlange, M. B. and Selker, J. S. 2010. On the Diurnal Soil Water Content Dynamics during Evaporation using Dielectric Methods. Vadose Zone J., **9**:709–718.

Bellingham, K. 2007. The Stevens Hydra Probe Inorganic Soil Calibrations. Stevens Water Monitoring Systems Inc.

Bom, M. and Boland, G. J. 2000. Evaluation of disease forecasting variables for sclerotinia stem rot (Sclerotinia sclerotiorum) of canola. Can. J. Plant Sci., **80**:889–898.

Campbell, J. E. 1990. Dielectric properties and influence of conductivity in soils at one to fifty megahertz. Soil Sci. Soc. Am. J., **54**:332–341.

Chandler, D. G., Seyfried, M., Murdock, M. and McNamara, J. P. 2004. Field calibration of water content reflectometers. Soil Sci. Soc. Am. J., **68**:1501–1507.

Chen, Y. and Or, D. 2006. Effects of Maxwell-Wagner polarization on soil complex dielectric permittivity under variable temperature and electrical conductivity. Water Resour. Res., **42**:1–14.

Chow, L., Xing, Z., Rees, H. W., Meng, F., Monteith, J. and Lionel, S. 2009. Field Performance of Nine Soil Water Content Sensors on a Sandy Loam Soil in New Brunswick, Maritime Region, Canada. Sensors, **9**:9398–9413.

Cosh, M., Jackson, T. J., Bindlish, R. and Prueger, J. 2004. Watershed scale temporal and spatial stability of soil moisture and its role in validating satellite estimates. Remote Sens. Environ., **92**:427–435.

Decagon Devices, Inc. 2012. EC-5 Soil Moisture Sensor User's Manual. Available at http://www.decagon.com.br/assets/Uploads/13876-01-Manual-EC-5.pdf (verified 27 November 2013).

Delta-T Devices Ltd. 1999. ThetaProbe Soil Moisture Sensor - Type ML2x. User Manual. Available at ftp://ftp.dynamax.com/manuals/ML2x_Manual.pdf (verified 26 November 2013).

Dobriyal, P., Qureshi, A., Badola, R. and Hussain, S. A. 2012. A review of the methods available for estimating soil moisture and its implications for water resource management. J. Hydrol., **458**–**459**:110–117.

Durigon, A., Alex dos Santos, M., de Jong van Lier, Q. and Metselaar, K. 2012. Pressure Heads and Simulated Water Uptake Patterns for a Severely Stressed Bean Crop. Vadose Zone J., **11**:1–14.

Egea, G., González-Real, M. M., Baille, A., Nortes, P. A., Sánchez-Bel, P. and Domingo, R. 2009. The effects of contrasted deficit irrigation strategies on the fruit growth and kernel quality of mature almond trees. Agric. Water Manag., **96**:1605–1614.

Egea, G., Nortes, P. A., González-Real, M. M., Baille, A. and Domingo, R. 2010. Agronomic response and water productivity of almond trees under contrasted deficit irrigation regimes. Agric. Water Manag., **97**:171–181.

Entekhabi, D., Njoku, E. G., O'Neill, P. E., Kellogg, K. H., Crow, W. T., Edelstein, W. N., Entin, J. K., Goodman, S. D., Jackson, T. J., Johnson, J., Kimball, J., Piepmeier, J. R., Koster, R. D., Martin, N., McDonald, K. C., Moghaddam, M., Moran, S., Reichle, R., Shi, J. C., Spencer, M. W., Thurman, S. W., Tsang, L. and Van Zyl, J. 2010. The Soil Moisture Active Passive (SMAP) Mission. Proc. IEEE, **98**:704–716.

Evett, S. R., Tolk, J. A. and Howell, T. A. 2006. Soil Profile Water Content Determination: Sensor Accuracy, Axial Response, Calibration, Temperature Dependence, and Precision. Vadose Zone J., **5**:894–907.

Fares, A. and Alva, A. K. 2000. Soil water components based on capacitance probes in a sandy soil. Soil Sci. Soc. Am. J., **64**:311–318.

Fares, A., Buss, P., Dalton, M., El-Kadi, A. I. and Parsons, L. R. 2004. Dual field calibration of capacitance and neutron soil water sensors in a shrinking–swelling clay soil. Vadose Zone J., **3**:1390–1399.

Fares, A., Hamdhani, H. and Jenkins, D. M. 2007. Temperature-Dependent Scaled Frequency: Improved Accuracy of Multisensor Capacitance Probes. Soil Sci. Soc. Am. J., **71**:894–900.

Gabriel, J. L., Lizaso, J. I. and Quemada, M. 2010. Laboratory versus Field Calibration of Capacitance Probes. Soil Sci. Soc. Am. J., **74**:593–601.

Geesing, D., Bachmaier, M. and Schmidhalter, U. 2004. Field Calibration of a capacitance soil water probe in heterogeneous fields. Aust. J. Soil Res., **42**:289–299.

Groves, S. J. and Rose, S. C. 2004. Calibration equations for Diviner 2000 capacitance measurements of volumetric soil water content of six soils. Soil Use Manag., **20**:96–97.

Haberland, J., Gálvez, R., Kremer, C. and Carter, C. 2014. Laboratory and Field Calibration of the Diviner 2000 Probe in Two Types of Soil. J. Irrig. Drain. Eng., **140**:.

Hanesiak, J. M., Raddatz, R. L. and Lobban, S. 2004. Local initiation of deep convection on the Canadian prairie provinces. Bound.-Layer Meteorol., **110**:455–470.

Holcomb, J. C., Sullivan, D. M., Horneck, D. A. and Clough, G. H. 2011. Effect of Irrigation Rate on Ammonia Volatilization. Soil Sci. Soc. Am. J., **75**:2341–2347.

Huang, Q., Akinremi, O. O., Sri Rajan, R. and Bullock, P. 2004. Laboratory and field evaluation of five soil water sensors. Can. J. Soil Sci., **84**:431–438.

Kaleita, A. L., Heitman, J. L. and Logsdon, S. D. 2005. Field calibration of the Theta Probe for Des Moines Lobe soils. Am. Soc. Agric. Eng., **21**:865–870.

Kelleners, T. J., Paige, G. B. and Gray, S. T. 2009. Measurement of the Dielectric Properties of Wyoming Soils Using Electromagnetic Sensors. Soil Sci. Soc. Am. J., **73**:1626–1637.

Kelleners, T. J., Seyfried, M. S., Blonquist, J. M., Bilskie, J. and Chandler, D. G. 2005. Improved Interpretation of Water Content Reflectometer Measurements in Soils. Soil Sci. Soc. Am. J., **69**:1684–1690.

Kelleners, T. J., Soppe, R. W. O., Ayars, J. E. and Skaggs, T. H. 2004. Calibration of capacitance probe sensors in a saline silty clay soil. Soil Sci. Soc. Am. J., **68**:770–778.

Kerr, Y. H., Waldteufel, P., Wigneron, J.-P., Delwart, S., Cabot, F., Boutin, J., Escorihuela, M.-J., Font, J., Reul, N., Gruhier, C., Juglea, S. E., Drinkwater, M. R., Hahne, A., Martín-Neira, M. and Mecklenburg, S. 2010. The SMOS Mission: New Tool for Monitoring Key Elements ofthe Global Water Cycle. Proc. IEEE, **98**:666–687.

Koyama, C. N., Korres, W., Fiener, P. and Schneider, K. 2010. Variability of Surface Soil Moisture Observed from Multitemporal C-Band Synthetic Aperture Radar and Field Data. Vadose Zone J., **9**:1014–1024.

Kulasekera, P. B., Parkin, G. W. and Bertoldi, P. von. 2011. Using Soil Water Content Sensors to Characterize Tillage Effects on Preferential Flow. Vadose Zone J., **10**:683–696.

Logsdon, S. D. 2009. CS616 Calibration: Field versus Laboratory. Soil Sci. Soc. Am. J., **73**:1–6.

Logsdon, S. D., Green, T. R., Seyfried, M., Evett, S. R. and Bonta, J. 2010. Hydra Probe and Twelve-Wire Probe Comparisons in Fluids and Soil Cores. Soil Sci. Soc. Am. J., **74**:5–12.

Logsdon, S. D. and Hornbuckle, B. K. 2006. Soil Moisture Probes for a Dispersive Soil (p. 14). Presented at the International Symposium and Workshop on Time Domain Reflectometry for Innovative Soils Applications (TDR 2006), Purdue University, West Lafayette, USA. Retrieved from https://engineering.purdue.edu/TDR/Papers/Papers/13_Paper.pdf

Lukanu, G. and Savage, M. J. 2006. Calibration of a frequency-domain reflectometer for determining soil-water content in a clay loam soil. Water A, **32**:37–42.

Ma, F., Kang, S., Li, F., Zhang, J., Du, T., Hu, X. and Wang, M. 2007. Effect of water deficit in different growth stages on stem sap flux of greenhouse grown pear-jujube tree. Agric. Water Manag., **90**:190–196.

Matheron, M. E. and Porchas, M. 2005. Influence of Soil Temperature and Moisture on Eruptive Germination and Viability of Sclerotia of *Sclerotinia minor* and *S. sclerotiorum*. Plant Dis., **89**:50–54.

McMichael, B. and Lascano, R. J. 2003. Laboratory evaluation of a commercial dielectric soil water sensor. Vadose Zone J., **2**:650–654.

Mittelbach, H., Lehner, I. and Seneviratne, S. I. 2012. Comparison of four soil moisture sensor types under field conditions in Switzerland. J. Hydrol., **430–431**:39–49.

Nachabe, M., Masek, C. and Obeysekera, J. 2004. Observations and modeling of profile soil water storage above a shallow water table. Soil Sci. Soc. Am. J., **68**:719–724.

Odubanjo, O. O., Fasinmirin, J. T., Oguntunde, P. G. and Olufayo, A. A. 2013. ECH2O probe calibration for soil moisture content determination in the tropical climate of Akure, Nigeria. Int. J. AgriScience, **3**:718–727.

Ojo, E. R. 2012. Modeling soil moisture from real-time weather data. MSc. Thesis, University of Manitoba. Available at http://mspace.lib.umanitoba.ca/handle/1993/5009 (verified 18 November 2013).

Paige, G. B. and Keefer, T. O. 2008. Comparison of Field Performance of Multiple Soil Moisture Sensors in a Semi-Arid Rangeland [1]. JAWRA J. Am. Water Resour. Assoc., **44**:121–135.

Paltinean, I. C. and Starr, J. L. 1997. Real-time Soil Water Dynamics Using Multisensor Capacitance Probes: Laboratory Calibration. Soil Sci. Soc. Am. J., **61**:1576–1585.

Paraskevas, C., Georgiou, P., Ilias, A., Panoras, A. and Babajimopoulos, C. 2012. Calibration equations for two capacitance water content probes. Int. Agrophysics, **26**:285–293.

Plauborg, F., Iversen, B. V. and Lærke, P. E. 2005. In Situ Comparison of Three Dielectric Soil Moisture Sensors in Drip Irrigated Sandy Soils. Vadose Zone J., **4**:1037–1047.

Polyakov, V., Fares, A. and Ryder, M. H. 2005. Calibration of a Capacitance System for Measuring Water Content of Tropical Soil. Vadose Zone J., **4**:1004–1010.

Raddatz, R. L., Shaykewich, C. F. and Bullock, P. R. 1994. Prairie crop yield estimates from modelled phenological development and water use. Can. J. Plant Sci., **74**:429–436.

Raes, D., Steduto, P., Hsiao, T. C. and Fereres, E. 2012. AquaCrop Version 4.0 - User Guide. Available at http://www.fao.org/nr/water/docs/AquaCropV40Chapter2.pdf (verified 1 December 2013).

Robinson, D. A., Campbell, C. S., Hopmans, J. W., Hornbuckle, B. K., Jones, S. B., Knight, R., Ogden, F., Selker, J. and Wendroth, O. 2008. Soil Moisture Measurement for Ecological and Hydrological Watershed-Scale Observatories: A Review. Vadose Zone J., **7**:358–389.

Robock, A., Vinnikov, K. Y., Srinivasan, G., Entin, J. K., Hollinger, S. E., Speranskaya, N. A., Liu, S. and Namkhai, A. 2000. The Global Soil Moisture Data Bank. Bull. Am. Meteorol. Soc., **81**:1281–1299.

Rosenbaum, U., Huisman, J. A., Weuthen, A., Vereecken, H. and Bogena, H. R. 2010. Sensor-to-Sensor Variability of the ECHO EC-5, TE, and 5TE Sensors in Dielectric Liquids. Vadose Zone J., **9**:181–186.

Rowlandson, T. L., Berg, A. A., Bullock, P. R., Ojo, E. R., McNairn, H., Wiseman, G. and Cosh, M. H. 2013. Evaluation of several calibration procedures for a portable soil moisture sensor. J. Hydrol., **498**:335–344.

Sakaki, T., Limsuwat, A. and Illangasekare, T. H. 2011. A Simple Method for Calibrating Dielectric Soil Moisture Sensors: Laboratory Validation in Sands. Vadose Zone J., **10**:526–531.

Schwank, M. and Green, T. R. 2007. Simulated effects of soil temperature and salinity on capacitance sensor measurements. Sensors, **7**:548–577.

Schwank, M., Green, T. R., Mätzler, C., Benedickter, H. and Flühler, H. 2006. Laboratory Characterization of a Commercial Capacitance Sensor for Estimating Permittivity and Inferring Soil Water Content. Vadose Zone J., **5**:1048–1064.

Schwartz, R. C., Evett, S. R. and Bell, J. M. 2009. Complex permittivity model for time domain reflectometry soil water content sensing: II. Calibration. Soil Sci. Soc. Am. J., **73**:898–909.

Sentek Technologies. **2011**. Calibration Manual for Sentek Soil Moisture Sensors. V 2.0.

Seyfried, M. S. and Grant, L. E. 2007. Temperature Effects on Soil Dielectric Properties Measured at 50 MHz. Vadose Zone J., **6**:759–765.

Seyfried, M. S., Grant, L. E., Du, E. and Humes, K. 2005. Dielectric Loss and Calibration of the Hydra Probe Soil Water Sensor. Vadose Zone J., **4**:1070–1079.

Seyfried, M. S. and Murdock, M. D. 2004. Measurement of soil water content with a 50-MHz soil dielectric sensor. Soil Sci. Soc. Am. J., **68**:394–403.

Starr, J. L. and Rowland, R. 2007. Soil Water Measurement Comparisons Between Semi-Permanent and Portable Capacitance Probes. Soil Sci. Soc. Am. J., **71**:51–52.

Todd, M. C., Washington, R., Cheke, R. A. and Kniveton, D. 2002. Brown locust outbreaks and climate variability in southern Africa. J. Appl. Ecol., **39**:31–42.

Topp, G.C., G.W. Parkin and T.P.A. Ferré. 2008. Soil water content. *In* Soil Sampling and Methods of Analysis (Carter, M.R. and E.G. Gregorich, eds.), CRC Press, Boca Raton, Fl. p. 939-961.

Vaz, C. M. P., Jones, S., Meding, M. and Tuller, M. 2013. Evaluation of Standard Calibration Functions for Eight Electromagnetic Soil Moisture Sensors. Vadose Zone J., **12**:1–16.

Walker, G. K. 1989. Model for operational forecasting of western Canada wheat yield. Agric. For. Meteorol., **44**:339–351.

Walker, J. P., Willgoose, G. R. and Kalma, J. D. 2004. In situ measurement of soil moisture: a comparison of techniques. J. Hydrol., **293**:85–99.

3. CALIBRATION AND EVALUATION OF A FDR SENSOR FOR REAL-TIME *IN SITU* MONITORING IN AN AGRICULTURAL SOIL MOISTURE NETWORK

3.1 Abstract

Soil spatial heterogeneity poses a challenge to accurate soil moisture determination. Remote sensing, especially via sensors which acquire data at microwave frequencies, is being used to overcome this challenge. *In situ* soil moisture monitoring can be used to validate remotely sensed surface soil moisture estimates and as inputs for agronomic and hydrologic models. Nine *in situ* soil moisture stations were established in Manitoba (Canada) and instrumented with Stevens Hydra Probes. The sensors were installed in triplicate with vertical orientation at the surface and with horizontal orientation at 5, 20, 50 and 100 cm depths. To ensure accuracy of measured soil moisture, both laboratory and field calibrations were conducted. These calibrated soil moisture values were compared to the probe default values and those generated using published calibrations such as Topp et al. (1980) and Logsdon et al. (2010). Overall, results obtained showed that the field calibration was superior (coefficient of determination, r^2 of 0.95) to the laboratory calibration (r^2 of 0.89). In addition, coarse textured sites generally performed better than the fine textured, high cation exchange capacity (CEC) sites. At the Kelburn site with high clay and CEC, use of field calibration reduced the root mean

square error (RMSE) from 0.188 m^3 m^{-3} to 0.026 m^3 m^{-3}. However, at the low clay and CEC Treherne site, gains in accuracy were minimal, about 0.005 m^3 m^{-3}. The laboratory calibration consistently underestimated soil moisture at all the evaluation sites whereas both Topp and Logsdon calibrations overestimated soil moisture.

3.2   Introduction

There is an increasing relevance of soil moisture determination in understanding global weather dynamics, flooding and drought severity, ecosystem carbon sink-source cycling, crop yield estimation as well as many other applications. This increased demand for soil moisture data has led to the development of various techniques to quantify soil moisture. Although destructive in nature, time-consuming and temporally limited, the thermogravimetric method remains important in calibrating indirect methods of measuring soil moisture (Walker et al., 2004; Robinson et al., 2008). One indirect method is the Frequency Domain Reflectometry (FDR) which uses the electrical properties of a medium at a specific frequency to determine the dielectric constant of the medium. In the soil, the electrical capacitance is formed by using embedded rods to propagate electrical signals and the soil as a dielectric (Lukanu and Savage, 2006). The dielectric constant is then related to the volumetric water content of the soil (Topp et al., 1980) based on the difference in dielectric constant of water (about 80 at ambient temperature) and soil mineral particles (between 4-8). Thus, the dielectric constant of soil increases with increasing soil wetness.

The Stevens Hydra Probe® is a FDR sensor which has been widely used to measure soil moisture. The Soil Climate Analysis Network of the Natural Resource Conservation Service uses the Hydra probe to monitor soil moisture in the United States (Cosh et al., 2004; Seyfried et al., 2005). The probe outputs a number of parameters including soil temperature, real and imaginary electrical conductivities as well as real and imaginary dielectric constants (The Hydra Probe® Soil Sensor, 2008). Using the Hydra probe to measure soil moisture, Verma and Kelleners (2012) evaluated depth-wise carbon dioxide (CO_2) production and flux in a rangeland soil and quantified the control of soil temperature and moisture on soil CO_2 production. Jabro et al. (2014) studied soil compaction under repeated freeze-thaw cycles as well as under unfrozen soil conditions in a clay loam soil using the Hydra probes. Similarly, Van Klaveren and McCool (2010) used the Hydra probe in studying the effects of freeze-thaw and water tension on soil detachment by determining erodibility and critical shear coefficients.

Several published studies have evaluated the accuracy of the Hydra probe in determining volumetric soil moisture using the real dielectric (Bosch, 2004; Seyfried et al., 2005; Kelleners and Verma, 2010; Logsdon et al., 2010; Vaz et al., 2013). Many of these studies concluded that accuracy is enhanced with soil specific calibrations and that the sensor's default calibration may suffice in coarse and medium textured soils but not in fine textured soil. For heavy clay soils, *in situ* calibration is necessary. In an experiment that compared the electrical response of water in four different types of clay and silty clay soils measured from 30 MHz to 3 GHz, Saarenketo (1998) observed that there was an orderly arrangement of water molecules around the soil particles comprised of Kaolinitic clay with a low cation exchange capacity (CEC) of 3.2 meq/100g and that the dielectric

values of the bound water layers were almost independent of measurement frequency. However, as the CEC increased, such as the Beaumont clay with CEC of 38.2 meq/100g, the author noted that the molecular structure of the bound water layers is disturbed, leading to high dielectric dispersion and increasing imaginary permittivity. In the preceding chapter, five soil moisture sensors in vertisolic, heavy clay soils with CEC >40 meq/100g were compared and the result showed that the Hydra probe default calibration yielded a root mean squared error of 0.129 m^3 m^{-3}. However, using a calibration developed *in situ*, the error was reduced to 0.014 m^3 m^{-3}. This underscored the importance of conducting calibration when establishing a soil moisture network with this sensor.

In Canada, Agriculture and Agri-Food Canada (AAFC) installed two *in situ* soil moisture monitoring networks- one in western Canada (Manitoba) and a second in the eastern part of the country (Ontario). AAFC also added four monitoring stations to an existing network in Saskatchewan, operated by Environment Canada and the University of Guelph. The stations record meteorological conditions (precipitation, air temperature, relative humidity, wind speed and wind direction), and are outfitted with Hydra probe soil moisture sensors. The network is known as the Real-time *In situ* Monitoring for Agriculture (RISMA). Manitoba-RISMA was established in 2012 and comprised of nine stations around the Carman-Elm Creek area which is within the Red River Basin in south-central Manitoba. The network was established to provide near-real time information on soil moisture conditions in an agricultural area prone to both drought and excess moisture risks, and to provide a data set that can be used holistically with remotely-sensed and modelled data products for calibration and validation of agronomic,

hydrologic and climate models (McNairn et al., 2015). This region is ideal for a soil moisture sensor network because of the economic importance of crop production in this area, the vulnerability of the watershed to moisture extremes as well as the opportunity to build on existing research activities. In addition, the Red River is a trans-boundary basin which stretches across the Canada-U.S. boundary facilitating bilateral research collaboration (Walker, 2012). In this study, we discuss the design of the soil moisture network and, more importantly, the calibration of Hydra probes and their evaluation at other locations outside the network.

3.3   Materials and Methods

3.3.1   Site Description

The RISMA soil moisture network in Manitoba consists of nine *in situ* monitoring stations distributed to be proportionally representative of different soil textural classes within a texturally-diverse agricultural region with comparative climatic and management conditions (Figure 3.1). The dominant land use in this area is agricultural crop production and the network extends about 29 km north-south by 5 km east-west. The geographical coordinates of the southernmost and northernmost fields, MB 2 and MB 8, are 49°29'33" N, 97°56'02" W and 49°45'11" N, 97°59'01" W, respectively. There is a distinct and abrupt textural difference with stations on the east side (stations labelled MB 2, 3, 5, 6 and 8) located on medium to fine textured soils developed on Glacial Lake Agassiz (glaciolaustrine) sediments of the Red River Valley. Stations on the west side (MB 1, 4, 7

and 9) are located on coarse textured soils developed on lacustrine beach deposits of the Lower Assiniboine Delta.
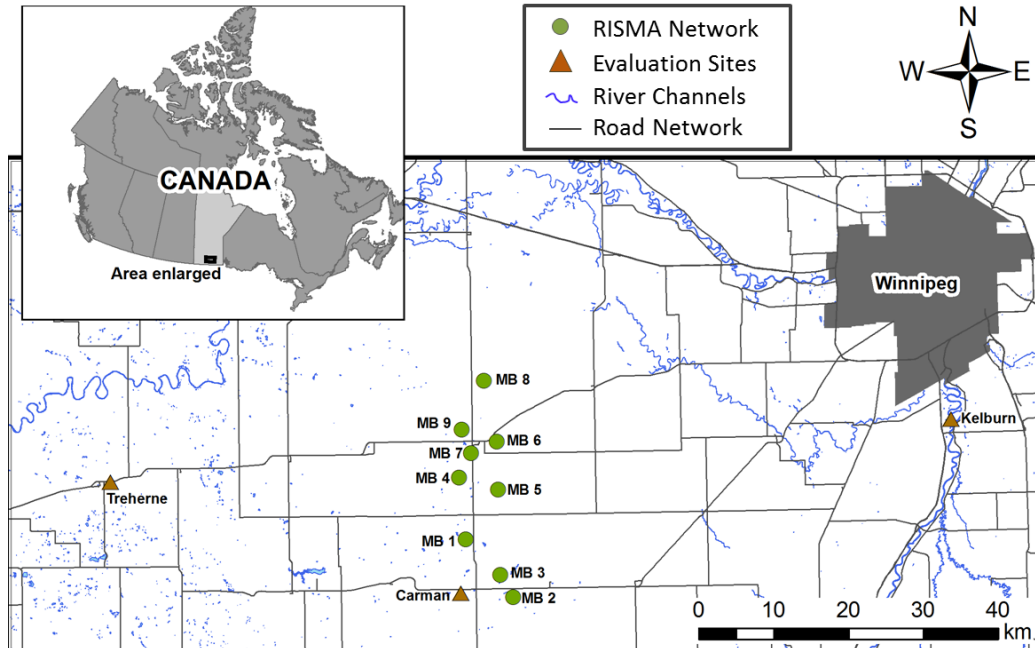
Figure 3.1   Location of RISMA network and evaluation sites.

Table 3.1 gives detailed textural composition, bulk density and the CEC of each station. All the stations are situated on agricultural fields and expectedly, the soil bulk density at the surface was lower than at depth at all the sites except at MB 5. Coarse textured soils were associated with high bulk density but low CEC. CEC tends to increase with increasing clay content. MB 6 and 8 were distinctly heavy clay soils with about 70% clay content and CEC values around 35 meq/100g. These locations experience frequent shrinking and swelling during the dry-wet cycles due to the presence of smectite clays.

Sites MB 1, 4, 7 and 9 are less reactive with CEC less than 15 meq/100g and clay content typically less than 14%. The pH values at all the sites except at MB 4 were

between 7.0 and 8.5 (data on pH not shown). MB 4 had slightly acidic soil with a pH of 5.0 in the top 20 cm layer. At lower depths, the soil had neutral pH of about 7.5.

MB 2 and 3 are medium textured soils with CEC about 21 meq/100g in the top 20 cm layer. These two sites tend to show characteristics associated with Solonetzic soils rather than the Chernozemic soils predominant in the area. In Chernozemic soils, the ratio of exchangeable calcium (Ca^{2+}) to exchangeable sodium (Na^+) is usually > 20. However, at MB 2 and 3, the ratios of the cations were 2 and 7 respectively in the top 20 cm layer. The high sodium content at these sites could have been due to the deposition of salts from groundwater when the water was close to the surface and subsequently lost by evaporation or plant uptake. The deposited salts may bind with the fine clay particles to create an impermeable, concrete-like surface that restricts water penetration. This impervious layer was observed at the two sites, especially at MB 2 and often led to the insensitivity of installed soil moisture instruments to rainfall events. Thus, the nine sites in the network provided adequate representation of the varying degree of soil textural class and ionic activity within the watershed.

Table 3.1 Physical properties of soils within the soil moisture network.

Station	Crop (2013)	Depth (cm)	Density (g/cm^3)	CEC[†] (meq/100g)	Texture (%) Sand – Silt - Clay
MB 1	Corn	5	1.28	8.37	79-10-11
		20	1.56	8.50	80-08-12
		50	1.54	8.94	82-08-10
		100	1.57	5.14	81-07-12
MB 2	Corn	5	1.35	24.3	45-21-34
		20	1.63	21.5	63-13-24
		50	1.63	12.2	66-13-21
		100	1.57	6.02	75-15-10
MB 3	Soybean	5	1.47	21.0	47-21-32
		20	1.52	21.9	46-21-33
		50	1.44	19.4	31-24-45
		100	1.41	15.8	70-18-12
MB 4	Soybean	5	1.33	5.14	90-01-09
		20	1.50	6.02	88-02-10
		50	1.60	6.50	88-02-10
		100	1.58	4.43	86-05-09
MB 5	Corn	5	1.46	22.9	41-18-41
		20	1.41	20.3	23-19-58
		50	1.33	25.5	04-27-69
		100	1.32	25.8	03-28-69
MB 6	Soybean	5	1.21	41.0	04-24-72
		20	1.39	36.3	04-21-75
		50	1.31	32.2	02-26-72
		100	1.31	30.9	01-27-72
MB 7	Corn	5	1.40	12.2	78-09-13
		20	1.59	12.4	82-06-12
		50	1.57	12.6	78-09-13
		100	1.58	5.36	80-08-12
MB 8	Soybean	5	1.22	40.7	04-33-63
		20	1.38	39.7	03-23-74
		50	1.38	37.6	04-23-73
		100	1.50	35.6	01-28-71
MB 9	Oat	5	1.53	9.34	81-06-13
		20	1.60	10.3	86-03-11
		50	1.53	12.8	83-05-12
		100	1.58	9.31	87-07-06

[†]CEC = Cation Exchange Capacity

In order to evaluate the calibration equations at different locations, data were collected from three sites that showed some physical and chemical similarities with sites within the network (Figure 3.1). Evaluating the calibration equations at other sites outside the network acted as an independent test for the reliability of the overall field calibration equation developed from the sites within the network. Table 3.2 provides some details of the evaluation sites. The Treherne site is a Rego Humic Gleysol developed on poorly drained fine loamy lacustrine sediment. The location was native grassland and the CEC is comparable to the < 15 meq/100g, coarse textured sites MB 1, 4, 7 and 9. The Carman site consists of an Orthic Black Chernozem, non-eroded, non-stony soil with high natural fertility. The medium textural classification and CEC between 15 – 30 meq/100g is comparable to MB 2, 3 and 5 (except at 50 cm depth at MB 2). The Kelburn site is a heavy clay soil consisting of a poorly drained Rego Humic Gleysol with high available water holding capacity. The fine texture and CEC > 30 meq/100g at this site is similar to MB 6 and 8. This classification was used in developing CEC-based calibrations.

Table 3.2 Physical properties of soils at the evaluation sites.

Station	Crop (2013)	Depth (cm)	CEC[†] (meq/100g)	Texture (%) Sand – Silt - Clay
Treherne	Native Grass	5	12.9	75-13-12
		20	12.8	67-18-15
		50	17.2	57-27-16
		100	nd[‡]	51-26-23
Carman	Alfalfa	5	22.8	41-24-35
		20	24.3	31-25-44
		50	20.9	19-31-50
		100	nd	19-36-45
Kelburn	Wheat	5	35.0	06-31-63
		20	35.6	06-33-61
		50	47.0	04-29-67
		100	nd	03-31-66

[†]CEC = Cation Exchange Capacity

[‡]nd= not determined.

3.3.2   Network Design

At each of the nine locations, a weather station is located at the edge of the field powered by solar panels and batteries. These stations collect rainfall, wind speed, wind direction, air temperature and humidity data at fifteen-minute intervals. Soil moisture sensors were installed about 10-20 m from the weather station to ensure ease of access to the location while limiting field edge effects on soil moisture. A soil pit about 1.0 m wide and 1.2 m deep was dug and Stevens Hydra probes were installed horizontally in triplicates at 5, 20, 50 and 100 cm. This redundancy was implemented to ensure sensor data would continue to be captured in the event of sensor failure, and to provide an indication of within-site variability in moisture conditions. Three additional probes were installed vertically at the surface to capture integrated surface soil moisture over a 6 cm

depth. Similar to the weather stations, the Hydra probe variables are collected in fifteen-minute intervals and include soil volumetric water content (using Stevens default dielectric conversion model), soil temperature in degree Celsius, soil real dielectric permittivity and soil conductivity.

During installation, firm contact between the probes and the soil was ensured. Soil core samples were collected at the location of each probe installation and preserved for a soil moisture dry-down calibration procedure in the laboratory as well as for soil texture and bulk density analysis. In order to ensure that similar vegetation and micro-climatic conditions were maintained between the location of the installed probes and the rest of the field, the areas around the probes were hand-seeded close to the time farmers' planting operations were carried out.

3.3.3   The Hydra Probe

The Hydra Probe® Soil Sensor from Stevens Water Monitoring Systems has four 0.3 cm diameter stainless steel tines which are 5.7 cm long. The arrangement is such that three tines in equi-triangular position with a 3.0 cm diameter surround a central tine. A 50-MHz signal is generated from a 4.2 cm diameter cylindrical head and the signal is transmitted to the tines. The cylindrical measurement region or sensing volume is the soil between the tines. The tine assembly is often referred to as the wave guide and the probe signal is the average of that from the soil in the sensing volume (Seyfried and Murdock, 2004; The Hydra Probe® Soil Sensor, 2008).

3.3.4 Calibration Procedure

3.3.4.1 Laboratory Calibration. During site preparation, three core samples 5.1 cm in internal diameter and 10.2 cm in length were taken at each depth of interest (5 cm, 20 cm, 50 cm and 100 cm) and used for a soil moisture dry-down calibration in the laboratory. Each sample was uniformly saturated using reverse-osmotic water and a probe was inserted. Analysis for inter-sensor variability was conducted by inserting the Hydra probes close to each other in a container of moist soil to determine differences in soil moisture that may arise due to the use of multiple sensors. Sensor-to-sensor variability was found to be negligible. This is similar to Seyfried and Murdock (2004) who observed that the precision of the Hydra Probe sensor in fluid had $< 1\%$ coefficient of variation and inter-sensor variability was low. Each probe was weighed (W_P) before being inserted in the wet soil and thereafter, a total weight (W_T, wet soil + probe) was determined. The probe was attached to a data logger that monitored and recorded soil moisture, temperature, real dielectric and electrical conductivity every five minutes. To monitor the evaporative soil moisture loss, total weight was determined every 24 hours at the early stage of the experiment and $48 - 72$ hours at the later drying stages. The oven dry weight (W_D) was determined after significant drying has ceased, usually after $12 - 22$ days depending on the soil texture. This experiment was conducted at temperatures ranging from 17 °C to 22 °C and the observed soil moisture on day i is given as:

$$\theta = \left(\frac{\rho_{b*} \left(W_{T_i} - W_P - W_D \right) / W_D}{\rho_w} \right) \qquad [3.1]$$

where θ is the volumetric water content, ρ_b is the soil bulk density and ρ_w is the density of water. $\left(W_{T_i} - W_P - W_D \right) / W_D$ is the gravimetric water content.

Calibration equations were developed by relating the real dielectric (ε_r) from the Hydra probe at the time of weighing to the observed soil moisture. Two relationship forms have been used in several publications (Bosch, 2004; Seyfried et al., 2005; Kelleners and Verma, 2010; Logsdon et al., 2010; Vaz et al., 2013; Rowlandson et al., 2013) and were investigated as shown in equations 3.2 and 3.3. A, B, C and D are coefficients determined empirically.

$$\theta = A\varepsilon_r^{1/2} + B \qquad\qquad [3.2]$$

$$\theta = A + B\varepsilon_r + C\varepsilon_r^2 + D\varepsilon_r^3 \qquad\qquad [3.3]$$

3.3.4.2   Field Calibration.   After soil sensor installation, two core samples 7 cm in length and 7.2 cm in internal diameter were taken within 2 m of the installed probes. Two samples were taken nine times at each location during the 2013 cropping season at about 1 – 8 cm, 16 – 23 cm and 46 – 53 cm in depth to calibrate probes installed at 5 cm, 20 cm and 50 cm respectively. *In situ* calibration was not conducted for probes installed at 100 cm partly because of the similarity in CEC and soil texture observed at 50 and 100 cm at most sites (except for MB 2, 3 and 7) and partly due to the relatively large digging area required for sampling at 100 cm which could lead to the disturbance of the installed probes. A similar Hydra probe to the ones installed was used to take soil moisture, temperature, real dielectric and conductivity data of the extracted soil samples before the samples were weighed and oven dried for at least 24 hours at 105 °C to determine the gravimetric water content. Volumetric water content was determined by multiplying the gravimetric water content with the soil bulk density, divided by the density of water. Soil temperature during most of the sampling periods ranged between 15 and 30 °C. The effect of soil temperature was not considered in this calibration study. Calibration

equations were developed at each site using the same equations as for the laboratory calibration earlier discussed (equations 3.2 and 3.3).

3.3.5 Data Analysis

Statistical indicators used to compare the default, laboratory and field calibrations included the coefficient of determination (r^2), the root mean square error (RMSE), the normalized root mean square error (NRMSE) and the mean bias error (MBE).

$$\text{RMSE} = \left(\frac{\Sigma(D_i - Obs_i)^2}{n}\right)^{0.5} \qquad\qquad [3.4]$$

$$NRMSE = \frac{1}{Obs}\sqrt{\frac{\Sigma(D_i - Obs_i)^2}{n}}\,100 \qquad\qquad [3.5]$$

$$MBE = \frac{1}{n}[\Sigma_{i=1}^{N}(D_i - Obs_i)] \qquad\qquad [3.6]$$

where D is the Hydra probe soil moisture value from either the default, field or laboratory calibrations and Obs is the observed soil moisture value on day i. Depth-specific calibration was not reported due to the limited number of samples obtained for field calibration at each depth (n < 20) as well as the limited range of soil water content especially at the 50 cm depth. Outliers were not included in the dataset and defined as samples that showed unrealistically high dielectric (> 70) which could be due to dissolved ions from reactive clay. This was observed mostly in the field data at the 20 and 50 cm depths at MB 6.

3.4 Results and Discussion

3.4.1 Laboratory Calibration

Although both calibration equations [3.2] and [3.3] have been used in several publications, no significant difference was found in the coefficient of determination using either equation. This was determined by conducting a test of the equality of two dependent correlation coefficients with one variable in common (Steiger, 1980). Therefore, to simplify the analysis, the square root values of the real dielectric constant were used. Also, instead of using the third order polynomial, quadratic equations were found to suffice at locations that showed a non-linear relationship (Figure 3.2). Table 3.3 lists the r^2 statistics and derived calibration equations for each site and all sites combined. Sites MB 6 and 8 had the greatest scatter and lowest r^2 of 0.85 and 0.92 respectively. All the other sites had r^2 values >0.95. The lower r^2 values corresponded with the locations with higher clay content and CEC.

Table 3.3 The laboratory calibration equations developed for each location.

Station	n	r^2	Equation[†]
MB 1	132	0.98	$\theta = 0.1127\varepsilon_r^{0.5} - 0.2025$
MB 2	124	0.95	$\theta = 9.779*10^{-3}\varepsilon_r + 2.7476*10^{-2}\varepsilon_r^{0.5} - 7.289*10^{-2}$
MB 3[††]	70	0.98	$\theta = 1.899*10^{-2}\varepsilon_r - 6.1939*10^{-2}\varepsilon_r^{0.5} + 9.876*10^{-2}$
MB 4	132	0.96	$\theta = 1.085*10^{-2}\varepsilon_r - 1.2122*10^{-2}\varepsilon_r^{0.5} + 3.082*10^{-2}$
MB 5	104	0.98	$\theta = 9.207*10^{-3}\varepsilon_r + 4.962*10^{-2}\varepsilon_r^{0.5} - 1.039*10^{-1}$
MB 6	109	0.85	$\theta = 6.090*10^{-3}\varepsilon_r + 2.0246*10^{-2}\varepsilon_r^{0.5} + 9.746*10^{-3}$
MB 7	132	0.99	$\theta = 0.1084\varepsilon_r^{0.5} - 0.1949$
MB 8	127	0.92	$\theta = 8.066*10^{-3}\varepsilon_r + 8.76*10^{-4}\varepsilon_r^{0.5} + 3.9367*10^{-2}$
MB 9	115	0.98	$\theta = 0.1131\varepsilon_r^{0.5} - 0.2116$
All Sites	1045	0.89	$\theta = 0.0870\varepsilon_r^{0.5} - 0.1425$

[†] θ is the volumetric soil moisture content and ε_r is the real dielectric.

[††] Data for the 100 cm depth not included due to large variation in the soil water content of replicates.
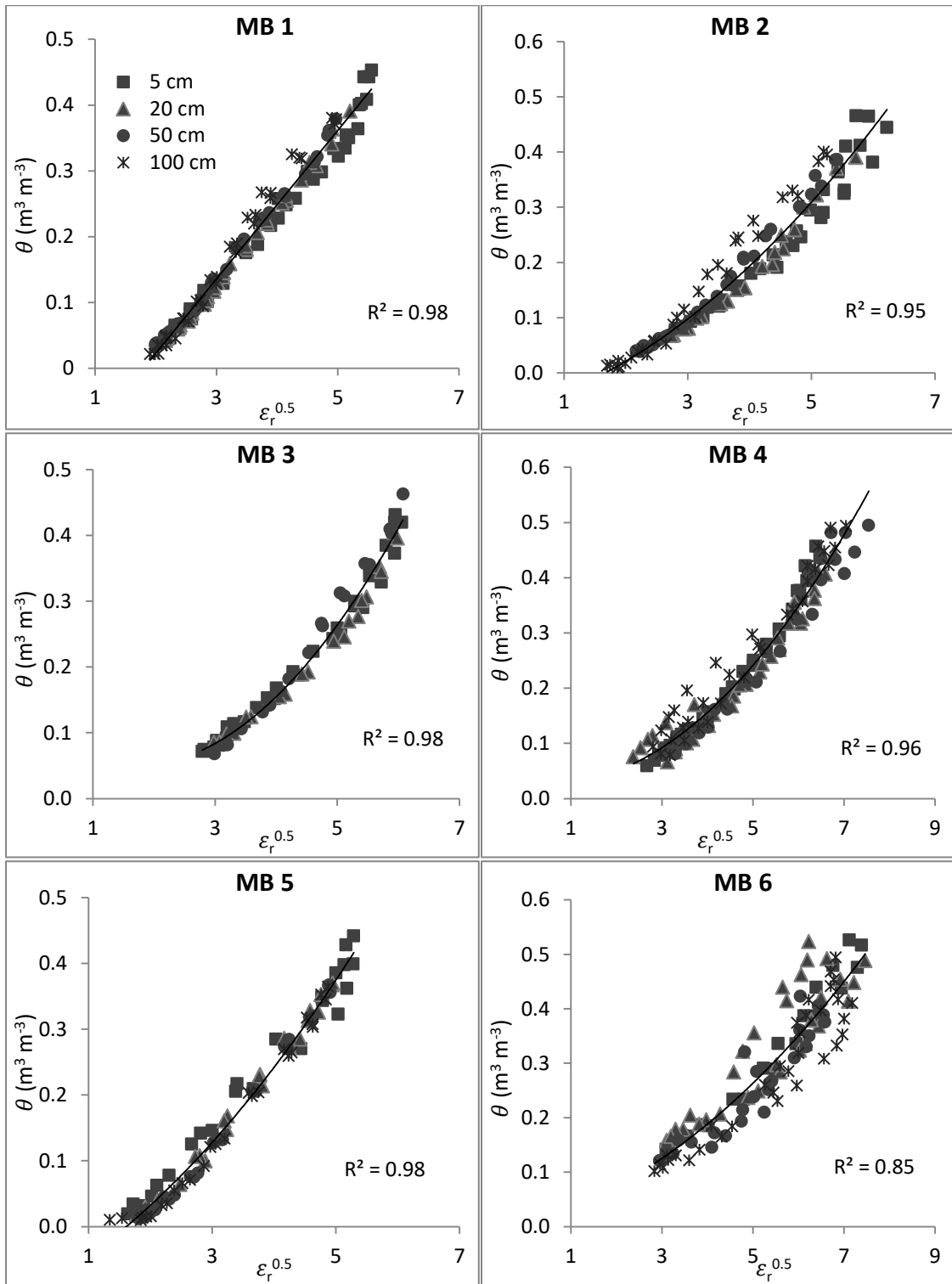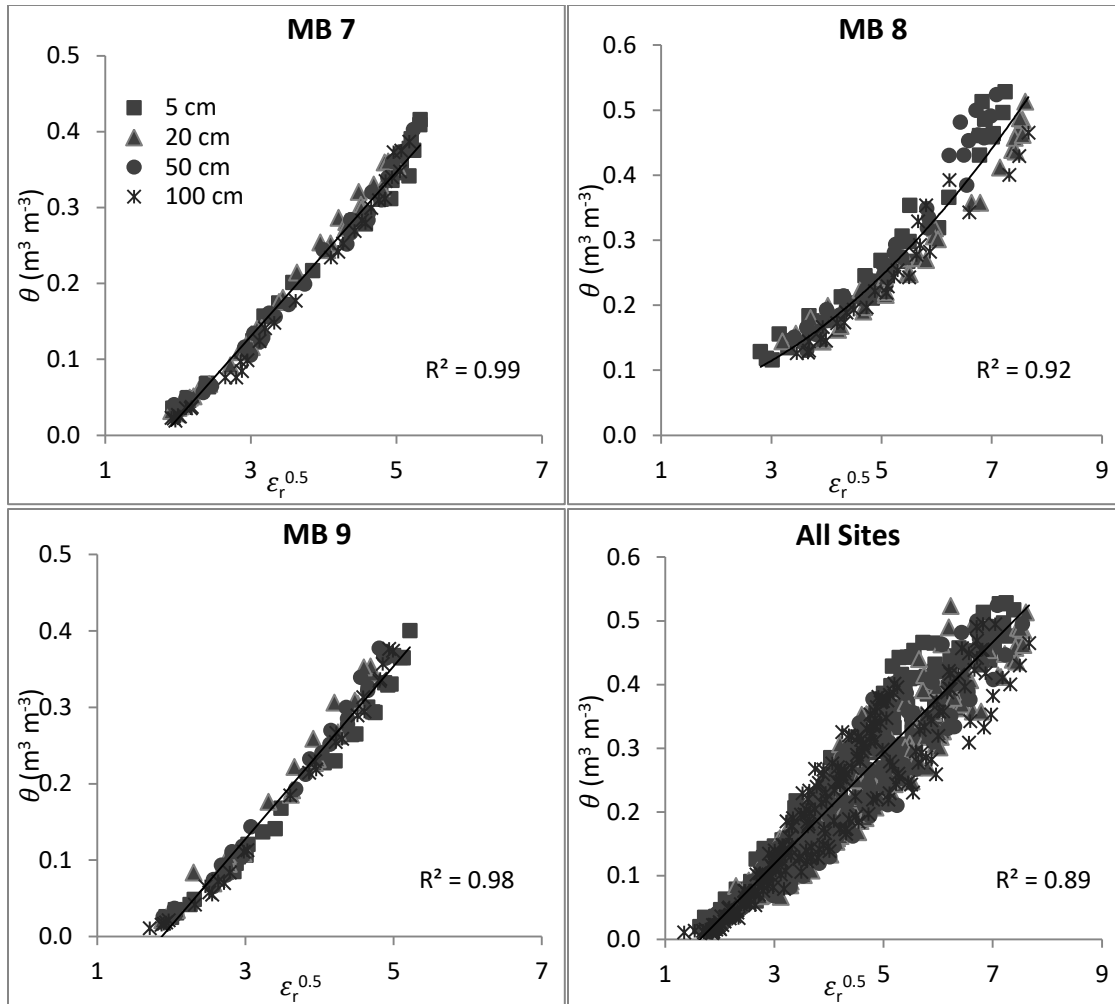
Figure 3.2   Data points for the laboratory calibration at MB 1-9 and all sites combined, showing the relationship between observed moisture content (y-axis, $m^3 \ m^{-3}$) and the square root of the real dielectric constant (x-axis, no unit). Note that the scale of the axes varies from image to image.

The trend line at the 100 cm depth at MB 2, 4 and 6 appeared to be different from the other depths; therefore a depth-specific calibration for 100 cm at these locations may improve soil moisture estimation. The results at 100 cm for MB 3 were not included in the analysis because they showed unreasonably high variability. Also, $\varepsilon_r > 80$ were recorded at MB 6 and those data points were not used in the analysis. The overall laboratory calibration equation [3.7] developed using the data from all nine locations (n=

1045) had an r^2 value of 0.89 with soil moisture content ranging between 0.01 – 0.54 m^3 m^{-3}.

$$\theta = 0.087\varepsilon_r^{0.5} - 0.1425 \hspace{3cm} [3.7]$$

3.4.2 Field Calibration

All the nine sites showed a linear relationship between the square root of the real dielectric, $\varepsilon_r^{0.5}$ and the observed soil moisture, θ (Figure 3.3). Similar to the laboratory calibration, $\varepsilon_r > 80$ were recorded at MB 6 and these data points were not used in the analysis. The lowest r^2 value of 0.60 was obtained at MB 8 (Table 3.4) and this could be due to the greater scatter within a narrow range of soil moisture content at this location. The soil moisture content used for calibration at MB 8 ranged from 0.31 m^3 m^{-3} to 0.50 m^3 m^{-3}. This result was different from the higher r^2 of 0.84 obtained at MB 6. Although both fields have similar textural classification and CEC values, the calibration equation developed at MB 6 had a wider range of soil moisture between 0.22 – 0.52 m^3 m^{-3}. The difficulty in obtaining the desired range of water content was listed by Robinson (2001) as one of the main challenges in developing field calibration. At the coarse textured locations (MB 1, 4, 7 and 9), the r^2 values were > 0.90 except at MB 9 which demonstrated that depth-specific calibration, especially at 50 cm depth, may be important at this location.
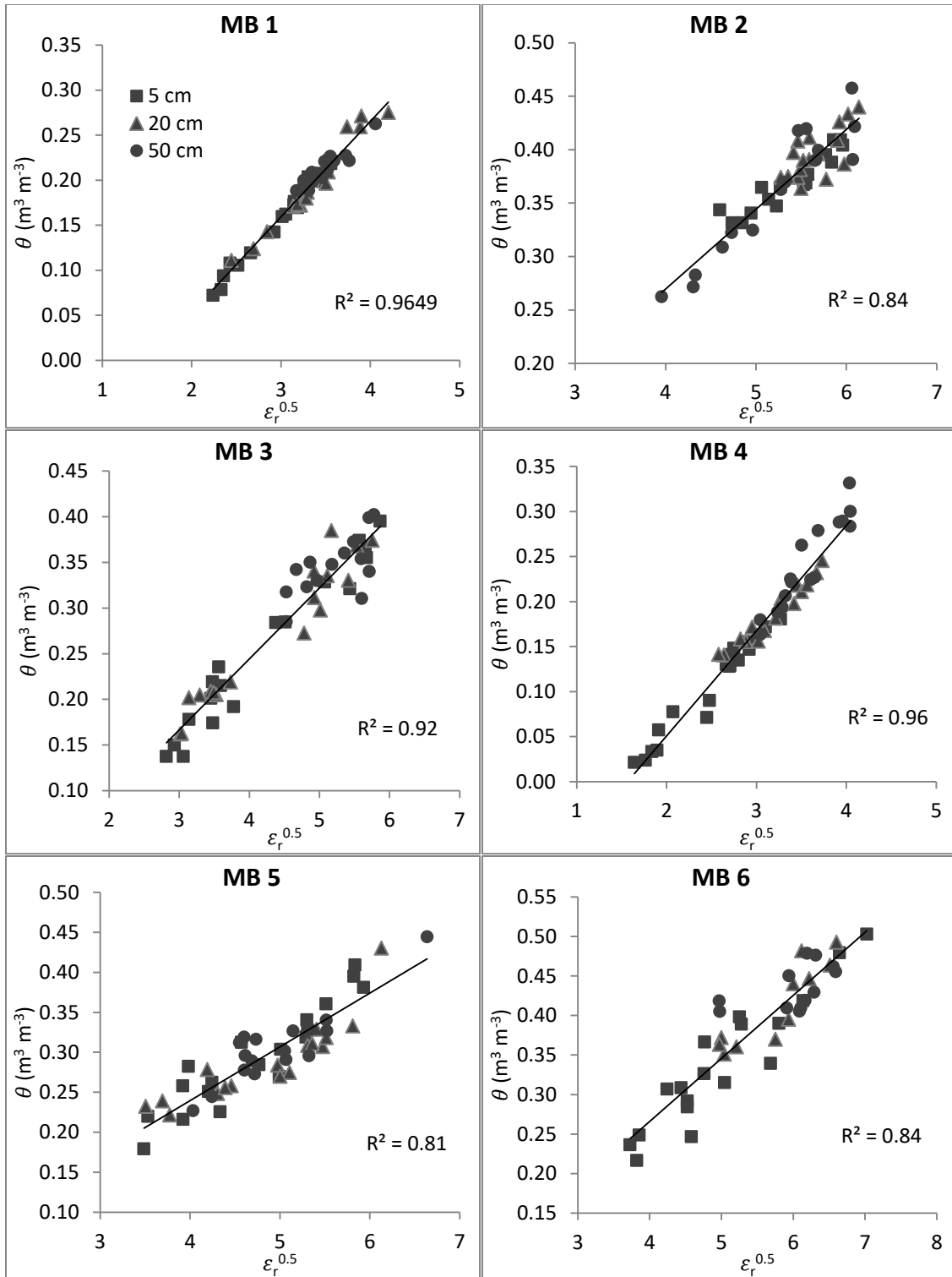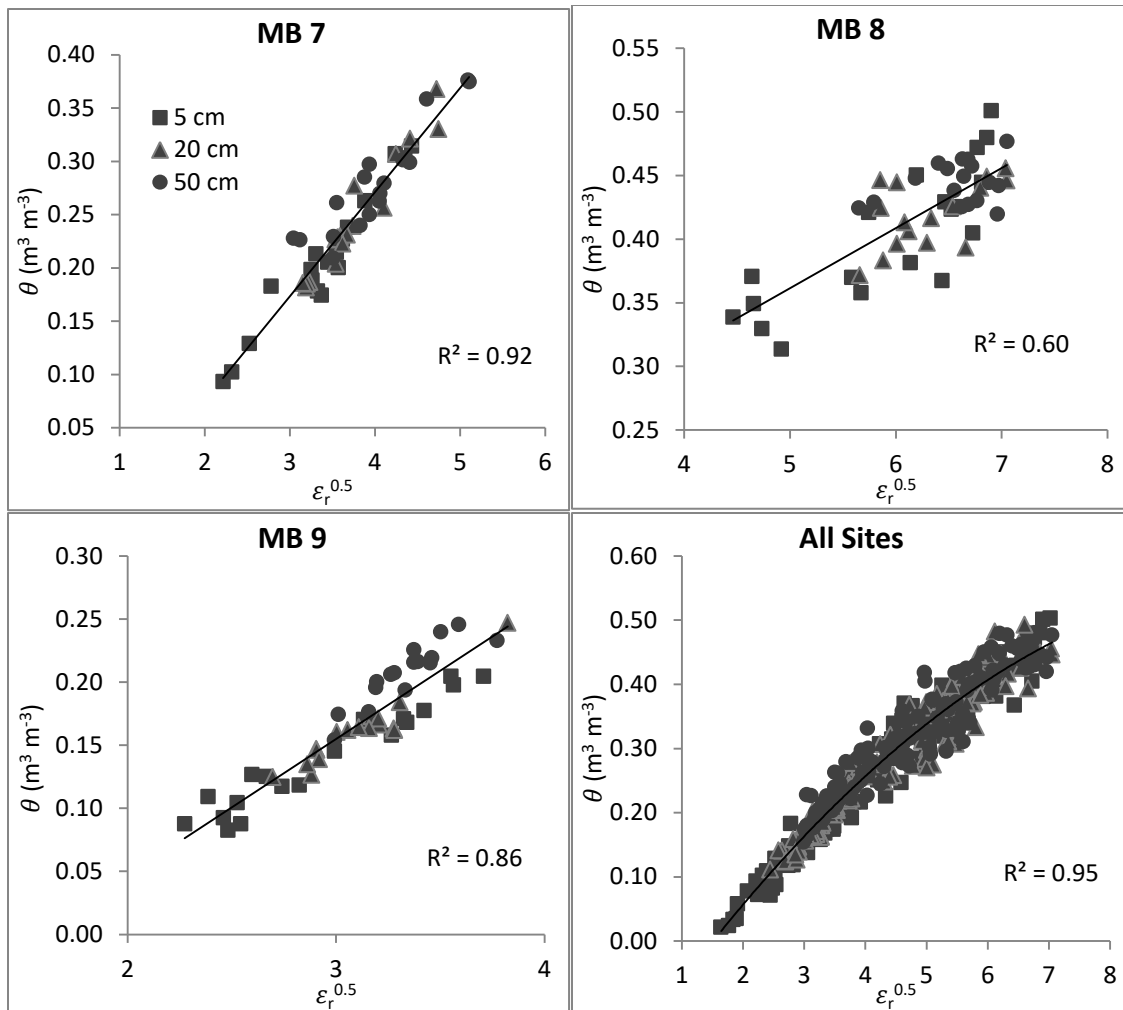
Figure 3.3   Data points for the field calibration at MB 1-9 and all sites combined, showing the relationship between observed moisture content (y-axis, m^3 m^{-3}) and the square root of the real dielectric constant (x-axis, no unit). Note that the scale of the axes varies from image to image.

The r^2 value of the field calibration equation [3.8] developed from the data points at all nine locations was 0.95, which is greater than the r^2 of 0.89 for the laboratory calibration at all sites. The contrary was expected based on the relatively controlled environment provided in the laboratory compared to the field. The soil moisture values used in developing the overall field calibration equation ranged between 0.02 – 0.52 m^3

m^{-3}. Linear equations sufficed at the individual stations, however, when data points from all the sites were combined, a second order function was a better fit for the data trend.

$$\theta = -0.006301\varepsilon_r + 0.1379\varepsilon_r^{0.5} - 0.1937 \qquad [3.8]$$
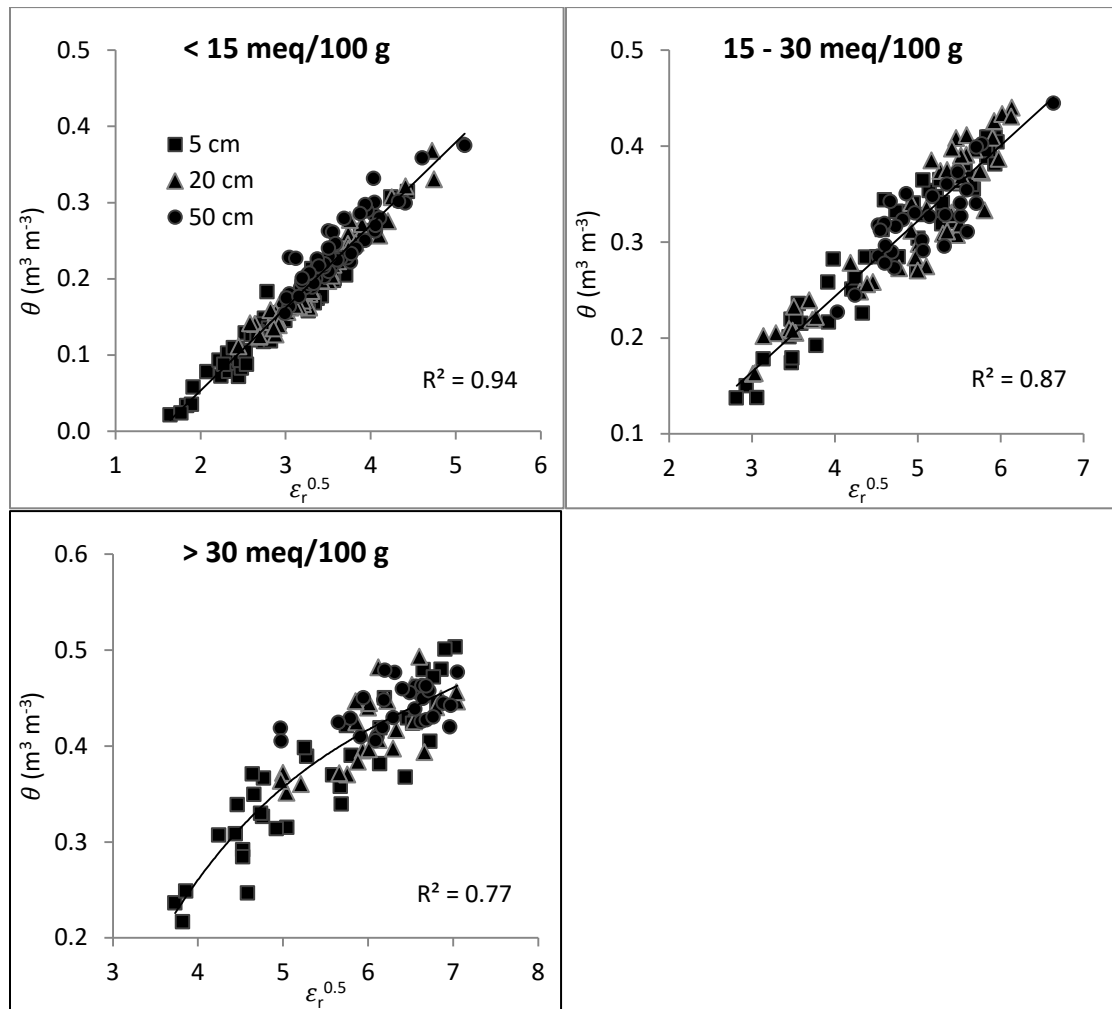
Figure 3.4   Data points for the field calibration based on sites with CEC < 15 meq/100 g, 15-30 meq/100 g and > 30 meq/ 100 g. Note that the scale of the axes varies from image to image.

Data from sites MB 1, 4, 7 and 9 were combined to develop a calibration equation that represents sites with low CEC (< 15 meq/100 g). The linear relationship between $\varepsilon_r^{0.5}$

and θ (Figure 3.4) had an r^2 of 0.94. MB 2, 3 and 5 sites had medium CEC between 15 –

30 meq/100 g. The calibration equation developed using data from these three sites,

excluding 50 cm depth at MB2, had an r^2 of 0.87 (Table 3.5). The high CEC sites, MB 6

and 8 had > 30 meq/ 100 g showed a non-linear relationship with an r^2 of 0.77. As the

CEC increased in the three categories, the r^2 of the calibration equation decreased.

Table 3.4 The *in situ* calibration equations developed for each location.

Station	n	r^2	Equation[†]
MB 1	51	0.96	$\theta = 0.1059\varepsilon_r^{0.5} - 0.1582$
MB 2	48	0.84	$\theta = 0.0748\varepsilon_r^{0.5} - 0.0299$
MB 3	50	0.92	$\theta = 0.0776\varepsilon_r^{0.5} - 0.0660$
MB 4	53	0.96	$\theta = 0.1169\varepsilon_r^{0.5} - 0.1831$
MB 5	53	0.81	$\theta = 0.0672\varepsilon_r^{0.5} - 0.0294$
MB 6	41	0.84	$\theta = 0.0797\varepsilon_r^{0.5} - 0.0530$
MB 7	53	0.92	$\theta = 0.0978\varepsilon_r^{0.5} - 0.1200$
MB 8	52	0.60	$\theta = 0.0473\varepsilon_r^{0.5} + 0.1247$
MB 9	52	0.86	$\theta = 0.1086\varepsilon_r^{0.5} - 0.1707$
All Sites	453	0.95	$\theta = -6.301*10^{-3}\varepsilon_r + 1.379*10^{-1}\varepsilon_r^{0.5} - 1.937*10^{-1}$

[†] θ is the volumetric soil moisture content and ε_r is the real dielectric.

Table 3.5 Field calibration equations based on CEC categories.

CEC Category (meq/ 100g)	Sites	n	R^2	Equation[†]
CEC < 15	1, 4, 7 and 9	209	0.94	$\theta = 0.1084\varepsilon_r^{0.5} - 0.1633$
CEC 15 – 30	2, 3 and 5[‡]	136	0.87	$\theta = 0.0786\varepsilon_r^{0.5} - 0.0714$
CEC > 30	6 and 8	93	0.77	$\theta = 3.32*10^{-3}\varepsilon_r^{1.5} - 6.784*10^{-2}\varepsilon_r + 5.047*10^{-1}\varepsilon_r^{0.5} - 8.85*10^{-1}$

[†] θ is the volumetric soil moisture content and ε_r is the real dielectric.

[‡] Data at the 50 cm depth at MB 2 was omitted because the CEC at that depth does not fall within this category.

3.4.3 Evaluating Calibration Equations

Three sites (Trehrene, Carman and Kelburn) were used to evaluate and compare seven different calibration equations as follows:

(i)   The loam default calibration equation [3.9] was used at the Treherne and Carman sites while the default clay calibration equation [3.10] was used at the Kelburn site as suggested by the manufacturer (Bellingham, 2007);

(ii)   *In situ* calibration equations were developed at each of the three sites using the procedure described earlier under the field calibration section;

(iii)   The overall laboratory equation [3.7];

(iv)   The overall field equation [3.8];

(v)   CEC-based calibration (Table 3.5). Low CEC calibration equation was used at the Treherne site; mid CEC at the Carman site and high CEC calibration at Kelburn;

(vi)   Topp et al. (1980) calibration equation [3.11];

(vii)   Logsdon et al. (2010) calibration equation [3.12].

$$\theta = 0.109\varepsilon_r^{0.5} - 0.179 \hspace{3cm} [3.9]$$

$$\theta = 0.000032414\varepsilon_r^{3} - 0.002464\varepsilon_r^{2} + 0.06553\varepsilon_r - 0.2093 \hspace{1cm} [3.10]$$

$$\theta = 0.0000043\varepsilon^{3} - 0.00055\varepsilon^{2} + 0.0292\varepsilon - 0.053 \hspace{1.5cm} [3.11]$$

$$\theta = 0.00000514\varepsilon^{3} - 0.00047\varepsilon^{2} + 0.0224\varepsilon \hspace{2cm} [3.12]$$

In this study, *in situ* calibration refers to use of the calibration equations developed at each of the three evaluation sites (Figure 3.5). The overall field calibration equation (or simply, field calibration) refers to equation 3.8 which was developed by combining all the data at all depths from the nine RISMA sites. Similar to this study, the

Logsdon et al. (2010) calibration equation was developed from soil samples taken at several states in the United States using 50 MHz Hydra Probe. However, the Topp et al. (1980) calibration equation was derived using Time Domain Reflectometry (TDR) technique at 1 GHz.
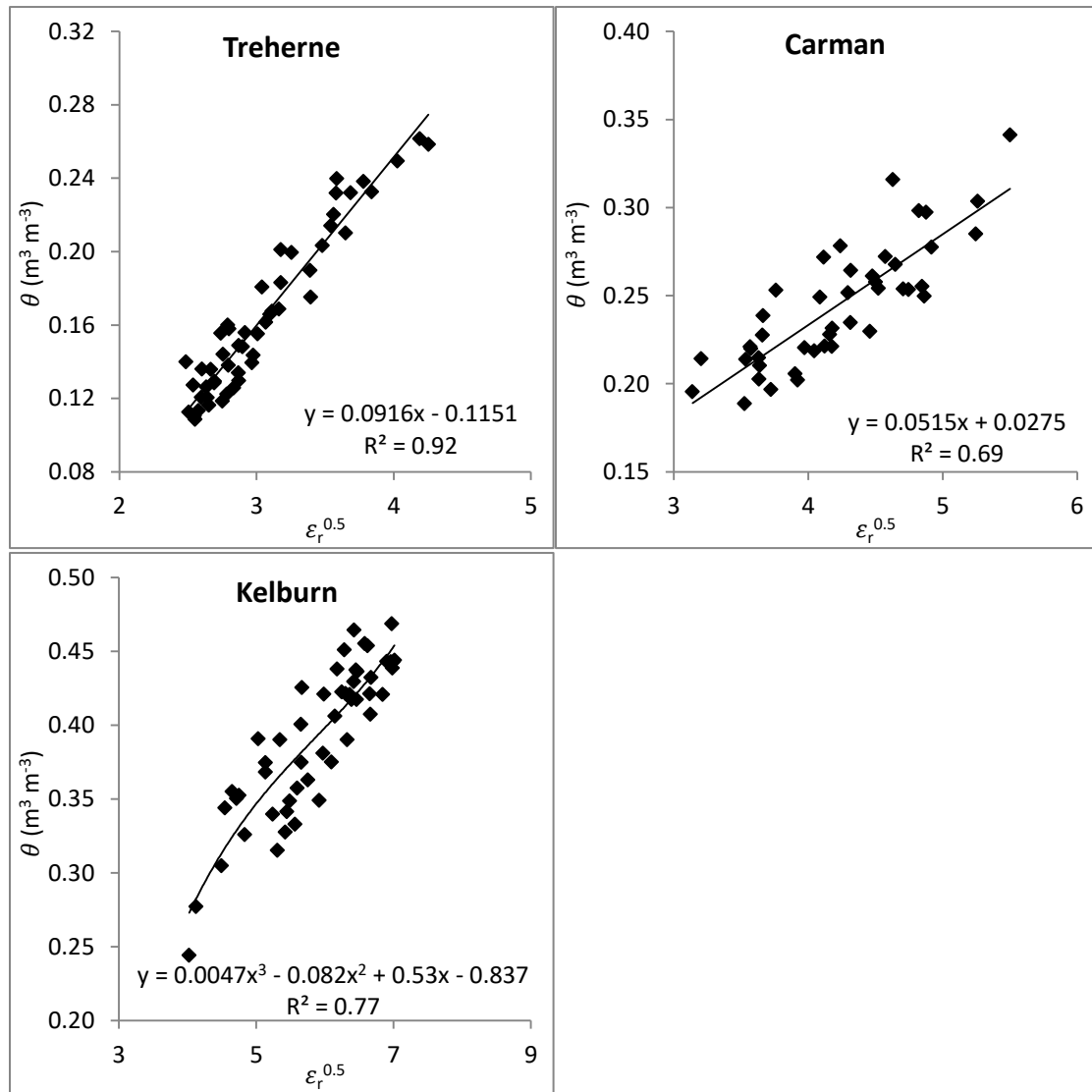
Figure 3.5   Data points for the *in situ* calibration of evaluation sites. Note that the scale of the axes varies from image to image.

Figure 3.6 shows an increased amount of scatter as the sites varied from coarse textured soil at Treherne to the fine textured site at Kelburn. At the Treherne location, all the tested calibration equations produced RMSE values less than 0.04 m^3 m^{-3}, except for the laboratory-developed equation which underestimated soil moisture by 0.042 m^3 m^{-3} (Table 3.6).
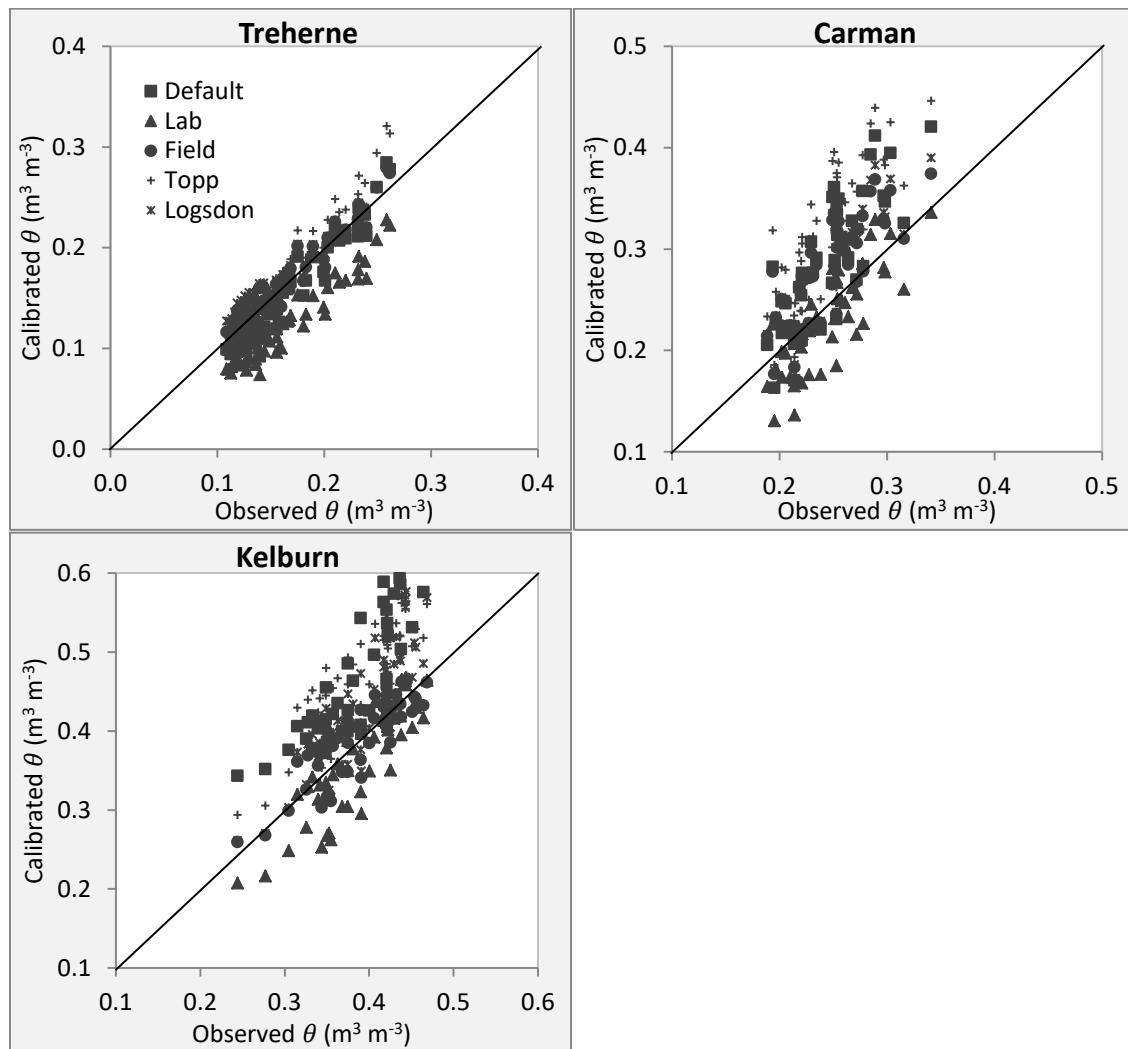
Figure 3.6   Comparison (1:1) between observed volumetric water content and volumetric water content determined by calibration at Treherne, Carman and Kelburn. Note that the scale of the axes varies from image to image.

In line with part of the goals of some satellite missions such as the Soil Moisture and Ocean Salinity (SMOS) and the Soil Moisture Active Passive (SMAP) to develop volumetric soil moisture products with an accuracy of 0.04 m^3 m^{-3} (Entekhabi et al., 2010; Kerr et al., 2010), the RMSE of the Hydra probe's loam default calibration was observed to be within the acceptable range. The *in situ*, field, low CEC and Logsdon calibrations showed little improvement to the default with a RMSE of 0.012 m^3 m^{-3}, 0.013 m^3 m^{-3}, 0.015 m^3 m^{-3} and 0.015 m^3 m^{-3} respectively compared to 0.018 m^3 m^{-3} from the default calibration. Therefore, developing *in situ* calibration may not be critical for low reactive, coarse textured soils.

At the Carman site, as expected, the *in situ* calibration produced the best statistics with a RMSE of 0.019 m^3 m^{-3}, followed by the mid-CEC calibration with a RMSE of 0.029 m^3 m^{-3}. Although the mid-CEC calibration is a subset of the data used in developing the overall field calibration, its performance at the Carman site, which is a mid-CEC soil, showed that it gave a better representation than the overall field calibration which had RMSE of 0.040 m^3 m^{-3}. The laboratory calibration was also better than the overall field calibration with RMSE and NRMSE values of 0.034 m^3 m^{-3} and 13.9% respectively. The Hydra probe loam default calibration equation overestimated soil moisture at the location by 0.036 m^3 m^{-3} and yielded a RMSE of 0.052 m^3 m^{-3}. Similar to the results obtained at the Treherne site, the field, mid-CEC and Logsdon calibrations were better than the default calibration. Topp's calibration was the least accurate with an overestimation of 0.069 m^3 m^{-3} and RMSE of 0.080 m^3 m^{-3}.

Table 3.6 Accuracy of different calibration equations at three evaluation sites

Validation Location	Calibration	RMSE ($m^3\ m^{-3}$)	NRMSE (%)	MBE ($m^3\ m^{-3}$)
Treherne (n=52)	Default	0.018	11.1	-0.011
	In situ	0.012	7.1	0.001
	Lab	0.043	26.3	-0.042
	Field	0.013	7.8	0.003
	Low CEC	0.015	9.1	0.003
	Topp	0.021	13.0	0.011
	Logsdon	0.015	8.9	0.008
Carman (n=44)	Default	0.052	21.2	0.036
	In situ	0.019	7.8	0
	Lab	0.034	13.9	-0.020
	Field	0.040	16.2	0.029
	Mid CEC	0.029	11.8	0.016
	Topp	0.080	32.6	0.069
	Logsdon	0.044	17.9	0.033
Kelburn (n=52)	Default	0.188	48.0	0.139
	In situ	0.025	6.5	0.007
	Lab	0.042	10.7	-0.022
	Field	0.026	6.7	0.004
	High CEC	0.027	7.0	0.011
	Topp	0.088	22.5	0.081
	Logsdon	0.065	16.5	0.044

The range of results obtained was highest at the heavy clay, high CEC site at Kelburn. The Hydra probe clay default calibration was the least accurate producing unrealistically high soil moisture at $\varepsilon_r > 45$ and overestimating soil moisture by 0.139 m^3 m^{-3} with an error of 0.188 m^3 m^{-3}. Out of the seven calibrations tested, the *in situ*, high CEC and overall field calibrations were within the <0.04 m^3 m^{-3} error threshold with RMSE values of 0.025 m^3 m^{-3}, 0.027 m^3 m^{-3} and 0.026 m^3 m^{-3} respectively.

For all the three evaluation sites, the laboratory-developed equation underestimated soil moisture which is in agreement with the findings of Logsdon (2009) who observed that under field conditions, the apparent permittivity was higher for similar water content than in the undisturbed columns in the laboratory taken from the same sites and depths. However, unlike Logsdon (2009), less scatter was found in the overall field calibration (Figure 3.3) than with the overall laboratory results (Figure 3.2). Both this study and Logsdon (2009) showed that laboratory calibrations are not always adaptable for use under field conditions.

The RMSE and MBE values for the Logsdon calibration were similar to the field calibration at the coarse and medium textured evaluation sites. A large difference was observed at the fine textured evaluation site (Kelburn) with the overall field calibration yielding RMSE of 0.026 m^3 m^{-3} compared to Logsdon's equation which yielded 0.065 m^3 m^{-3}. This may be due to the smaller proportion of fine-textured, smectite clay soils used in developing the Logsdon calibration compared to the proportion at our network sites. Topp, Logsdon, field and CEC-based calibrations overestimated soil moisture at all three evaluation sites. The Topp calibration was consistently higher than Logsdon and field calibrations. Overall, *in situ* calibration showed the best result followed by the CEC-based calibration. The overall field calibration seemed adequate under diverse soil conditions and textural class. This result, similar to conclusions reached by Cosh et al. (2005) and Polyakov et al. (2005) reinforces the need to conduct field calibration to ensure better accuracy in soil moisture determination using the Hydra probes especially in high reactive, medium to fine textured soils.

In this study, both the calibration and evaluation sites were categorised and described based on their textural classification and their CEC. Many of the factors that affect the behaviour and response of water to an applied electromagnetic field can be related to these two properties. For a given temperature and signal frequency, the degree to which water molecules are bound to soil particles is dependent on the soil type and the amount of water in the soil. Clay soils are usually associated with high water holding capacity because of their high porosity facilitated by the presence of many micropores and bound water. However, as discussed earlier, the arrangement of water molecules around the soil particles was different in Kaolinitic clay vs Smectite clay but dependent on the CEC. Increased distortion was observed as the CEC of the soil increased (Saarenketo, 1998).

3.5 Conclusions

A Real-time *In Situ* Monitoring for Agriculture (RISMA) network was established over several sites in Canada (Manitoba, Saskatchewan and Ontario) for the purpose of validating remote sensing products and to serve as input for hydrologic and agronomic models. The RISMA network in Manitoba consists of nine stations that represent the diverse soil textural variation within the Carman - Elm Creek area and collects soil moisture, soil temperature, dielectric values and soil conductivity using the Stevens Hydra probes. To ensure the highest accuracy of the instruments, calibration analyses were conducted in the laboratory and in the field, and compared against the default readings from the probe as well as published calibration equations from Topp and

Logsdon. The laboratory-derived calibration underestimated soil moisture at all the three sites used for evaluation and the performance was poorer than the default calibration at the coarse textured site. However, both the *in situ*, CEC-based and the overall field calibrations performed better than the default calibration at all the evaluation sites. The greatest improvement was observed at the high CEC, fine textured site where the default equation produced unrealistic soil moisture values.

Surface soil moisture products obtained via remote sensing are often calibrated by conducting campaigns such as the Soil Moisture Active Passive Validation Experiment 2012 (SMAPVEX12), National Airborne Field Experiment of 2006 (NAFE'06), and Soil Moisture Experiments (SMEX) between 2002 – 2005 (Rowlandson et al., 2013). These campaigns involve taking soil moisture measurements using handheld sensors at specific locations across the field. Establishing soil moisture networks such as RISMA in many countries will help in long term assessment of soil moisture retrieval algorithms under various climate and land use areas. Similar to other point-based volumetric water content determination, the use of Hydra probe is limited to a very small sampling volume. Also, the instrument's sensitivity to temperature and salinity at the low operating frequency (50 MHz) is a drawback to the use of the Hydra Probe,

For future applications, *in situ* derived calibration is recommended to ensure that the instruments are calibrated to local conditions. However, due to the labour requirements, time constraints and other limitations for creating *in situ* calibrations, CEC-based calibration may provide a suitable alternative and has shown significant promise at the evaluation sites used in this study. Calibrations developed based on the CEC of the soil are expected to provide better reliability in other regions of the world than texture-

based calibrations because similarly classified soil texture may not always show similar behaviour in water. The development of CEC-based and an overall field calibration for the study area was important to ensure that models used within the watershed have the most accurate soil moisture input values possible. Also, it ensures that remotely sensed products are assessed against accurate soil moisture values. Dependence on uncalibrated sensors can lead to erroneous conclusions.

3.6   Acknowledgements

3.7   References

Bellingham, K. 2007. The Stevens Hydra Probe Inorganic Soil Calibrations. Stevens Water Monitoring Systems Inc. Available at http://www.stevenswater.com/catalog/products/soil_sensors/datasheet/The%20Stevens%20Hydra%20Probe%20Inorganic%20Soil%20Calibrations.pdf (verified 19 June 2014).

Bosch, D. D. 2004. Comparison of capacitance-based soil water probes in coastal plain soils. Vadose Zone J., **3**:1380–1389.

Cosh, M. H., Jackson, T. J., Bindlish, R., Famiglietti, J. S. and Ryu, D. 2005. Calibration of an impedance probe for estimation of surface soil water content over large regions. J. Hydrol., **311**:49–58.

Cosh, M., Jackson, T. J., Bindlish, R. and Prueger, J. 2004. Watershed scale temporal and spatial stability of soil moisture and its role in validating satellite estimates. Remote Sens. Environ., **92**:427–435.

Entekhabi, D., Njoku, E. G., O'Neill, P. E., Kellogg, K. H., Crow, W. T., Edelstein, W. N., Entin, J. K., Goodman, S. D., Jackson, T. J., Johnson, J., Kimball, J., Piepmeier, J. R., Koster, R. D., Martin, N., McDonald, K. C., Moghaddam, M., Moran, S., Reichle, R., Shi, J. C., Spencer, M. W., Thurman, S. W., Tsang, L. and Van Zyl, J. 2010. The Soil Moisture Active Passive (SMAP) Mission. Proc. IEEE, **98**:704–716.

Jabro, J. D., Iversen, W. M., Evans, R. G., Allen, B. L. and Stevens, W. B. 2014. Repeated Freeze-Thaw Cycle Effects on Soil Compaction in a Clay Loam in Northeastern Montana. Soil Sci. Soc. Am. J., **78**:737–744.

Kelleners, T. J. and Verma, A. K. 2010. Measured and Modeled Dielectric Properties of Soils at 50 Megahertz. Soil Sci. Soc. Am. J., **74**:744–752.

Kerr, Y. H., Waldteufel, P., Wigneron, J.-P., Delwart, S., Cabot, F., Boutin, J., Escorihuela, M.-J., Font, J., Reul, N., Gruhier, C., Juglea, S. E., Drinkwater, M. R., Hahne, A., Martín-Neira, M. and Mecklenburg, S. 2010. The SMOS Mission: New Tool for Monitoring Key Elements ofthe Global Water Cycle. Proc. IEEE, **98**:666–687.

Logsdon, S. D. 2009. CS616 Calibration: Field versus Laboratory. Soil Sci. Soc. Am. J., **73**:1–6.

Logsdon, S. D., Green, T. R., Seyfried, M., Evett, S. R. and Bonta, J. 2010. Hydra Probe and Twelve-Wire Probe Comparisons in Fluids and Soil Cores. Soil Sci. Soc. Am. J., **74**:5–12.

Lukanu, G. and Savage, M. J. 2006. Calibration of a frequency-domain reflectometer for determining soil-water content in a clay loam soil. Water A, **32**:37–42.

McNairn, H., Jackson, T. J., Wiseman, G., Belair, S., Berg, A., Bullock, P., Colliander, A., Cosh, M. H., Kim, S.-B., Magagi, R., Moghaddam, M., Njoku, E. G., Adams, J. R., Homayouni, S., Ojo, E., Rowlandson, T., Shang, J., Goita, K. and Hosseini, M. 2015. The Soil Moisture Active Passive Validation Experiment 2012 (SMAPVEX12): Prelaunch Calibration and Validation of the SMAP Soil Moisture Algorithms. IEEE Trans. Geosci. Remote Sens., **53**:2784–2801.

Polyakov, V., Fares, A. and Ryder, M. H. 2005. Calibration of a Capacitance System for Measuring Water Content of Tropical Soil. Vadose Zone J., **4**:1004–1010.

Robinson, D. A. 2001. Comments on 'Field calibration of a capacitance water content probe in fine sand soils'. Soil Sci. Soc. Am. J., **65**:1570–1571.

Robinson, D. A., Campbell, C. S., Hopmans, J. W., Hornbuckle, B. K., Jones, S. B., Knight, R., Ogden, F., Selker, J. and Wendroth, O. 2008. Soil Moisture Measurement

for Ecological and Hydrological Watershed-Scale Observatories: A Review. Vadose Zone J., **7**:358–389.

Rowlandson, T. L., Berg, A. A., Bullock, P. R., Ojo, E. R., McNairn, H., Wiseman, G. and Cosh, M. H. 2013. Evaluation of several calibration procedures for a portable soil moisture sensor. J. Hydrol., **498**:335–344.

Saarenketo, T. 1998. Electrical properties of water in clay and silty soils. J. Appl. Geophys., **40**:73–88.

Seyfried, M. S., Grant, L. E., Du, E. and Humes, K. 2005. Dielectric Loss and Calibration of the Hydra Probe Soil Water Sensor. Vadose Zone J., **4**:1070–1079.

Seyfried, M. S. and Murdock, M. D. 2004. Measurement of soil water content with a 50-MHz soil dielectric sensor. Soil Sci. Soc. Am. J., **68**:394–403.

Steiger, J. H. 1980. Tests for comparing elements of a correlation matrix. Psychol. Bull., **87**:245–251.

The Hydra Probe® Soil Sensor. 2008. Stevens Water Monitoring System, Inc. Available at http://www.fondriest.com/pdf/stevens_hydra_manual.pdf (verified 16 June 2014).

Topp, G. C., Davis, J. L. and Annan, A. P. 1980. Electromagnetic determination of soil water content: Measurements in coaxial transmission lines. Water Resour. Res., **16**:574–582.

Van Klaveren, R. W. and McCool, D. K. 2010. Freeze–Thaw and Water Tension Effects on Soil Detachment. Soil Sci. Soc. Am. J., **74**:1327–1338.

Vaz, C. M. P., Jones, S., Meding, M. and Tuller, M. 2013. Evaluation of Standard Calibration Functions for Eight Electromagnetic Soil Moisture Sensors. Vadose Zone J., **12**:1–16.

Verma, A. K. and Kelleners, T. J. 2012. Depthwise Carbon Dioxide Production and Transport in a Rangeland Soil. Soil Sci. Soc. Am. J., **76**:821–828.

Walker, B. D. 2012. Agri-Environmental Monitoring – Manitoba: Methodology and landscape descriptions, pp 29. Agriculture and Agri-Food Canada, Agri-Environmental Services Branch.. Winnipeg, MB and Ottawa, ON.

Walker, J. P., Willgoose, G. R. and Kalma, J. D. 2004. In situ measurement of soil moisture: a comparison of techniques. J. Hydrol., **293**:85–99.

4.   MODELLING SURFACE AND ROOT-ZONE SOIL MOISTURE FOR CONTRASTING MANITOBA AGRICULTURAL SOILS USING THE VERSATILE SOIL MOISTURE BUDGET

4.1   Abstract

The use of agrometeorological models in addition to soil moisture observation using instruments is important to overcome the natural complexity posed by the temporal and spatial variability of soil moisture. The Versatile Soil Moisture Budget (VSMB) is a one-dimensional model that has been widely used to simulate soil moisture on the Canadian prairie. With a growing area planted to soybean and corn on the Prairie, it is important to enhance the capability of the VSMB to simulate soil moisture at fields where these crops are grown. In 2013 and 2014, simulation of surface and root-zone soil moisture with the VSMB was tested at seven sites in Manitoba, Canada that provided observed soil moisture every fifteen minutes across a range of different soil texture and crop types. The results obtained showed that the four coarse textured sites had average RMSE of 0.048 m^3 m^{-3} and 0.056 m^3 m^{-3} for the surface moisture during the 2013 and 2014 growing seasons, respectively. For the surface layer of the medium-fine textured sites, the average RMSE was 0.068 m^3 m^{-3} in 2013 and 0.051 m^3 m^{-3} in 2014. The root zone soil moisture for the entire soil profile at the coarse textured sites had RMSE values

that ranged from 14 - 35 mm in 2013 and 17 - 56 mm in 2014. The average root-zone RMSE at the medium-fine textured sites was 37 mm (0.028 m^3 m^{-3}) in 2013 and 65 mm (0.050 m^3 m^{-3}) in 2014. This study raises questions on the representativeness of a single observed value for daily soil moisture especially in the coarse-textured soil surface layer with high hydraulic conductivity.

4.2   Introduction

Many hydrologic, agronomic and biochemical processes are dependent on the moisture content of the soil. For example, the rates of hydrologic processes such as surface runoff and evapotranspiration are highly correlated with the antecedent soil moisture content. Knowledge of the soil moisture variation can be used in agricultural applications to determine weed emergence (Bullied et al. 2012) and quantify the risk levels for outbreaks of insects and pathogens (Dufault et al. 2006). The quality and quantity of crop yield is correlated to soil moisture availability (Steduto et al. 2009). Soil biochemical processes such as nitrogen cycling and other soil redox reactions are influenced by soil moisture levels.

Soil moisture can be directly measured using the thermogravimetric method which is destructive to the soil sample. However, there are several non-destructive, indirect methods which include the use of instruments that are in contact with the soil (e.g. surface and multi-depth probes); non-contact remote sensing instruments (e.g. Cosmic Ray Soil Moisture Observing System, Soil Moisture Active and Passive Satellite)

as well as the use of models (e.g. physical, empirical or mixed models). These various methods present unique opportunities for monitoring soil moisture at varying temporal and spatial scales. However, there are several challenges, such as the application of soil moisture data collected at one scale to another scale. Robinson et al. (2008) presented a comprehensive review on the various methods of determining soil moisture.

Compared to the cost of soil moisture instruments, the use of models in estimating soil moisture is cheaper. The use of models has gained prominence resulting in an increase in the number of studies that are based on the use of agrometeorological models (Monteith 2000). The Versatile Soil Moisture Budget (VSMB) that models one-dimensional, vertical soil moisture fluxes was first introduced about five decades ago by Baier and Robertson (1966). Several users have modified the model to improve its performance. Akinremi et al. (1996) replaced the simplified reference evapotranspiration equation which used temperature and latitude with the Priestley-Taylor equation. They also replaced the infiltration and moisture redistribution process. The function used to estimate the drying curve in grasslands was modified by Hayashi et al. (2010). Ojo (2012) also replaced the evapotranspiration subroutine which uses the Priestley-Taylor equation with the Penman-Monteith evapotranspiration equation. The author included a five-stage physiological-day (P-day) accumulation, based on the original description by Sands et al. (1979) for the purpose of modelling canola development using threshold values developed by Wilson (2002).

Modelled soil moisture values from the VSMB have been validated against actual soil moisture measurements derived using other methods (Baier 1990; Hayhoe et al. 1993; Akinremi et al. 1996; Chipanshi et al. 2013). These authors have demonstrated

that the VSMB provided reasonable estimates of soil moisture content. However, the comparison between modelled and observed soil moisture were made on selected days during the growing season rather than on a continuous basis. One of the unique aspects of this study was the availability of daily soil moisture observations which provided an extensive dataset for model validation at the fourteen site-years described in the next section of this chapter. The VSMB has been adopted for various agrometeorology, climatology and hydrology applications such as snow accumulation and snowmelt (Mohammed et al. 2013), assessment of Prairie grassland evaporation rate (Hayashi et al. 2010), effect of water use on the yield of spring wheat on the Canadian Prairies (Qian et al. 2009) as well as the assessment of climate change on several agronomic practices such as seeding date and soil water content on the Canadian prairies (McGinn and Shepherd 2003).

Many of the aforementioned studies that used the VSMB to estimate soil moisture have focused on root-zone soil moisture simulation or assumed an upper soil layer with a thickness of 0.2 m or more. The shallow surface (~ 0 – 0.1 m), at the soil-atmosphere interface, is the most dynamic layer and has a significant impact on the accuracy of soil moisture simulated within the root zone. Remote sensing provides a unique capability to measure soil moisture in the surface layer on a frequent basis and across the entire globe. There is interest in comparing the VSMB modelled soil moisture in the surface layer to remotely-sensed estimates. Furthermore, the fourteen site-years in this study provided an extensive dataset for model validation because of the availability of daily soil moisture observations, something that has not been available in other published validations of the VSMB. Thus, the first objective of this study was to assess the accuracy of the VSMB to

simulate soil moisture variation in the top 0.1 m of the soil. This will help determine the model's capability as a validation tool for remote sensing techniques. The second objective of this study was to determine the accuracy of the VSMB to simulate root zone soil moisture across a wide range of soil textures and crops. Despite the wide use of VSMB for estimating soil moisture, it has been limited to mainly grasslands and cereal crops such as wheat (Akinremi et al. 1996; Hayashi et al. 2010) and recently canola (Ojo 2012). Soybean and corn are gradually becoming more prominent crops on the Canadian prairies. Statistics Canada (2015) reported that Soybean production in Manitoba has tripled from 413,700 metric tonnes in 2011 to 1,243,800 metric tonnes in 2015. Thus, there is a need to incorporate subroutines that will simulate the growth of a greater number of crops across a range of coarse to fine-textured soils and, thus, expand the soil moisture simulation capability of the VSMB.

4.3   Materials and Methods

4.3.1   Soil Moisture Observation Sites

Nine soil moisture monitoring sites (MB1-9) were established by Agriculture and Agri-Food Canada (AAFC) in Manitoba in 2012 as part of the Real-time In-situ Soil Monitoring for Agriculture (RISMA) network (Figure 3.1). However, results from sites MB 5 and 6 are not reported because of instrument failure early in the 2013 growing season. MB 1, 4, 7 and 9 are coarse textured soils with less than 15% clay content in the top 0.10 m depth. All other sites (MB 2, 3 and 8) are medium to fine textured soils with greater than 30% clay in the top soil. Soil moisture sensors (Hydra Probe, Stevens Water

Monitoring Systems, Inc.) were installed in triplicate at 0.05, 0.20, 0.50 and 1.0 m depths at each site and data logged every 15 minutes. In addition to soil moisture monitoring, a weather station was installed at each site to collect air temperature, humidity (HC2-S3, Campbell Scientific, Inc.), rainfall (CS 700, Campbell Scientific, Inc.) and wind speed data (05103L, RM Young). The weather data were used as inputs to run the VSMB. The network area (Figure 3.1) has been the site of intense soil moisture monitoring and remote sensing validation (McNairn et al. 2011, 2015) due to its distinct features such as the sharp soil texture change that occurs within a few kilometers.

The preceding chapter provided detailed information on the soil moisture network design, location and instrumentation. The authors conducted *in situ* calibration of the probes at all the sites to ensure better accuracy of the soil moisture data collected. The daily observed soil moisture data used in this study was obtained from the mean of the three calibrated soil moisture probes at each depth and each value is the average of 96, 15-minute readings for a 24 hour period. Table 4.1 provides information on the physical characteristics of the top soil as well as the crops grown at each site in 2013 and 2014.

Table 4.1 Physical properties of the surface (0 – 0.10 m) soil layer for sites within the soil moisture network

Station	Crop (2013)	Crop (2014)	Soil Bulk Density(g cm⁻³)	Sand–Silt–Clay (%)	Texture
MB 1	Corn	Wheat	1.28	79-10-11	Sandy Loam
MB 2	Corn	Bean	1.35	45-21-34	Clay Loam
MB 3	Soybean	Wheat	1.47	47-21-32	Sandy Clay Loam
MB 4	Soybean	Wheat	1.33	90-01-09	Sand
MB 5	Corn	Soybean	1.46	41-18-41	Clay
MB 6	Soybean	Wheat	1.21	04-24-72	Heavy Clay
MB 7	Corn	Oat	1.40	78-09-13	Sandy Loam
MB 8	Soybean	Wheat	1.22	04-33-63	Heavy Clay
MB 9	Oat	Corn	1.53	81-06-13	Sandy Loam

4.3.2 Model Description

The VSMB simulates soil moisture on a daily time step using the water balance method.

$$\theta v_{i,j} = \theta v_{(i-1),j} + P_i - RO_i - AET_{i,j} - D_{i,j} \qquad [4.1]$$

$\theta v_{i,j}$ is the moisture content at soil depth j on day i, $\theta v_{(i-1),j}$ is the soil moisture content from the previous day at depth j, $P_i - RO_i$ is the precipitation less runoff for the surface layer (or simply $I_{i,j}$ which is infiltration into layer j on day i), $AET_{i,j}$ is the actual evapotranspiration loss and $D_{i,j}$ is drainage loss to the adjacent layer. The actual evapotranspiration loss from all the layers is determined as:

$$AET = \sum_{i=1}^{n} [ET_o \times R_i \times DC(W_i/W_{ci})] \qquad [4.2]$$

where n is the total number of layers, ET_o is the potential evaporation using the Priestley Taylor equation, R_i is the empirically-derived root coefficient, DC is the drying curve and W_i/W_{ci} is the relative soil moisture content. Basic soil information such as the permanent

wilting point, field capacity, saturation as well as weather data such as rainfall, maximum and minimum temperatures are inputs needed to run the VSMB. Hayashi et al. (2010), Ojo (2012) and Mohammed et al. (2013) provide detailed information on the VSMB. A sample of both the input and output files is provided in the Appendix section of this thesis. In this study, the soil profile was divided into four layers: 0 – 0.10, 0.11 – 0.30, 0.31 – 0.70 and 0.71 – 1.30 m depth. The modelled soil moisture from each layer was compared to observed soil moisture from probes installed at 0.05, 0.20, 0.50 and 1.0 m, respectively. Although the VSMB has the capacity to run over multiple years, simulated soil moisture for both 2013 and 2014 was run separately and only during the growing season (May – September).

4.3.3   Model Parameterization

For each soil layer, the VSMB requires four soil moisture parameters: initial soil moisture at the start of simulation, soil saturation level, field capacity and permanent wilting point. Similar to Hayashi et al. (2010), the lowest observed daily soil moisture values for both years were averaged and used as the permanent wilting point. Field capacity was defined as the average of the maximum observed daily value for both years. This is different from the traditional definition of field capacity but was adopted because the VMSB uses field capacity as the moisture content to which a saturated soil will decline within a day. The traditional field capacity definition and measurement (soil moisture content of a soil allowed to drain freely without evaporative loss for 3 days after being saturated) does not provide values that are representative for the VSMB, especially for medium to fine textured sites where soil moisture can remain above field capacity for days after significant rainfall. Ojo (2012) showed that the VSMB underestimated soil

moisture using the traditional field capacity values. Saturation was taken as the maximum 15-min observed soil moisture which is always greater than the 24-h mean value. The model simulation was started during the last week in April, thus, the initial soil moisture was the observed moisture content on April 24. Table 4.2 shows the four soil moisture parameters used at the surface layer at the sites reported in this study. Plant available soil moisture during the growing season is expected to range between field capacity and permanent wilting point.

The VSMB model parameters used in both this chapter and chapter 5 were not calibrated to achieve the best possible fit between observed and modelled soil moisture values at the sites used in this study. Model calibrations conducted and reported in Ojo (2012) were used. Site-specific parameters that were adjusted in both chapters 4 and 5 are crop phenology, curve number and moisture regimes described in the preceding paragraph.

Table 4.2 Soil moisture parameters

Site[z]	Saturation	Field Capacity	Initial	Wilting Point
	---------------------------------- (m^3 m^{-3}) ----------------------------------			
MB 1	0.35	0.285	0.30	0.09
MB 2	0.55	0.480	0.45	0.26
MB 3	0.49	0.380	0.40	0.18
MB 4	0.39	0.253	0.30	0.02
MB 7	0.40	0.354	0.30	0.16
MB 8	0.62	0.526	0.55	0.31
MB 9	0.42	0.224	0.30	0.09

[z] Analysis was not conducted at MB 5 and 6 due to instrument failure.

4.3.4 Model Modification

The VSMB has a Bio-Meteorological Time Scale (BMTS) subroutine which is used to simulate the growth of wheat in response to temperature and photoperiod. The BMTS was also used to simulate oat growth. To simulate corn and soybean growth, a subroutine that accumulates crop heat units (CHU) was added to the model. Similar to Growing Degree Days (GDD), CHU measures the effect of heat accumulation on the growth and development of a crop. Its main distinction from GDD is that CHU treats day and night temperatures differently (equation 4.3). The daily minimum temperature (T_{min}) is used in a linear function with a minimum of 4.4°C. The daily maximum temperature (T_{max}) is used in a quadratic function with a minimum at 10°C and an optimum at 30°C (Brown 1969). It is important to note that when $T_{min} < 4.4$°C then T_{min} is set to 4.4°C. Also, when $T_{max} < 10$°C then T_{max} is set to 10°C.

$$CHU_{min} = 1.8(T_{min} - 4.4°C) \qquad [4.3]$$

$$CHU_{max} = 3.33(T_{max} - 10°C) - 0.084(T_{max} - 10°C)^2 \qquad [4.4]$$

$$CHU = (CHU_{max} + CHU_{min}) / 2 \qquad [4.5]$$

Table 4.3 Growth stages of corn and their corresponding cumulative crop heat units

Growth Stage	Cumulative CHU[†]
Seeding - First Leaf Collar	0 to 330
First Leaf Collar - Ear Initiation	330 to 780
Ear Initiation - Silking	780 to 1480
Silking - Dough	1480 to 2165
Dough - Maturity	2165 - 2600

[†]CHU – Crop Heat Units. Adapted from OMAFRA (2009)

Table 4.4 Growth stages of soybean and their corresponding cumulative crop heat units

Growth Stage	Cumulative CHU[†]
Seeding - Emergence	0 to 226
Emergence – 4th Trifoliolate	226 to 794
4th Trifoliolate – Beginning of Pod	794 to 1446
Beginning of Pod – Full Seed	1446 to 2136
Full Seed - Maturity	2136 - 2378

[†]CHU – Crop Heat Units. Adapted from Aaron Glenn (AAFC Brandon, unpublished data)

Among other factors, crop maturity is dependent on the variety planted. To mimic the five growth stages used for wheat growth in the model, five selected corn growth stages from the Ontario Ministry of Agriculture, Food and Rural Affairs (OMAFRA 2009) were adopted (Table 4.3). In this study, the maximum CHU necessary for corn maturity was modified from 2800 in OMAFRA (2009) to 2600 which reflects the highest CHU observed in corn varieties in the Manitoba corn hybrid performance trials in 2013 (Cott et al. 2013). For soybean, Aaron Glenn (AAFC Brandon, personal communication) conducted research that monitored the developmental stages of three soybean varieties of different maturity groups at multiple sites in Manitoba between 2011 and 2013. The CHU recorded (unpublished data) at the southernmost and northernmost sites were averaged for five selected growth stages (Table 4.4). The same subroutine used for soybean was used for the bean field.

4.3.5   Data Analysis

Statistical indicators used to compare both the surface and root zone VSMB modelled soil moisture to the observed were the root mean square error (RMSE) and the mean bias error (MBE).

$$RMSE = \left(\frac{\Sigma(M_i - Obs_i)^2}{n}\right)^{0.5} \qquad\qquad [4.6]$$

$$MBE = \frac{1}{n}[\Sigma_{i=1}^{N}(M_i - Obs_i)] \qquad\qquad [4.7]$$

where *M* is the modelled soil moisture from the VSMB and *Obs* is the observed soil moisture from calibrated probes on day *i*.

4.4   Results and Discussion

4.4.1   Surface Soil Moisture Analysis

4.4.1.1   Coarse Textured Soil. The 2013 results for modelled surface soil moisture showed that coarse textured soils generally had lower Root Mean Square Error (RMSE) compared to the medium-fine textured soils. This was expected because coarse textured soils hold less moisture compared to the medium to fine textured soils. Specifically, MB 1, 4, 7 and 9 had RMSEs of 0.047 m^3 m^{-3}, 0.072 m^3 m^{-3}, 0.041 m^3 m^{-3} and 0.031 m^3 m^{-3}, respectively. The Mean Bias Error (MBE) showed that the model overestimated soil moisture at all the coarse textured soils except at MB 9 which had a slight underestimation of -0.004 m^3 m^{-3} (Table 4.5). Generally, the model performed reasonably well in simulating soil moisture trends; however, the model did not effectively capture soil moisture peaks and nadirs (Figure 4.1).

Table 4.5 Statistical analysis for 2013 and 2014

Site	Surface RMSE (m³ m⁻³)		MBE (m³ m⁻³)		All Depths RMSE (mm)		MBE (mm)	
	2013	2014	2013	2014	2013	2014	2013	2014
MB 1	0.047	0.045	0.038	0.036	14	17	-10	-7
MB 4	0.072	0.065	0.057	0.046	27	56	11	-30
MB 7	0.041	0.058	0.031	0.044	35	35	-21	-2
MB 9	0.031	0.055	-0.004	0.036	29	53	12	-48
Average	0.048	0.056	0.031	0.041	26	40	-2	-22
MB 2	0.056	0.048	-0.029	0.035	38	25	-12	-1
MB 3	0.046	0.061	-0.002	0.048	30	69	11	68
MB 8	0.101	0.044	-0.090	-0.001	44	101	-11	98
Average	0.068	0.051	-0.040	0.027	37	65	-4	55

RMSE = Root Mean Square Error, MBE= Mean Bias Error.

Near the end of the growing season, the 2014 results showed a larger disparity between the modelled and observed soil moisture. This may be due to the fact that after harvest, the rate of evapotranspiration drops significantly because the model assumes that R_i in equation [4.2] is no longer contributing to actual evapotranspiration. Thus, lower evapotranspiration results in higher soil moisture.

2013   **2014**

Figure 4. 1   Plots showing the daily soil moisture trend between the observed (solid line, m^3 m^{-3}) and the VSMB modelled (dotted line, m^3 m^{-3}) at 0.05 m at the coarse textured sites- MB 1, 4, 7 and 9. Vertical bars represent daily precipitation (mm). VWC = Volumetric Water Content.

At MB 4, the field capacity value utilized in VSMB was 0.253 m^3 m^{-3}, which was the mean of the 2013 and 2014 maximum daily observed soil moisture values of 0.157 m^3 m^{-3} and 0.349 m^3 m^{-3}, respectively. It is unclear why the observed daily maximum value more than doubled in 2014 compared to 2013. The model overestimated soil moisture until mid-July in 2013 at this site, especially early in the growing season. In 2014, the modelled results were again higher than observed but not to the same extreme and mainly in the late growing season.

The 2013 growing season, with about 300 mm of precipitation, was drier than 2014 that had about 400 mm. As discussed in a later section of this paper, the timing of the precipitation event and the mode of data aggregation from 15-minute frequency to daily time-step were significant factors that affected the values used as the "observed daily soil moisture", especially on days with significant precipitation. Across the four coarse textured sites, the average RMSE in 2013 was 0.048 m^3 m^{-3} with an average MBE of 0.031 m^3 m^{-3}. In 2014 however, the average RMSE and MBE increased to 0.056 and 0.041 m^3 m^{-3}, respectively.

4.4.1.2 Medium-Fine Textured Soil. The rates of drying after rain events were faster in the modelled soil moisture compared to the observed. This may be due to the drying curve function used to run the model. As discussed in Ojo (2012), the drying curve function determines the rate of water loss between field capacity and permanent wilting point. The coefficients used were 1, 1, 1 and 0.7 to represent the dimensionless fitting parameters C_m, C_n, C_h and C_r, respectively. These coefficients assume that within the range of 50% to 100% available soil moisture, the soil is able to meet the evapotranspirative demand. Thus, rapid drying occurs in response to demand from

evaporation and transpiration. However, when the soil is drier than the 50% available soil

moisture value, evapotranspirative loss is reduced.

2013   **2014**
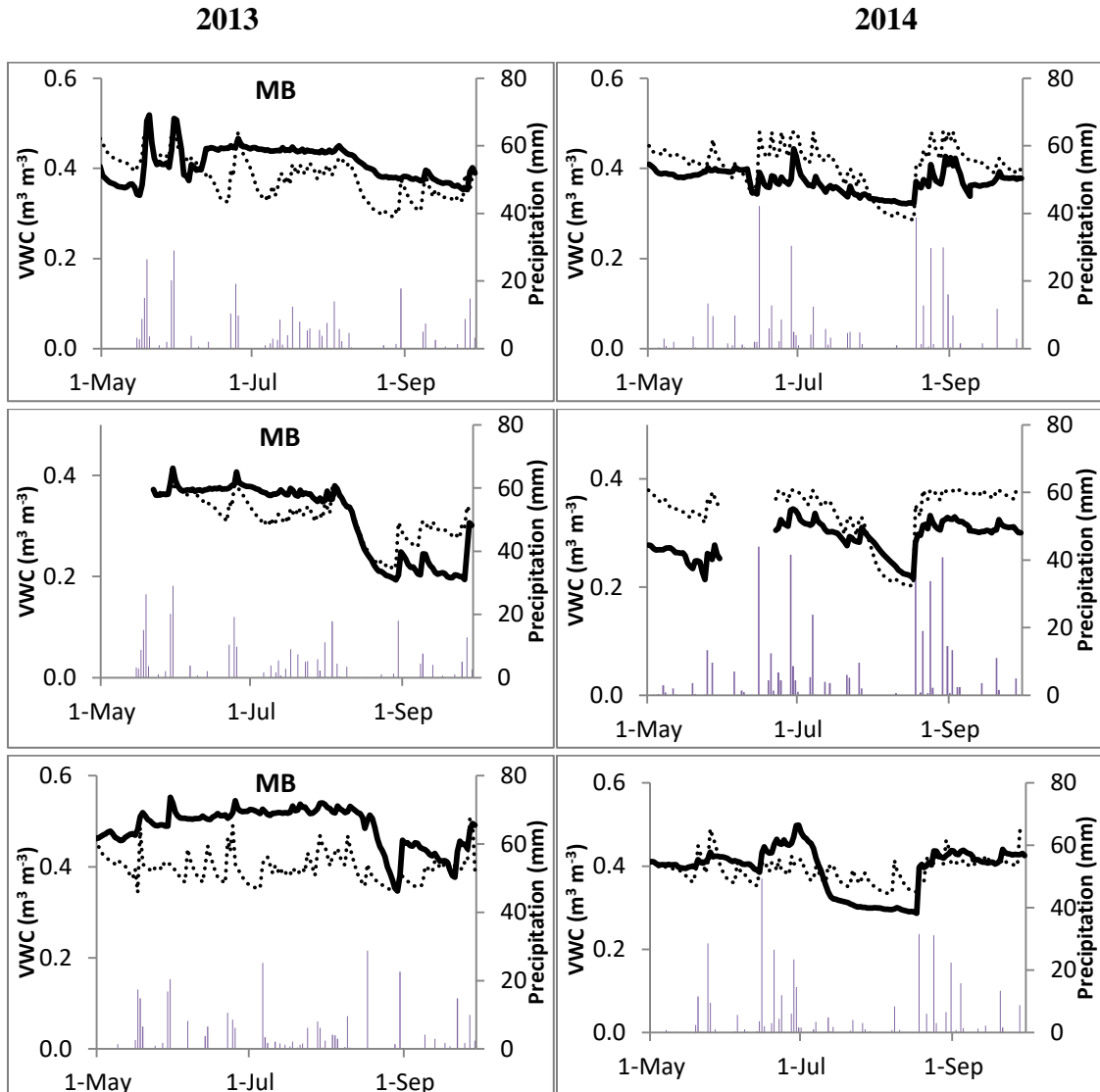
Figure 4.2   Plots showing the daily soil moisture trend between the observed (solid line, m^3 m^{-3}) and the VSMB modelled (dotted line, m^3 m^{-3}) at 0.05 m at the medium-fine textured sites- MB 2, 3 and 8. Vertical bars represent daily precipitation (mm). VWC = Volumetric Water Content.

The VSMB underestimated soil moisture throughout the 2013 growing season at MB 2 and 8 with MBE values of -0.029 and -0.090 respectively (Figure 4.2). Both sites had better RMSE in 2014 compared to 2013 (Table 4.3). No observed values were recorded in the first three weeks in May 2013 and June 2014 at MB 3 due to sensor failure. However, the model effectively captured the soil moisture trend despite the huge discrepancy at the beginning and towards the end of the 2014 growing season.

Across the three medium-fine textured sites, the average RMSE in 2013 was 0.068 m^3 m^{-3} with an average MBE of -0.040 m^3 m^{-3}. In 2014 however, the average RMSE decreased to 0.051 m^3 m^{-3} with a positive MBE of 0.027 m^3 m^{-3}. Sridhar et al. (2008) developed a soil moisture index for quantifying drought and compared observed soil moisture to the Robinson and Hubbard (1990) model. In their study, observed soil moisture was monitored using calibrated sensors (Theta Probe, Delta-T Devices Ltd.). The authors reported a RMSE range between 0.03 m^3 m^{-3} and 0.14 m^3 m^{-3} at 0.10 m for the 37 sites simulated. Across the fourteen site-years in this study, the RMSE obtained ranged from 0.031 m^3 m^{-3} and 0.101 m^3 m^{-3} which is comparable to results obtained by Sridhar et al. (2008).

4.4.2   Root Zone Soil Moisture Analysis

4.4.2.1   Coarse Textured Soil.   At each site, the soil profile was divided into four depths to facilitate the independent analysis of the top layer. However, the root zone soil moisture was derived from aggregating the data from the four depths (0 - 1.3 m). Due to the frequent harsh winter in Manitoba, soils are sometimes frozen at 1 m until late May or early June. Root zone soil moisture statistical analysis only included the frost-free

periods from May to September at all the depths. Similar to modelled surface soil moisture, the VSMB was able to reproduce the measured soil water within the profile with a reasonable degree of accuracy. Total root zone soil moisture (Figure 4.3) is not as dynamic as the surface soil moisture values. All the coarse textured sites except MB7 showed increased RMSE from 2013 to 2014. MB1 had the lowest RMSE of 14 and 17 mm in 2013 and 2014, respectively. The MBE at this site indicated that the model slightly underestimated soil moisture at both years. In 2013, the RMSE at all the coarse sites ranged from 14 mm to 35 mm with an average RMSE of 26 mm (or 0.020 m^3 m^{-3}). In 2014, the RMSE ranged from 17 mm to 56 mm with an average RMSE of 40 mm (or 0.031 m^3 m^{-3}). The average MBE across these sites increased from -2 mm in 2013 to -22 mm in 2014.

4.4.2.2   Medium-Fine Textured Soil. The RMSEs at MB 2, 3 and 8 were 38 mm, 30 mm and 44 mm in 2013 (Table 4.4). The only improvement in 2014 was at MB 2 with a RMSE of 25 mm. At both MB 3 and 8, the modelled soil moisture was consistently higher than the observed all through the growing season in 2014 (Figure 4.4) with MBE values of 68 mm and 98 mm, respectively. The average RMSE across the three medium-fine textured sites increased from 37 mm (or 0.028 m^3 m^{-3}) in 2013 to 65 mm (or 0.050 m^3 m^{-3}) in 2014.
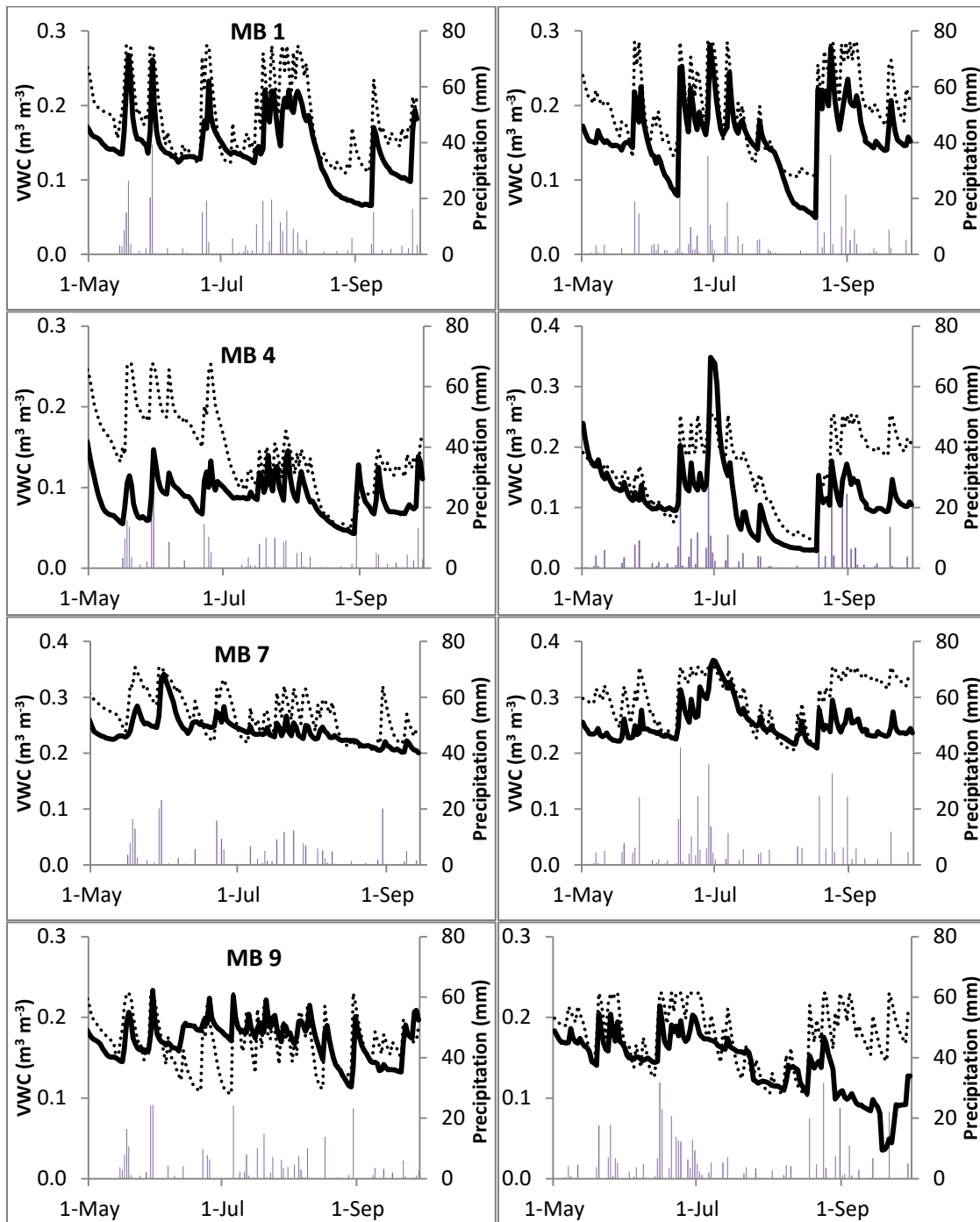
2013

2014
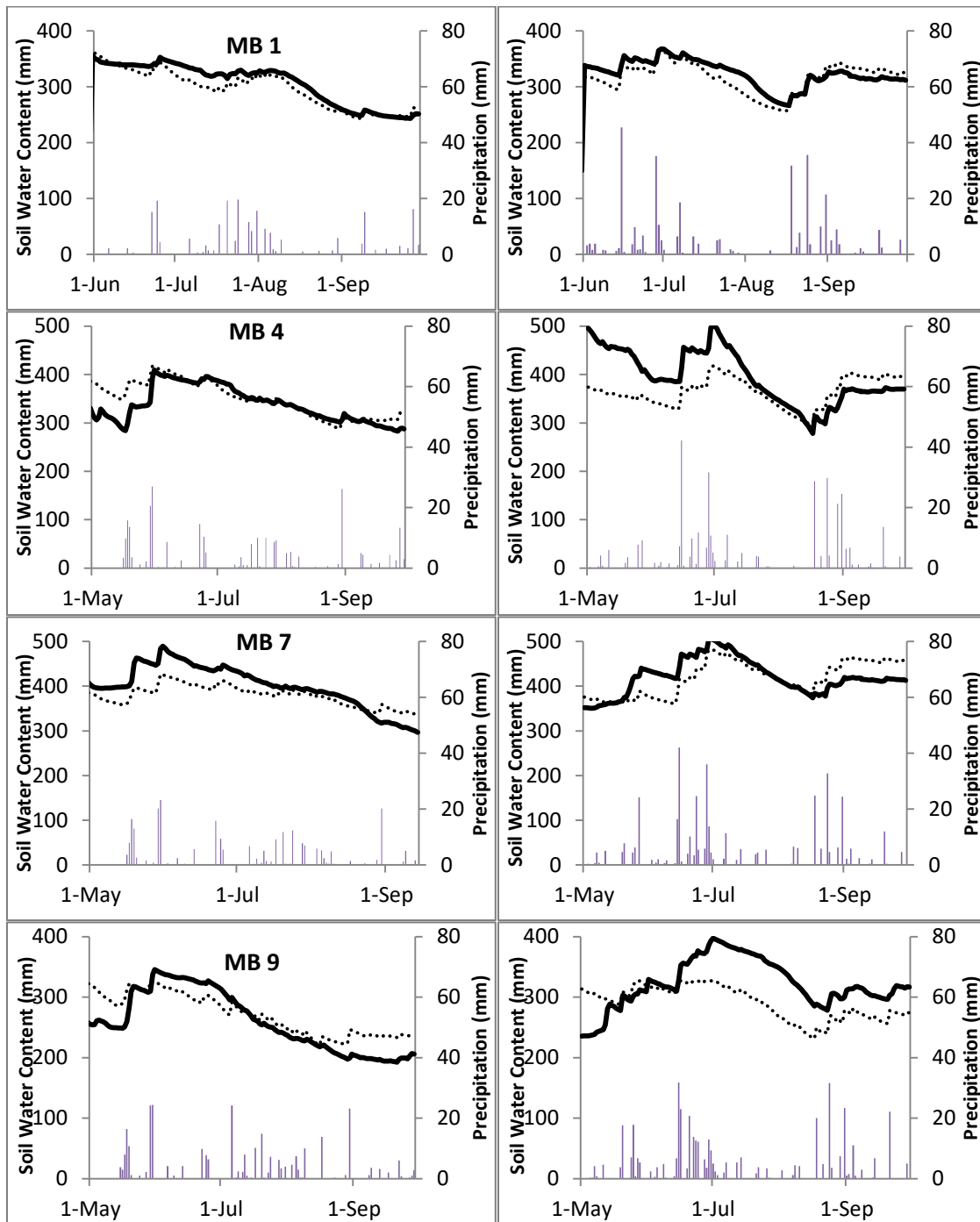
Figure 4.3   Plots showing the daily soil moisture trend between the observed (solid line, mm) and the VSMB modelled (dotted line, mm) for the 0 – 1.30 m depth at the coarse textured sites- MB 1, 4, 7 and 9. Vertical bars represent daily precipitation (mm).

2013   **2014**
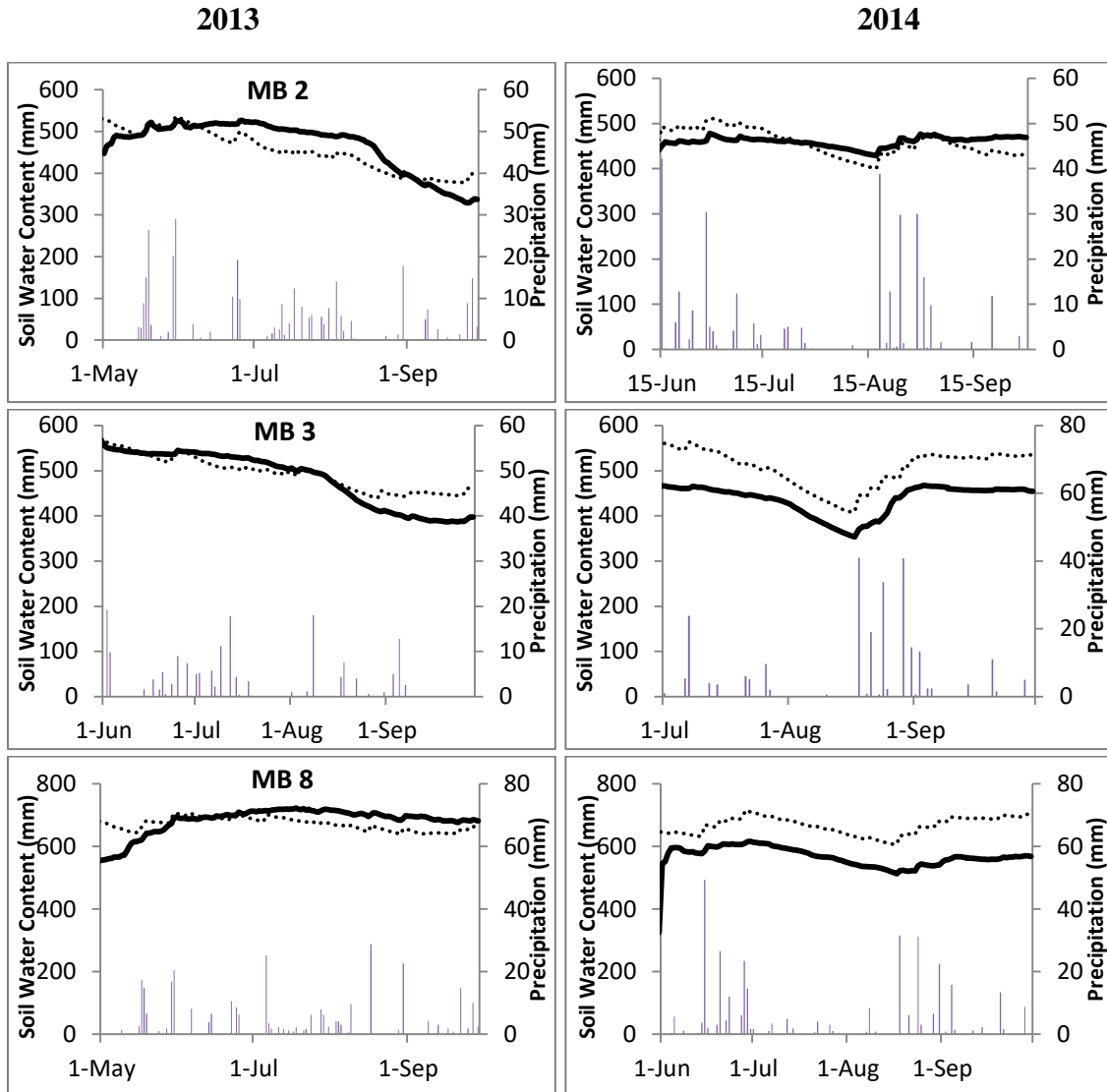
Figure 4.4   Plots showing the daily soil moisture trend between the observed (solid line, mm) and the VSMB modelled (dotted line, mm) for the 0 – 1.30 m depth at the medium-fine textured sites- MB 2, 3 and 8. Vertical bars represent daily precipitation (mm).

The performance of VSMB in simulating root-zone soil moisture was compared to other models that have been used. Gervais et al. (2010) simulated root zone soil moisture using the modified Prairie Agrometeorological Model (PAM). The authors observed a RMSE of 53 mm across the 19 site-years considered. Assessing the

performance of the FAO AquaCrop model for wheat grain yield and soil moisture simulation, Mkhabela and Bullock (2012) obtained a RMSE of 49 mm at the locations considered by Gervais et al. (2010). At a long-term simulation of soil-crop interactions study in Saskatchewan under a medium textured soil, Kersebaum et al. (2008) simulated root zone soil moisture over a period of 25 years using HERMES model and obtained a RMSE of 24 mm. Across the fourteen site-years, the average root zone RMSE obtained in this study is 42 mm which is slightly better than the results obtained from both the PAM and AquaCrop models. It should be noted that the aforementioned references compared modelled soil moisture to fewer observed soil moisture collected randomly across the growing season. In this study however, the comparisons were based on observed daily soil moisture throughout the growing season.

4.4.3 Observed Daily Soil Moisture Analysis

In this study, observed soil moisture from calibrated sensors was reported every 15 minutes. The VSMB modelled soil moisture on a daily time step. The output was compared to observed daily soil moisture which was calculated as the mean of 96, 15-minute readings on each 24 hour (midnight to midnight) period. Due to the dynamic nature of the soil surface layer, the representativeness of a mean observed value for daily soil moisture, especially in the coarse-textured soil surface layer with high hydraulic conductivity, is being questioned as a valid observation.
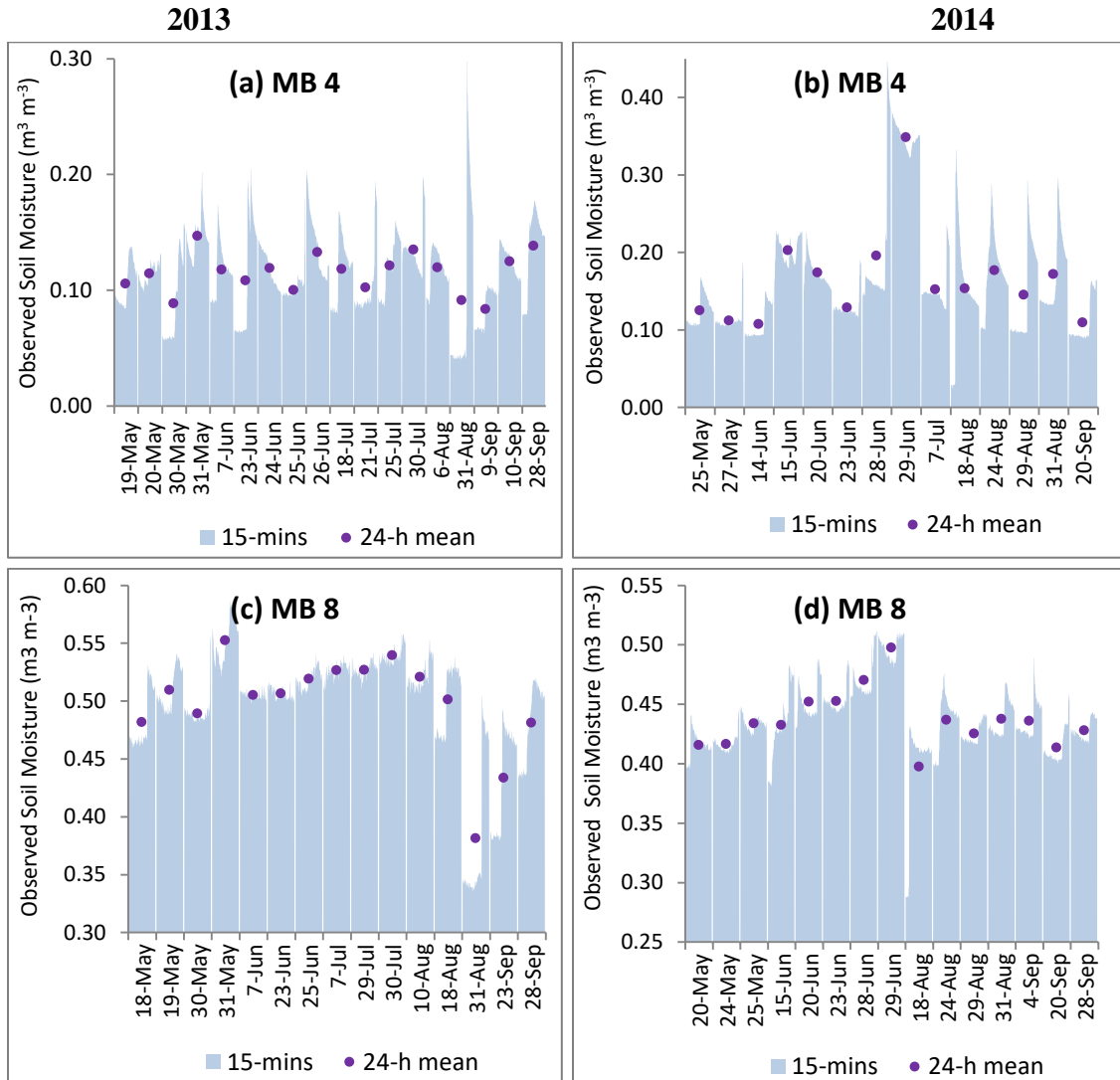
Figure 4.5   Volumetric soil moisture at 0.05 m on days with significant precipitation
events between May – September at (a) MB 4 in 2013 (b) MB 4 in 2014
(c) MB 8 in 2013 and (d) MB 8 in 2014.

Figure 4.5(a-d) shows the observed volumetric soil moisture content at the 0.05 m

depth on days with > 8mm rainfall at MB 4 (coarse texture) and MB 8 (fine texture) in

2013 and 2014. Similar to the data aggregation used in this study, the mean value of

hourly or semi-hourly readings have been used to represent daily soil moisture content

(Illston et al. 2004; Meng and Quiring 2008). During the entire 2013 growing season, the

largest range of recorded 15-minute volumetric moisture content within a day occurred on August 31st (Figure 4.5 a and c). At MB 4, volumetric moisture content changed from 0.044 m^3 m^{-3} at 4:30 pm to 0.298 m^3 m^{-3} at 5:15 pm due to the 16 mm rainfall that was recorded within the timeframe. However, in less than 7 hours, the soil moisture dropped to 0.161 m^3 m^{-3} just before midnight. The mean of all 96, 15-minute data was 0.091 m^3 m^{-3} and the moisture content at noon before the rainfall event was 0.042 m^3 m^{-3}. On August 31, 2013 at MB 8, soil moisture changed from 0.346 m^3 m^{-3} at 5 pm to 0.504 m^3 m^{-3} at 5:15 pm as a result of the 15 mm of rainfall within 15 minutes. The mean of all 96, 15-minute data at this site was 0.381 m^3 m^{-3}.

The mean daily value obtained is highly dependent on the timing of the rainfall event. For example, the largest range of 15-minute volumetric soil moisture recorded at MB 8 in 2014 occurred on August 18th (Figure 4.5d). However, unlike in 2013, the mean of the 96, 15-minute data was a relatively good representation because the rainfall occurred early in the day. Figure 4.5 c and d showed that the mean values were mostly representative of the 15-minute soil moisture trend at the fine textured site. However, towards the end of the 2013 growing season, especially on August 31, relatively low soil moisture and late afternoon rainfall resulted in the mean value being less representative.

The type of observed soil moisture data aggregation has significant implications for modelling. The use of the observed daily value from the mean of 15-minute data gave a maximum daily soil moisture value of 0.157 m^3 m^{-3} throughout the 2013 growing season at MB 4. However, Figure 4.5a shows several 15-minute data points above 0.157 m^3 m^{-3}. This type of data aggregation leads to an inadequate representation of observed soil moisture and may potentially increase the error of models that are compared to such

aggregated data. Thus, simulating surface soil moisture at coarse textured sites on a daily time-step under-represents the volatility observed during significant rainfall events. At MB 8 with low hydraulic conductivity, soil moisture remained high all day on September 1, 2013 due to the rainfall from the previous day. Thus, the mean observed soil moisture on September 1 (0.458 m^3 m^{-3}), which was a day without any rainfall, was higher than the mean soil moisture on August 31 (0.381 m^3 m^{-3}) which had a total rainfall of 21.8 mm occurring late afternoon. Depending on the antecedent soil moisture and the timing of rainfall, the use of daily time-step at fine textured soils can be less problematic due to their low hydraulic conductivity.
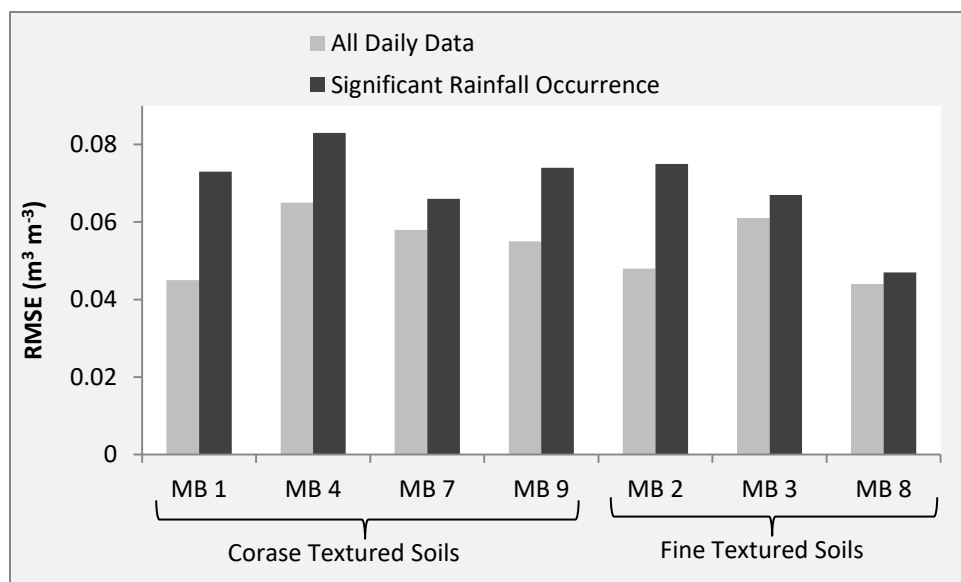
Figure 4.6   Agreement between modelled soil moisture data on all days and days with > 8 mm rainfall occurrence in 2014 compared to measurements from soil moisture instrument at 5 cm.

Figure 4.6 shows the overall results from the comparison of the observed to the modelled soil moisture at the surface layer to the results obtained on those days with significant rainfall occurrence (SRO). During the study period in 2014, the number of

days with > 8 mm of rainfall ranged between 11 and 15 days. The results showed that at all the coarse and fine textured locations; days with significant rainfall occurrence had higher RMSEs compared to the overall data. The rain effect was noticeable at three of the four coarse textured sites which had RMSE difference >0.015 m^3 m^{-3}. Only one of the three fine textured sites had >0.015 m^3 m^{-3} RMSE difference.

4.5   Conclusions

The Versatile Soil Moisture Budget (VSMB), a soil moisture model that has been widely used on the Canadian prairie was used to estimate soil moisture on seven fields with significant differences in soil texture and for a wide range of crops over two separate growing seasons. This study expanded the capability of the VSMB to simulate soil moisture under corn and soybean. The results show that the VSMB was effective at modelling the daily soil moisture trend considering the variation in both soil and crops but it was not effective at simulating the extremes of wetting/drying cycles. Further, the dynamic surface layer was more difficult than the root zone to model accurately. This study raised questions about whether it is appropriate to expect a daily time-step model to accurately represent the highly dynamic surface layer in coarse textured soils because it cannot capture the significant variability that occurs within a 24-hour period.

As more data become available both from RISMA and other *in situ* soil moisture networks, it is expected that VSMB model output accuracy will improve. However, the fourteen site-years in this study provided an extensive dataset for model validation

because of the availability of daily soil moisture observations. This study also shows that VSMB has great prospects for accurately modelling root-zone soil moisture. This is very important to the overall goal of achieving accurate estimates of soil moisture availability for agricultural crops as well as serving as an input in flood models. Remote sensing can only provide a measure of soil moisture at the surface and *in situ* soil moisture networks are limited and expensive to operate. Thus, the only means to provide root zone soil moisture across the vast extent of agricultural landscapes will be through the synergy of these methods which include the use of models such as VSMB.

4.6   Acknowledgements

4.7   References

Akinremi, O.O., McGinn, S. M. and Barr, A.G. 1996. Simulation of soil moisture and other components of the hydrological cycle using a water budget approach. Can. J. Soil Sci. **76**: 133–142.

Baier, W. 1990. Characterization of the environment for sustainable agriculture in semi-arid tropics. p. 90–128. *In* Proceedings of the International Symposium on Natural Resources Management for a Sustainable Agriculture. Indian Society of Agronomy, New Delhi.

Baier, W. and Robertson, G.W. 1966. A new versatile soil moisture budget. Can. J. Plant Sci. **46**: 299–315.

Brown, D.M. 1969. Heat units for corn in southern Ontario. Ministry of Agric. and Food, Guelph, ON, Canada.

Bullied, W. J., Van Acker, R.C. and Bullock, P.R. 2012. Review: Microsite characteristics influencing weed seedling recruitment and implications for recruitment modeling. Can. J. Plant Sci. **92**: 627-650

Chipanshi, A.C., Warren, R. T., L'Heureux, J., Waldner, D., McLean, H. and Qi, D. 2013. Use of the National Drought Model (NDM) in Monitoring Selected Agroclimatic Risks across the Agricultural Landscape of Canada. Atmosphere-Ocean **51**: 471–488.

Cott, M., Rocquigny, P., Billing, W., Murray, B., Veldman, G., Kaminsky, J. and Bergsma, T. 2013. 2013 Manitoba Corn Hybrid Performance Trials. [Online] Available: http://manitobacorn.ca/wp-content/uploads/2013/11/FINAL-2013-MCC-Brochure.pdf [2013 Jun. 26].

Dufault, N. S., deWolf, E. D., Lipps, P. E. and Madden, L. V. 2006. Role of temperature and moisture in the production and maturation of Gibberella zeae perithecia. Plant Disease **90**: 637-644.

Gervais, M., Bullock, P. R., Mkhabela, M., Finlay, G. and Raddatz, R. 2010. Improvements to the accuracy of modelled soil water content from the Second Generation Prairie Agrometeorological Model. Can. J. Soil Sci. **90**: 523–526.

Hayashi, M., Jackson, J. F. and Xu, L. 2010. Application of the Versatile Soil Moisture Budget Model to Estimate Evaporation from Prairie Grassland. Can. Water Resour. J. **35**: 187–208.

Hayhoe, H.N., Pelletier, R. G. and van Vliet, L. 1993. Estimation of snowmelt runoff in the Peace River region using a soil moisture budget. Can. J. Soil Sci. **73**: 489–501.

Illston, B.G., Basara, J. B. and Crawford, K.C. 2004. Seasonal to interannual variations of soil moisture measured in Oklahoma. Int. J. Climatol. **24**: 1883-1896.

Kersebaum, K.C., Wurbs, A., de Jong, R., Campbell, C. A., Yang, J. and Zentner, R. P. 2008. Long-term simulation of soil–crop interactions in semiarid southwestern Saskatchewan, Canada. Eur. J. Agron. **29**: 1–12.

McGinn, S.M. and Shepherd, A. 2003. Impact of climate change scenarios on the agroclimate of the Canadian prairies. Can. J. Soil Sci. **83**: 623–630.

McNairn, H., Jackson, T. J., Wiseman, G., Béliar, S., Berg, A., Bullock, P., Colliander, A., Cosh, M. H., Kim, S. B., Magagi, R., Moghaddam, M., Adams, J. R., Homayouni, S., Ojo, E. R., Rowlandson, T., Shang, J., Goïta, K. and Hossein, M. 2015. The Soil Moisture Active Passive Validation Experiment 2012 (SMAPVEX12): Pre-Launch Calibration and Validation of the SMAP Satellite. IEEE Trans. Geosci. Remote Sens. **53**: 2784–2801.

McNairn, H., Merzouki, A. and Pacheco, A . 2011. Monitoring soil moisture to support risk reduction for the agriculture sector using RADARSAT-2. p. 3618–3621. *In* IEEE International, Vancouver, BC, Canada.

Meng, L. and Quiring, S. M. 2008. A Comparison of Soil Moisture Models Using Soil Climate Analysis Network Observations. J. Hydrometeorol. **9**: 641–659.

Mkhabela, M.S. and Bullock, P. R. 2012. Performance of the FAO AquaCrop model for wheat grain yield and soil moisture simulation in Western Canada. Agric. Water Manag. **110**: 16–24.

Mohammed, G.A., Hayashi, M., Farrow, C. R. and Takano, Y. 2013. Improved characterization of frozen soil processes in the Versatile Soil Moisture Budget model. Can. J. Soil Sci. **93**: 511–531.

Monteith, J.L. 2000. Agricultural meteorology: evolution and application. Agric. For. Meteorol. **103**: 5–9.

Ojo, E.R. 2012. Modeling soil moisture from real-time weather data. University of Manitoba. Master's Thesis. [Online] Available: http://mspace.lib.umanitoba.ca/handle/1993/5009 [2015 Aug. 10].

Ontario Ministry of Agriculture, Food and Rural Affairs. 2009. Agronomy Guide for Field Crops: Corn Development. [Online] Available: http://www.omafra.gov.on.ca/english/crops/pub811/1corn.htm [2015Jun. 26].

Qian, B., De Jong, R. and Gameda, S. 2009. Multivariate analysis of water-related agroclimatic factors limiting spring wheat yields on the Canadian prairies. Eur. J. Agron. **30**: 140–150.

Robinson, D.A., Campbell, C. S., Hopmans, J. W., Hornbuckle, B. K., Jones, S. B., Knight, R., Ogden, F., Selker, J. and Wendroth, O. 2008. Soil Moisture Measurement for Ecological and Hydrological Watershed-Scale Observatories: A Review. Vadose Zone J. **7**: 358–389.

Robinson, J.M., and Hubbard, K. G. 1990. Soil water assessment model for several crops in the High Plains. Agron. J. **82**: 1141–1148.

Sands, P.J., Hackett, C. and Nix, H. A. 1979. A model of the development and bulking of potatoes (Solanum tuberosum L.). I. Derivation from well-managed field crops. Field Crops Research **2**: 309-331.

Sridhar, V., Hubbard, K. G., You, J. and Hunt, E. D. 2008. Development of the Soil Moisture Index to Quantify Agricultural Drought and Its "User Friendliness" in Severity-Area-Duration Assessment. J. Hydrometeorol. **9**: 660–676.

Statistics Canada. 2015. Table 001-0010: Estimated areas, yield, production and average farm price of principal field crops, in metric units. [Online] Available: http://www5.statcan.gc.ca/cansim/a26?lang=eng&retrLang=eng&id=0010010&pattern=&csid= [2015 Aug. 31].

Steduto, P., Hsiao, T. C., Raes, D. and Fereres, E. 2009. AquaCrop—The FAO Crop Model to Simulate Yield Response to Water: I. Concepts and Underlying Principles. Agron. J. **101**: 426–437.

Wilson, J. L. 2002. Estimation of phenological development and fractional leaf area of canola (Brassica napus L.) from temperature. University of Manitoba. Master's Thesis. [Online] Available: http://hdl.handle.net/1993/7805 [2015 Jul. 26].

5. UPSCALING THE VERSATILE SOIL MOISTURE BUDGET AND POINT-BASED SOIL MOISTURE TO FIELD SCALE

5.1 Abstract

Soil moisture determination from models provides unique opportunities for estimating soil moisture at various spatial extents. However, the accuracy of these models is often validated against observed data derived from a single point or limited spatial coverage. Soil moisture from a single location is often not representative of the field due to soil spatial heterogeneity. In this study, we investigated the errors obtained from two sources of soil moisture data when compared to observed soil moisture derived from 48 sampling points within the field (i) soil moisture from an in-field location, SM_{TS} (ii) modelled soil moisture from the Versatile Soil Moisture Budget, VSMB.. The results obtained showed that the single in-field location, though not always representative of the entire field, gave better soil moisture values than the modelled estimates. Coarse textured sites had an average root mean square error (RMSE) of 0.038 m^3 m^{-3} and 0.043 m^3 m^{-3} under the SM_{TS} and the VSMB, respectively. At the fine textured sites, both the SM_{TS} and the VSMB overestimated soil moisture. Two out of four fine textured sites had negative model efficiency values which indicated that the mean of the observed result was a better estimator of soil moisture than the VSMB.

5.2   Introduction

Rainfall is often used as an indicator of plant available soil moisture. The majority of farmers on the Canadian Prairie do not use soil-placed instruments to monitor soil moisture. Those farmers that do monitor soil moisture purchase a single or very limited number of instruments due to cost. This single instrument is randomly placed in the field at a location that appears to be representative of the farm and data from the point location is extrapolated across the entire field. The use of point measurements taken from instruments with < 0.1m spatial resolution to determine processes and trends occurring at field or watershed levels has been carried out over several decades. Over the last two decades, many studies have focused on the errors associated with this scaling effect (Wilson et al., 2004; De Lannoy et al., 2007; Brocca et al., 2012).

The term "upscaling" as used in this chapter implies taking information on scales smaller (e.g. points) than those of interest (field), smoothening such information (e.g. averaging) and assessing the outcome of the larger scale system (Delleur, 2006). This can be achieved via several means such as (i) sampling at specific field locations that are known to reflect the average field behaviour, (ii) averaging data obtained from various field locations, and (iii) interpolating data from several field locations. The need to develop sampling strategies that compare aerial estimates to data from point samples is vital due to the increasing use of remote sensing for soil moisture determination (Moran

et al., 2004; Thoma et al., 2008; McNairn et al., 2010; Kornelsen and Coulibaly, 2013; Pierdicca et al., 2013). Rowlandson et al. (2013) highlighted several field campaigns over the last 15 years that required ground *truthing*, using intensive soil moisture sampling, for calibrating and validating remotely sensed measurements. In order to determine the single soil moisture value that represents the spatial extent of interest based on field observation, factors such as the appropriate number of required samples as well as the determination of error associated with the point instrument used for sampling are considered.

Soil moisture measurements have traditionally been determined at point level with the use of various instruments such as the neutron probe calibrated by the thermogravimetric method. Frequency and time domain reflectometry point sensors have largely replaced the neutron probe because of their ability to provide continuous temporal measurement. These instruments have been used to create vast soil moisture monitoring networks (Seyfried and Murdock, 2004; Ojo et al., 2015) to which spatial comparison can be made.

The spatial variability of soil moisture at field and watershed scales as well as the number of point-based samples required to make reasonable conclusions on larger scales have been the focus of previous research. Grayson and Western (1998) promoted the time stability concept introduced by Vachaud et al. (1985) to demonstrate that soil moisture content at certain locations in the landscape consistently provide reasonable agreement with the average soil moisture content across the entire landscape. This concept premised that instead of undertaking intensive soil moisture sampling of an area, the average soil moisture can be determined from limited sample locations that consistently showed minimal deviation from the aerial estimates.

Time stability analysis was tested by Jacobs et al. (2004) on the ground-based data collected during Soil Moisture Experiment 2002 (SMEX02) to validate soil moisture products retrieved from remote sensors. They showed that a carefully selected single sampling point within a field can provide comparable accuracy to the field average from several measurements. Topography and soil characteristics such as texture are important considerations in selecting the single, representative point. Cosh et al. (2004) tested the temporal and spatial stability of soil moisture on a watershed scale (~ 100 km^2) and demonstrated that if spatial and temporal stability is known, single point in-situ measurements can provide reasonable estimates of area average soil moisture. Martinez-Fernandez and Ceballos (2005) studied two fields with different scales (1285 km^2 and 0.62 km^2) in Spain and at both spatial scales, temporal stability analysis showed stations that were consistently representative of the mean soil moisture condition irrespective of wet or dry conditions. Dente et al. (2012) observed that the spatial patterns of soil moisture monitored at the Tibetan Plateau were not always stable in time and used weighted spatial average to validate remotely-sensed soil moisture products.

The duration of most field campaigns for remote sensing validation are usually less than a month. It is impossible to accurately assess the spatial and temporal stability of an area as well as the dominant process controlling soil moisture patterns within this limited time frame. Martinez-Fernandez and Ceballos (2005) concluded that at least a year of measurements is required to determine the representative mean soil moisture. Since the time stability concept requires the comparison of field average soil moisture to single point measurements to determine which point(s) consistently show comparable soil

moisture content to the field average, this approach has merit in locations for which future field sampling is planned.

Installing field instruments for continuous, intensive soil moisture monitoring at a provincial scale is an impossible task. Therefore, models are used to increase the number of point measurements for locations at which soil moisture can be simulated using weather, soil and vegetation data. Estimating soil moisture from models that have been calibrated and validated can be cost-effective compared to the use of instruments. These models use a combination of atmospheric drivers such as precipitation and temperature and soil surface characteristics such as soil texture and vegetation type to estimate soil moisture. One such model is the Versatile Soil Moisture Budget (VSMB). It is a simple land-surface, water-balance model that has been widely used and validated across the Canadian Prairie (Akinremi et al., 1996; Sheppard et al., 2007; Hayashi et al., 2010).

The first objective of this study was to assess the accuracy of the VSMB to simulate field-scale surface soil moisture by comparing the model's estimate to the observed field average derived from 48 sampling locations within the field. Intensive field sampling is expected to help determine the ability of the model to accurately represent average surface soil moisture at field-scale. Validation of models, including VSMB, is often done by comparing the modelled result to in-field observations taken at a single location on the field (Xiao et al., 2006; Hayashi et al., 2010; Bellingham, 2013). This single location, however, may not be a good representation of the average field-scale soil moisture condition. The second objective was to determine the representativeness of soil moisture measurements from an arbitrarily selected single point in a field that *looks* representative of the area compared to the field average. This is similar to what a farmer

will do in assessing soil moisture status on the field or as mentioned earlier, models are sometimes validated using observations from a single location.

5.3   Materials and Methods

5.3.1   Site Location

This research was conducted in the Carman-Elm Creek area of Manitoba, Canada during the Soil Moisture Active Passive Validation EXperiment in 2012 - SMAPVEX12 (Figure 5.1). SMAPVEX12 was one of several calibration and validation experiments carried out to test algorithms used for soil moisture retrieval before the launch of the SMAP satellite on January 31, 2015. McNairn et al. (2015) published detailed information about SMAPVEX12 which included both the ground data and air-borne data collection. The study area is generally flat with <2% slope and included a varying range of soil texture from heavy clay soils with > 60% clay content to sandy soils with > 90% sand fraction. The validation campaign ran from June 7 through July 19, 2012 and covered an area about 13 km by 70 km consisting of various annual crops, pasture and forest.

The 1981-2010 climate normal for this area showed daily average temperature in June and July were 17.2°C and 19.4°C, respectively with 96.4 mm of rainfall in June and 78.6 mm in July (Environment Canada, 2014). During the study, the average temperatures were 17.7°C in June and 21.9°C in July with about 75 mm of rainfall in June and 65 mm in July. Several weather stations installed and managed by Environment

Canada, Manitoba Agriculture Weather Program and WeatherFarm are located within and around the study area. Agriculture and Agri-Food Canada (AAFC) installed tipping bucket rain gauges and soil moisture probes at nine locations within the study area (Figure 5.1). For this study, a subset of eight fields was selected from the fifty-five fields monitored during the campaign. Selection criteria for these eight fields were based on soil characteristics (equal representation of coarse and fine textured soil), availability of continuous hourly soil moisture measurements and proximity to a weather station for modeling purposes. Four of the selected fields were coarse textured with less than 15% clay and the other four were fine textured soils with ≥40% clay content (Table 5.1).
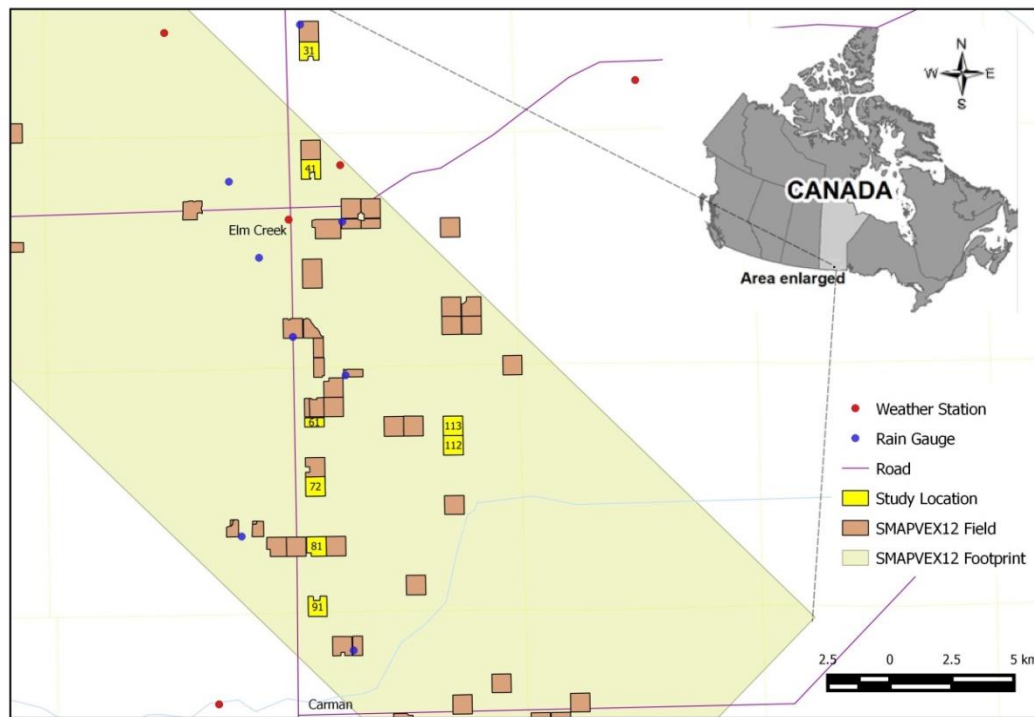
Figure 5.1   Overview of study location

5.3.2 Soil Moisture Monitoring

5.3.2.1   Field Observation. Observed surface soil moisture was determined using vertically inserted Stevens Hydra probes (0-6 cm) to take three replicates of soil moisture measurements at 16 pre-determined sampling points on each field. The 16 sampling points were divided into two transects parallel to crop row direction, each with 8 sampling points. Points within each transect were 75 m apart and the two transects were 200 m apart (Figure 5.2). Calibration of the soil moisture instrument was carried out using samples from a bulk density core which was collected on each sampling day.

Table 5.1 Physical properties of soils at 5 cm

Station ID	Crop	Sand – Silt – Clay (%)
31	Wheat	04-56-40
41	Wheat	04-32-64
61	Canola	83-05-12
72	Corn	93-02-05
81	Wheat	87-05-08
91	Wheat	88-04-08
112	Soybean	03-31-66
113	Soybean	03-33-64
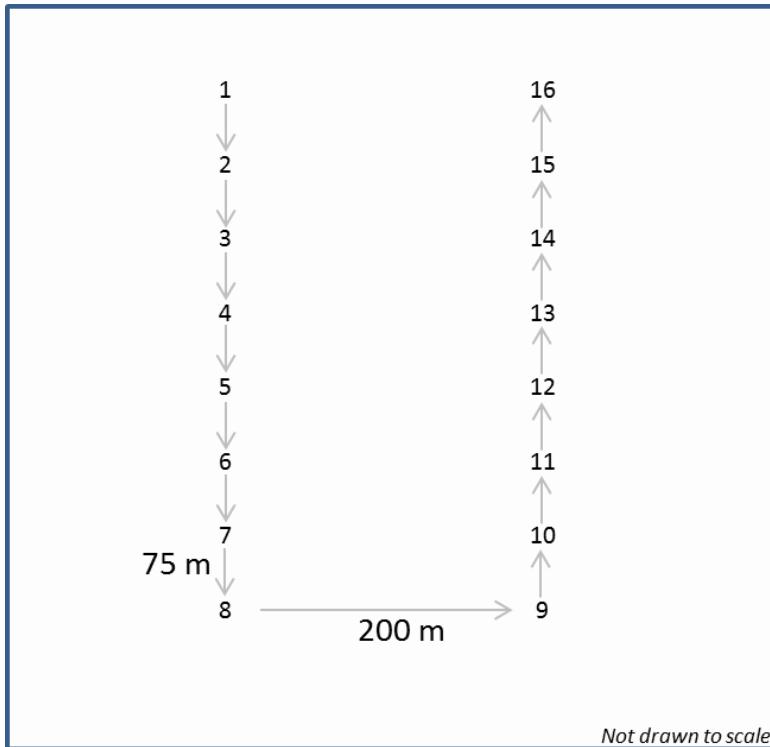
Figure 5.2   Layout of soil moisture field sampling

Rowlandson et al. (2013) evaluated several calibration procedures for the soil moisture probes during SMAPVEX12 and reported an average root mean square error (RMSE) value of 0.037 for field-specific calibration. On each soil moisture sampling day, the arithmetic mean of the 48 soil moisture measurements (three replicates at 16 points) collected in each field was used as the field observed soil moisture content. Other types of data aggregation such as geometric mean as well as the use of the median data were tried (data not shown) but none of these showed any significant difference from the arithmetic mean at most of the sites. This sampling for field-based surface soil moisture determination was carried out about 16 times during the duration of the campaign; however, not all fields were sampled on all sampling days. McNairn et al. (2015)

reported that the standard deviation for many of the intra-field soil moisture measurements was between 0.023 and 0.045 $m^3 m^{-3}$.

5.3.2.2   Temporary Stations.   Each field had a continuous soil moisture monitoring station located at point 1 (Figure 5.2). These temporary stations were provided by the United States Department of Agriculture and were installed prior to the start of SMAPVEX12. The stations remained in place throughout the duration of the campaign. Each station consisted of a Stevens soil moisture probe installed horizontally at 5 cm and a data-logger that recorded hourly soil moisture data and was powered by a battery that was charged using a solar panel. This single point installation, though limited in spatial extent, provided high temporal frequency data and is similar to what farmers interested in knowing the moisture status of their field may do. To coincide with the period when field observed soil moisture was determined, the mean of hourly data between 7 am and 12 pm was taken as the temporary station soil moisture (SM_{TS}).

5.3.2.3   Versatile Soil Moisture Budget (VSMB).   As described in the preceding chapter, VSMB is a model that simulates the vertical movement of soil moisture using weather data as well as soil and crop information. The model uses a simple water balance method to estimate soil moisture retention at each soil layer and has been widely used across the Canadian prairie (Hayhoe et al., 1993; Akinremi et al., 1996; Hayashi et al., 2010; Chipanshi et al., 2013). VSMB has user-defined soil layer depth and can run with minimal data input. Soil and crop information required to run the model include crop type, soil texture, water holding capacity, field capacity and the permanent wilting point. Soil texture data were obtained from the SMAPVEX12 database. The maximum and minimum volumetric water contents reached by the temporary soil moisture station

113

installed on each study field were taken as the water holding capacity and the permanent wilting point, respectively. Hayashi et al., (2010) published detailed information on the VSMB. Although the VSMB can simulate soil moisture at user-defined depths, the interest of this study lies in the dynamic surface layer which was defined as 0-10 cm.

The VSMB was used to estimate soil moisture at eight fields using the air temperature and precipitation data from the closest weather station. If the distance between a weather station and a field was greater than 5 km, a simple mean interpolation of the two closest weather stations was used to derive the air temperature data used for such fields. In all cases, the tipping bucket rain gauge data closest to each field was used and all precipitation data used to run the VSMB for each field were collected within 7 km of the field.

5.3.3 Data Analysis

Both the VSMB modelled soil moisture and soil moisture from temporary station (SM_{TS}) were compared to field observed soil moisture using statistical indicators such as the root mean square error (RMSE), the mean bias error (MBE) and the model efficiency (E). Better agreement with observed measurement is achieved when RMSE and MBE values are closer to 0. E ranges from - ∞ to 1 and the closer E is to 1, the better the model performance. Negative E values infer that the mean of the observations is a better predictor than the model.

$$\text{RMSE} = \left(\frac{\Sigma (M_i - Obs_i)^2}{n} \right)^{0.5} \qquad\qquad [5.1]$$

$$MBE = \frac{1}{n} \left[\sum_{i=1}^{n} (M_i - Obs_i) \right] \qquad\qquad [5.2]$$

$$E = 1 - \frac{\sum_{i=1}^{n}(M_i - Obs_i)^2}{\sum_{i=1}^{n}(Obs_i - \overline{Obs})^2} \qquad\qquad [5.3]$$

where *M* is the soil moisture from the VSMB or from SM_{TS} and *Obs* is the observed soil moisture on day *I* averaged over 48 points. Soil moisture from SM_{TS} (7 am – 12 pm) and the VSMB provided a time-continuous data record, however, field sampling for observed soil moisture was carried out 16 times during the SMAPVEX12 campaign on specific dates. Statistical analysis considered only the days when field sampling for soil moisture was done.

5.4   Results and Discussion

5.4.1   Coarse Textured Soil

The six week duration of the campaign was adequate to capture a range of soil moisture conditions from relatively wet at the start of the campaign through a dry-down period midway into the experiment. Out of the four coarse textured fields used in this study, two fields (61 and 72) had 16 days of soil moisture sampling. Fields 81 and 91 had 11 and 14 soil moisture sampling days, respectively. The MBE values for the comparison between VSMB and *Obs* ranged from -0.014 to 0.04 m^3 m^{-3} and VSMB overestimated observed soil moisture at two of the four coarse textured fields. The RMSE values ranged from 0.037 to 0.05 m^3 m^{-3} (Table 5.2). The comparison between SM_{TS} and *Obs* resulted in RMSE values that ranged from 0.023 to 0.05 m^3 m^{-3} with MBE values ranging from -0.045 to 0.009 m^3 m^{-3}. Three of the four fields showed that SM_{TS} underestimated soil

moisture. Similar to this study, Adams et al. (2015) compared the field-mean soil moisture to observations at a point location, SM_{TS}, on some SMAPVEX fields (different from the locations used in this study). At two coarse textured sites monitored, the authors observed RMSE < 0.04 m^3 m^{-3} which was better than the result obtained in this study.

Table 5.2 Statistical analysis

Site	n	RMSE (m^3 m^{-3})		MBE (m^3 m^{-3})		E	
		SM_{TS}	VSMB	SM_{TS}	VSMB	SM_{TS}	VSMB
61	16	0.037	0.037	-0.012	0.018	0.33	0.31
72	16	0.023	0.050	0.009	0.040	0.65	-0.66
81	11	0.050	0.046	-0.045	-0.014	-0.21	0.01
91	14	0.043	0.039	-0.033	0	0.23	0.34
Average		0.038	0.043	-0.020	0.011		
31	14	0.057	0.081	0.040	0.048	0.56	0.11
41	14	0.068	0.085	-0.044	0.054	0.48	0.15
112	16	0.074	0.108	0.059	0.099	-0.09	-1.42
113	16	0.036	0.128	0.021	0.112	0.84	-1.09
Average		0.059	0.101	0.019	0.078		

RMSE = Root Mean Square Error, MBE= Mean Bias Error and E = Model Efficiency.

Irrespective of the type of soil moisture monitoring, similar trends and response to rainfall events as well as dry-down periods in response to evaporative demands were observed (Figure 5.3). However, the magnitude of these responses varied. With the exception of field 72, both the VSMB and the SM_{TS} mostly underestimated observed soil moisture towards the end of the campaign which was characterized by localized rainfall events (Figure 5.4). Overall, using a soil moisture value obtained from a randomly selected location on the field (SM_{TS}) was better than a VSMB modelled soil moisture value.
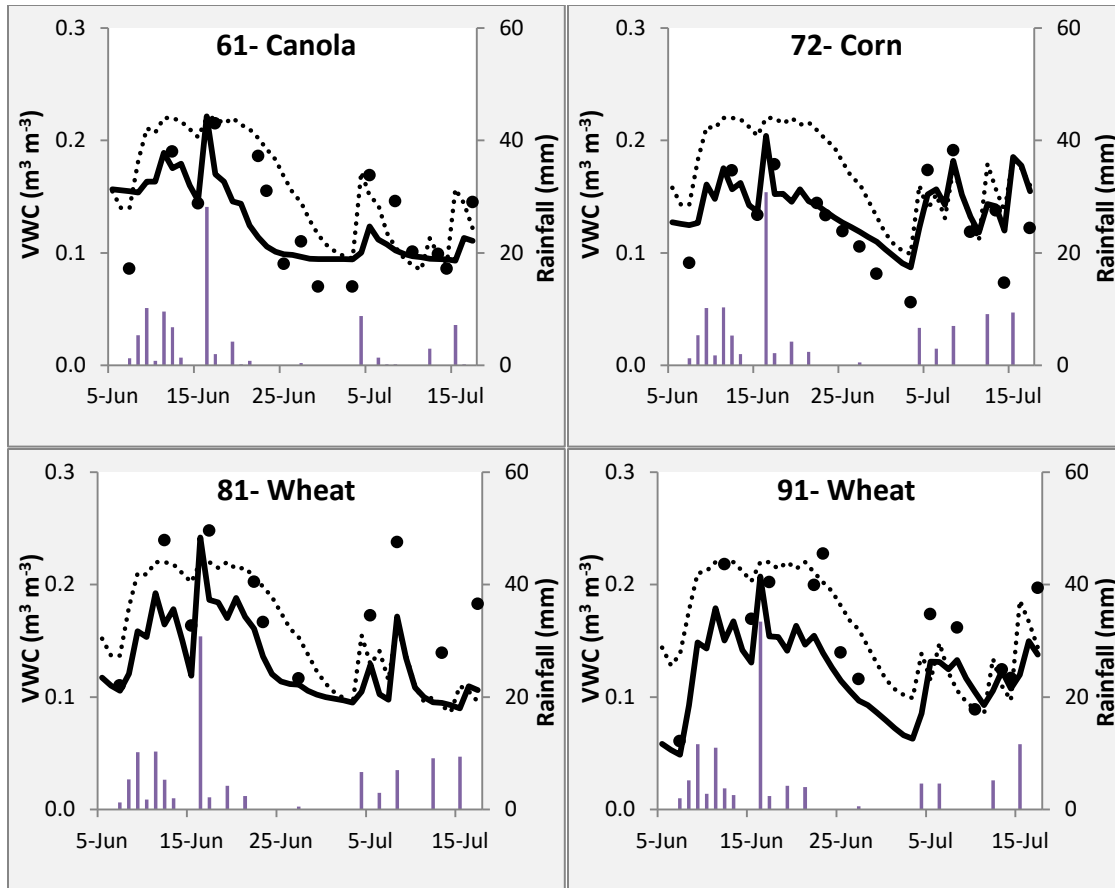
Figure 5.3   Soil moisture trend at 5 cm at the coarse textured sites showing VSMB modelled (dotted line), temporary station (SM_{TS}, solid black line) and field observed (black circles) volumetric water content (VWC). Vertical bars represent rainfall.

Across all four coarse textured sites, SM_{TS} had a lower RMSE of 0.038 m^3 m^{-3} compared to the value obtained from model analysis which was 0.043 m^3 m^{-3}. The result of the comparison between VSMB and *Obs* obtained from this study is better than the result reported in preceding chapter that showed an average RMSE value of 0.052 m^3 m^{-3} across eight coarse textured site-years. Meng and Quiring (2008) compared the accuracy of three models (DSSAT, VIC and CWB) to simulate soil moisture. The results obtained at a coarse textured site (Powder Mill) had RMSE and *E* values that ranged from 0.03 m^3 m^{-3} to 0.13 m^3 m^{-3} and -5.94 to 0.73, respectively. Bellingham (2013) had better results

using the HYDRUS 1D model at a coarse-textured site with 71% sand and 25% silt. The author reported RMSE, MBE and E values of 0.01 m^3 m^{-3}, 0.01 m^3 m^{-3} and 0.36, respectively.
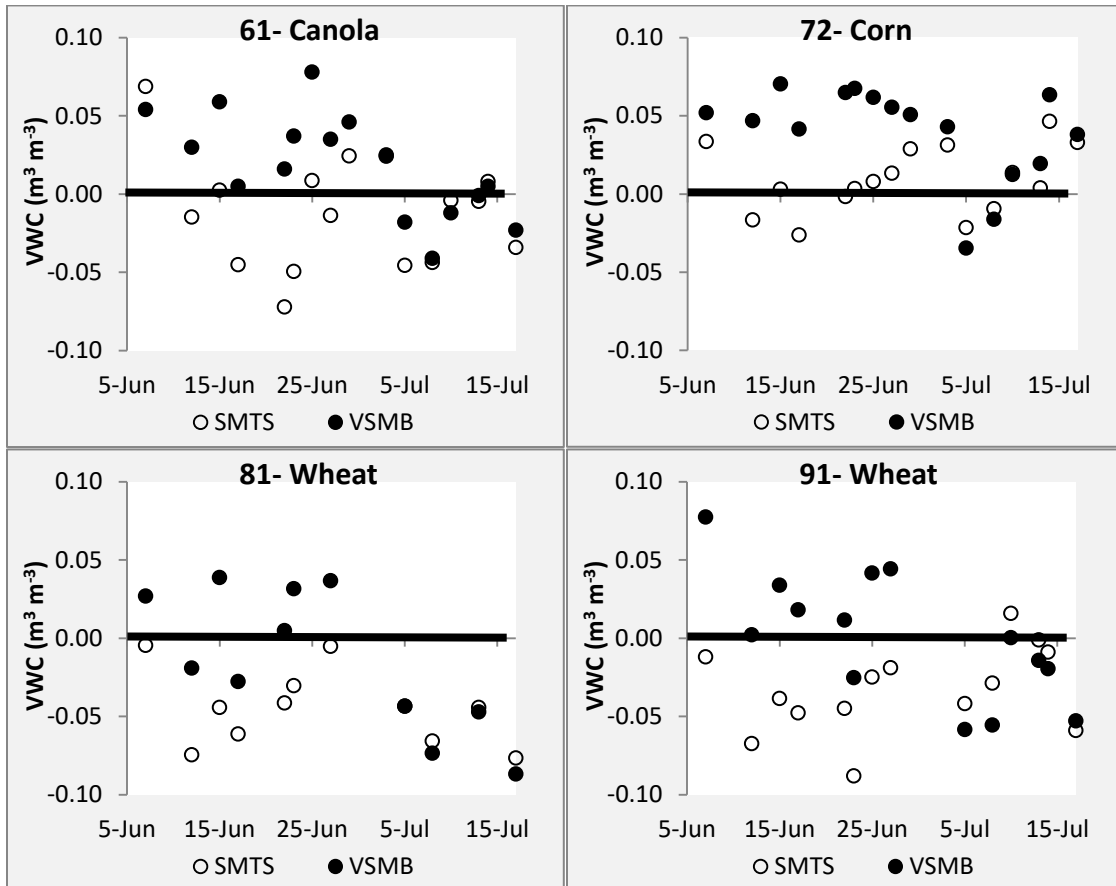
Figure 5.4   Deviation of VSMB modelled and temporary station soil moisture from field observed volumetric water content (VWC) at coarse textured fields.

Model efficiency (E) was highest under SM$_{TS}$ at field 72. This field also had the best RMSE and MBE values of 0.023 m^3 m^{-3} and 0.009 m^3 m^{-3}, respectively. The mean of observed soil moisture was a better predictor than SM$_{TS}$ at field 81 which had E value of -0.21 as well as the worst RMSE and MBE values of the four coarse-textured fields considered. Under the VSMB, E values ranged from -0.66 at site 72 to 0.34 at site 91.

118

Only site 72 had a negative E value which indicated that the mean of observed soil moisture was a better predictor of soil moisture than the VSMB.

VSMB soil moisture results at sites 72 and 81 were simulated using precipitation data that was collected about 4 km from the fields and both sites had relatively poor statistical indicators compared to sites 61 and 91 which had precipitation data collected within 2 km of the field. Towards the end of the campaign, observed soil moisture at site 81 showed relatively high response to rainfall compared to marginal response shown by both the VSMB and the SM_{TS}. Dyck and Gray (1977) investigated the spatial characteristics of Prairie rainfall over 8 years in west central Saskatchewan by determining the minimum gauge density (number of rain gauges per square mile) that is comparable to their dense network of one rain gauge per square mile. The authors reported that for cumulative monthly and seasonal rainfall, 0.38 (or one gauge per 6.8 km^2) and 0.10 (or one gauge per 25.9 km^2) gauge densities, respectively, would suffice. Although the gauge density for daily rainfall was not analysed, the result would be expected to be in the order of one gauge in less than 2 km^2 area.
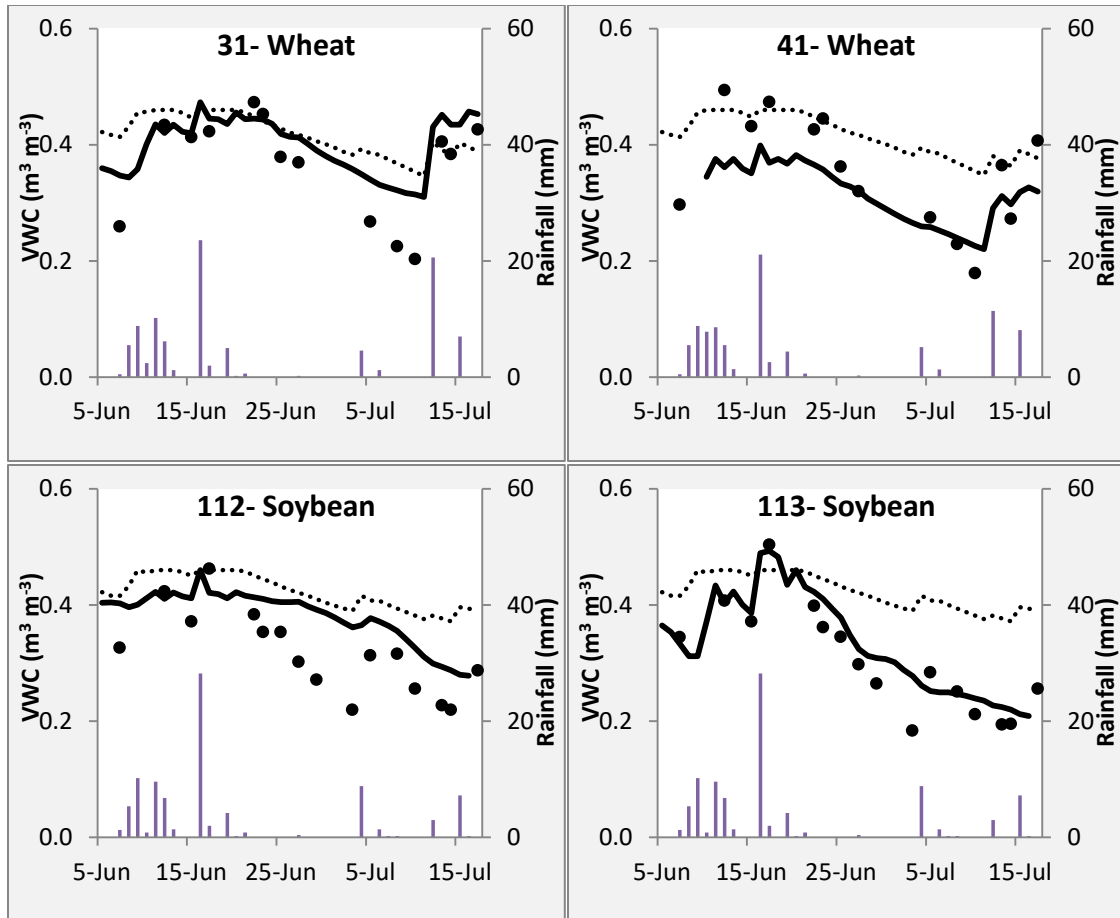
Figure 5.5   Soil moisture trend at 5 cm at the fine textured sites showing VSMB modelled (dotted line), temporary station (SMTS, solid black line) and field observed (black circles) volumetric water content (VWC). Vertical bars represent rainfall.

5.4.2   Fine Textured Soil

Figures 5.5 and 5.6 showed that the VSMB overestimated surface soil moisture at all the four fine textured sites, especially, during the dry-down period. The modelled drying rate was slower compared to the observed. The MBE values obtained from the VSMB ranged from 0.048 to 0.112 m^3 m^{-3} compared to -0.044 to 0.059 m^3 m^{-3} MBE values obtained from SM_{TS}. The SM_{TS} results showed that the sampling location selected for this study at three of the four fine textured sites was wetter than most areas of the field and this

120

impacted the field-scale soil moisture assessment. Except at site 41, SM_{TS} overestimated soil moisture but to a lesser magnitude compared to VSMB.
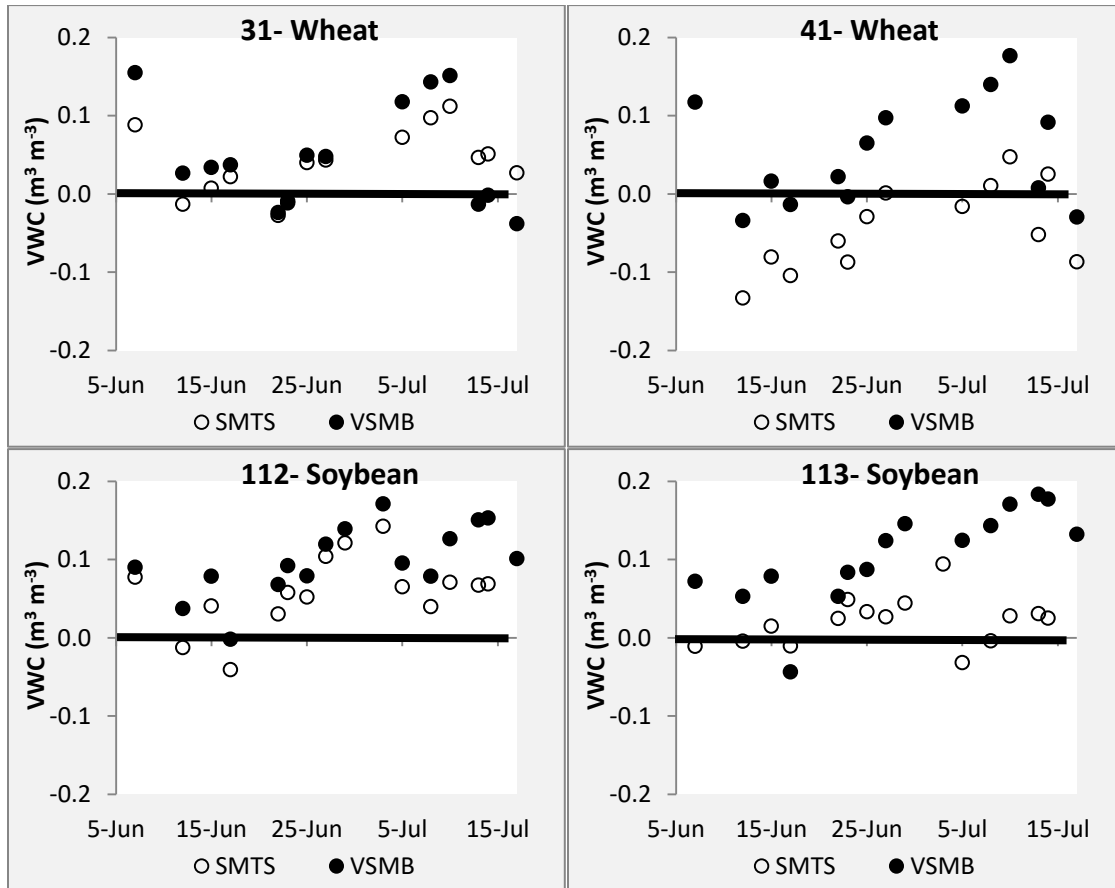
Figure 5.6   Deviation of VSMB modelled and temporary station soil moisture from field observed volumetric water content (VWC) at fine textured fields.

Field 112 had the worst RMSE value of 0.074 m^3 m^{-3} under SM_{TS}. However, this result was better than field 31 which had the best RMSE value of 0.081 under VMSB. The average RMSE values across all four fine textured sites for the modelled and SM_{TS} were 0.101 m^3 m^{-3} and 0.059 m^3 m^{-3}, respectively (Table 5.2). The results obtained in this study are comparable to those by Meng and Quiring (2008) at a silty clay site. Their

results showed that RMSE values obtained with the three models ranged from 0.05 – 0.14 m^3 $m^{-3}$and the E values ranged from -1.50 to 0.56.

Although precipitation is one of the main drivers of soil moisture, the high bias from the VSMB at the fine textured soils was as a result of the overestimated soil moisture during dry-down periods due to lower rate of drying compared to the observed soil moisture. Despite using the same empirical drying curve function and coefficients, this result contrasts what was observed at the RISMA sites in the preceding chapter where the VSMB had faster drying rates compared to the observed soil moisture. The empirical drying curve function should be independently studied to validate the coefficients used in the function. A model sensitivity test conducted by Hayashi et al., (2010) reported that the drying curve function had a highly significant influence in determining the model's evaporation rate.

The SM_{TS} was quite representative of the observed soil moisture. However, it overestimated soil moisture during the dry-down period at sites 31 and 112. Similar to this study, Adams et al. (2015) reported RMSE values that ranged from 0.06 – 0.15 m^3 m^{-3} at locations with high clay content compared to RMSE values between 0.036 – 0.74 m^3 m^{-3} recorded in this study. The reduction in the level of bias in our study compared to Adams et al. (2015) could be due to the use of mean hourly data between 7 am and 12 pm for the temporary station soil moisture (SM_{TS}) to coincide with the period when field observed soil moisture was determined. The performance of SM_{TS} at coarse textured soil was better than at fine textured soil. However, Adams et al. (2015) showed that fine textured soils had more divergent RMSE when both vertically and horizontally installed point measurements were compared to the observed field average. The authors reported a

difference of over 0.05 m^3 m^{-3} in the RMSEs at a location. The vertically installed probes had lower RMSEs at all the fine-textured sites. The 48 field samples were collected by inserting the probes vertically into the soil but the horizontal installation data were used for (SM$_{TS}$) in this study. Horizontal installation is often preferred for mid-long term monitoring due to the potential occurrence of surface runoff or surface cracking in dry clay soils which may limit the probe-soil matrix contact, thereby introducing low measurement bias.

5.5   Conclusions

Soil moisture from a single location on the field and simulated soil moisture using VSMB were compared to field-averaged observed soil moisture. This study showed that monitoring soil moisture at an arbitrarily selected location on the field generally gave a better result than the VSMB model. Although modelling has many benefits, such as limited costs and reasonable agreement with observed soil moisture, the need to have monitoring stations cannot be over-emphasized. In modelling, greater focus is often given to the main output of interest, which is soil moisture in this case; validating other areas of the hydrological processes such as evapotranspiration (influenced by the drying curve function) that are being simulated alongside should be given equal attention. Future validation of the VSMB should ensure that data input to the model, especially precipitation data, are obtained from weather stations which are installed at or close to the study location.

5.6 Acknowledgements

5.7 References

Adams, J. R., McNairn, H., Berg, A. A. and Champagne, C. 2015. Evaluation of near-surface soil moisture data from an AAFC monitoring network in Manitoba, Canada: Implications for L-band satellite validation. J. Hydrol., **521**:582–592.

Akinremi, O. O., McGinn, S. M. and Barr, A. G. 1996. Simulation of soil moisture and other components of the hydrological cycle using a water budget approach. Can. J. Soil Sci., **76**:133–142.

Bellingham, B. K. 2013. New quality assurance technique for meteorological stations based on a physically-based hydrological model (pp. 1–12). Presented at the Western Snow Conference, Wyoming, USA.

Brocca, L., Tullo, T., Melone, F., Moramarco, T. and Morbidelli, R. 2012. Catchment scale soil moisture spatial–temporal variability. J. Hydrol., **422**–**423**:63–75.

Chipanshi, A. C., Warren, R. T., L'Heureux, J., Waldner, D., McLean, H. and Qi, D. 2013. Use of the National Drought Model (NDM) in Monitoring Selected Agroclimatic Risks Across the Agricultural Landscape of Canada. Atmosphere-Ocean, **51**:471–488.

Cosh, M., Jackson, T. J., Bindlish, R. and Prueger, J. 2004. Watershed scale temporal and spatial stability of soil moisture and its role in validating satellite estimates. Remote Sens. Environ., **92**:427–435.

De Lannoy, G. J. M., Houser, P. R., Verhoest, N. E. C., Pauwels, V. R. N. and Gish, T. J. 2007. Upscaling of point soil moisture measurements to field averages at the OPE3 test site. J. Hydrol., **343**:1–11.

Delleur, J. W. (Ed.). 2006. The handbook of groundwater engineering. CRC press.

Dente, L., Vekerdy, Z., Wen, J. and Su, Z. 2012. Maqu network for validation of satellite-derived soil moisture products. Int. J. Appl. Earth Obs. Geoinformation, **17**:55–65.

Dyck, G. and Gray, D. 1977. Spatial characteristics of prairie rainfall (pp. 110–116). Presented at the Conference on Hydrometeorology, Toronto, Ont. (Canada): American Meteorological Society.

Environment Canada. 2014. 1981-2010 Climate Normals and Averages. Available at http://climate.weather.gc.ca/climate_normals/stnselect_1981_2010_e.html?province=MAN&lang=e&provBut=Go&page=12014

Grayson, R. B. and Western, A. W. 1998. Towards areal estimation of soil water content from point measurements: time and space stability of mean response. J. Hydrol., **207**:68–82.

Hayashi, M., Jackson, J. F. and Xu, L. 2010. Application of the Versatile Soil Moisture Budget Model to Estimate Evaporation from Prairie Grassland. Can. Water Resour. J., **35**:187–208.

Hayhoe, H. N., Pelletier, R. G. and Vliet, L. van. 1993. Estimation of snowmelt runoff in the Peace River region using a soil moisture budget. Can. J. Soil Sci., **73**:489–501.

Jacobs, J. M., Mohanty, B. P., Hsu, E.-C. and Miller, D. 2004. SMEX02: Field scale variability, time stability and similarity of soil moisture. Remote Sens. Environ., **92**:436–446.

Kornelsen, K. C. and Coulibaly, P. 2013. Advances in soil moisture retrieval from synthetic aperture radar and hydrological applications. J. Hydrol., **476**:460–489.

Martínez-Fernández, J. and Ceballos, A. 2005. Mean soil moisture estimation using temporal stability analysis. J. Hydrol., **312**:28–38.

McNairn, H., Jackson, T. J., Wiseman, G., Belair, S., Berg, A., Bullock, P., Colliander, A., Cosh, M. H., Kim, S.-B., Magagi, R., Moghaddam, M., Njoku, E. G., Adams, J. R., Homayouni, S., Ojo, E., Rowlandson, T., Shang, J., Goita, K. and Hosseini, M. 2015. The Soil Moisture Active Passive Validation Experiment 2012 (SMAPVEX12): Prelaunch Calibration and Validation of the SMAP Soil Moisture Algorithms. IEEE Trans. Geosci. Remote Sens., **53**:2784–2801.

McNairn, H., Merzouki, A. and Pacheco, A. 2010. Estimating Surface Soil Moisture Using RADARSAT-2 (Vol. XXXVIII, Part 8, pp. 576–579). Presented at the Networking the World with Remote Sensing, Kyoto, Japan: International Archieves of the Photogrammetry.

Meng, L. and Quiring, S. M. 2008. A Comparison of Soil Moisture Models Using Soil Climate Analysis Network Observations. J. Hydrometeorol., **9**:641–659.

Moran, M. S., Peters-Lidard, C. D., Watts, J. M. and McElroy, S. 2004. Estimating soil moisture at the watershed scale with satellite-based radar and land surface models. Can. J. Remote Sens., **30**:805–826.

Ojo, E. R., Bullock, P. R., L'Heureux, J., Powers, J., McNairn, H. and Pacheco, A. 2015. Calibration and Evaluation of a Frequency Domain Reflectometry Sensor for Real-Time Soil Moisture Monitoring. Vadose Zone J., **14**:.

Pierdicca, N., Pulvirenti, L., Bignami, C. and Ticconi, F. 2013. Monitoring Soil Moisture in an Agricultural Test Site Using SAR Data: Design and Test of a Pre-Operational Procedure. IEEE J. Sel. Top. Appl. Earth Obs. Remote Sens., **6**:1199–1210.

Rowlandson, T. L., Berg, A. A., Bullock, P. R., Ojo, E. R., McNairn, H., Wiseman, G. and Cosh, M. H. 2013. Evaluation of several calibration procedures for a portable soil moisture sensor. J. Hydrol., **498**:335–344.

Seyfried, M. S. and Murdock, M. D. 2004. Measurement of soil water content with a 50-MHz soil dielectric sensor. Soil Sci. Soc. Am. J., **68**:394–403.

Sheppard, S. C., De Jong, R., Sheppard, M. I., Bittman, S. and Beaulieu, M. S. 2007. Estimation of ammonia emission episodes for a national inventory using a farmer survey and probable number of field working days. Can. J. Soil Sci., **87**:301–313.

Thoma, D. P., Moran, M. S., Bryant, R., Rahman, M. M., Collins, C. D. H., Keefer, T. O., Noriega, R., Osman, I., Skrivin, S. M., Tischler, M. A., Bosch, D. D., Starks, P. J. and Peters-Lidard, C. D. 2008. Appropriate scale of soil moisture retrieval from high resolution radar imagery for bare and minimally vegetated soils. Remote Sens. Environ., **112**:403–414.

Vachaud, G., De Silans, A. P., Balabanis, P. and Vauclin, M. 1985. Temporal Stability of Spatially Measured Soil Water Probability Density Function. Soil Sci. Soc. Am. J., **49**:822–828.

Wilson, D. J., Western, A. W. and Grayson, R. B. 2004. Identifying and quantifying sources of variability in temporal and spatial soil moisture observations. Water Resour. Res., **40**:1–10.

Xiao, W., Yu, Q., Flerchinger, G. N. and Zheng, Y. 2006. Evaluation of SHAW Model in Simulating Energy Balance, Leaf Temperature, and Micrometeorological Variables within a Maize Canopy. Agron. J., **98**:722.

6. SYNTHESIS

6.1 Important Findings and Implications

This dissertation reported the accuracy and suitability of various soil moisture instruments in highly reactive clays and suggested a novel approach of using cation exchange capacity-based categorization in developing a universal calibration equation for a Frequency Domain Reflectometry instrument. The field-scale representativeness of a widely used model on the prairie and a single soil moisture station were also reported.

The impacts of soil moisture on the quantity and quality of crop yield have been long understood (Denmead and Shaw, 1960; Aspinall et al., 1964; Heapy et al., 1976; Walker, 1989). However, many recent studies have focused on the influence of soil moisture in global and regional climate (Hanesiak et al., 2004; Seneviratne et al., 2010; Wei and Dirmeyer, 2012). Identifying a single soil moisture value that will represent a specified spatial extent requires strategic soil sampling techniques which usually include careful integration of several representative ground measurements. With many instruments available to monitor soil moisture at a point-scale, it is imperative to analyze the adaptability of these instruments under various environmental conditions before extensive use. The level of uncertainty introduced at the point level will be transferred

and magnified when determining up-scaled soil moisture values from these point measurements.

The findings reported in the study that analyzed the performance of five soil moisture instruments in heavy clay soils is the first multi-sensor assessment in highly reactive smectite clay soils with over 70% clay content. The study affirms that sensor calibration is an important exercise in improving the accuracy of these soil moisture instruments. All the five instruments tested had improved accuracy after calibration. The Theta probe had the best pre-calibration performance and showed very minimal post-calibration gain. Analyzing 24 independent data points, the pre-calibration equation yielded a RMSE value of 0.027 m^3 m^{-3} and this was slightly improved after calibration with a RMSE of 0.023 m^3 m^{-3}. The Hydra probe had the worst pre-calibration result yielding a RMSE value of 0.129 m^3 m^{-3} but had the best post-calibration performance with an impressive RMSE of 0.014 m^3 m^{-3}. Overall, the pre-calibration accuracy of the three pronged sensors; Theta probe, ECHO EC5 and the Hydra Probe; aligned with the increase in their operating frequency. Theta probe, ECHO EC5 and the Hydra Probe operate at 100 MHz, 70 MHz and 50 MHz, respectively and the pre-calibration accuracy was reduced with lower operating frequency. This finding is similar to Logsdon and Hornbuckle (2006) who suggested that the Hydra probes' sensitivity to electrical conductivity may be influenced by its lower operating frequency.

Two multi-depth sensors, EnviroSCAN and Diviner, operate at a frequency of 100 MHz and were included in the instrument comparisons. These sensors are widely used for monitoring soil moisture at different depths and require the installation of an access tube. They measure the moisture content of the soil volume within 10 cm diameter

of the tube. At low soil moisture contents, both devices underestimated observed soil moisture and this is speculated to be due, in part, to the presence of cracks within the sensing volume. Cracked areas were avoided in the soil samples collected for calibration and this may not be representative of the soil matrix within the sensing volume of the two multi-depth sensors. Cracks are normal occurrence in the matrix of dry heavy clay soil as a result of the swell-shrink cycles in response to wetting and drying. Calibration evidently improved the accuracy of all the devices tested, including the two multi-depth sensors.

Post-calibration bias was highest in the EnviroSCAN and Diviner compared to the three-pronged sensors. The calibration equations developed in this study yielded comparable RMSE values with the calibration equation suggested by the manufacturer developed at a cracking clay site (Sentek Technologies, 2011). Although the textural breakdown of the cracking clay site was not indicated in the publications, Sentek Technologies estimated 50-60% clay content at the sites used in developing the calibration equation (Diane Atkinson pers. comm.). Other published calibration equations developed at other clay textured sites resulted in RMSE values greater than 0.07 m^3 m^{-3}, much higher than those derived in this study and above the often-stated target of 0.04 m^3 m^{-3}.

This study provides a critical insight that would assist producers, agronomists, researchers and government agencies to decide which instrument to select in monitoring soil moisture in heavy clay soils. The Manitoba 2011 flood review report (Manitoba Government, 2013) highlighted the need to have observed soil moisture data in the province and recommended that soil moisture monitoring sites be established. For widespread deployment where developing site-specific calibration may not be feasible,

this study indicates that Theta probes may be the best-suited sensor under such circumstances. Remote sensing campaigns such as SMAPVEX12, that compared massive ground data to remotely sensed soil moisture, used calibrated hydro probes (Rowlansdson et al., 2013). Several considerations can impact which instrument will be selected for soil moisture monitoring. This study provides valuable information on the pre-calibration and post calibration accuracies. Other factors that may be considered include cost, ease of deployment and maintenance, mode and duration of data collection as well as soil depth(s) of interest.

The first study established that calibrated Hydra probes had the lowest RMSE for soil moisture measurement. These sensors were further studied to develop a broad calibration strategy that can be adapted to a wide range of soils. Laboratory-derived calibrations developed from soils collected at nine sites with varying soil physical properties were compared to field calibrations developed after instrument installation. The result showed that the laboratory calibration for all sites and depth had r^2 of 0.89 compared to 0.95 obtained from field calibration and the field-derived equation provides better correlation with observed soil moisture. Logsdon (2009) observed that in similar water content, apparent permittivity was higher under field conditions than in undisturbed columns in the laboratory.

For the purpose of generating a generic calibration that can be widely used, a soil texture-based approach was suggested by Stevens Hydra Probe (Bellingham, 2007). However, Saarenketo (1998) observed that depending on the cation exchange capacity (CEC) of clays, the arrangement of water molecules around the soil particles behave differently. The implication is that a calibration equation developed from a less reactive

130

clay soil such as Kaolinitic clays will yield a high bias to Hydra probe values from highly reactive Smectite clay. CEC was determined at the nine sites described in the second study and were divided into 3 groups: Low, Mid and High categories based on the range of the CEC. Data from all the sites under each category was used to develop calibration equations which were applied to an independent dataset at three evaluation sites; one for each CEC category. Seven different calibration equations were compared and the *in situ* derived calibration had the best performance followed by the CEC-based calibration.

This study has important implications for deployments of a large number of Hydra probes across variable soils for many soil moisture monitoring networks. An example is the Real-time *In situ* Monitoring for Agriculture (RISMA) used in validating remotely sensed soil moisture products. *In situ* calibration, although desirable, may be a daunting undertaking. CEC-based calibration can provide a suitable alternative and was shown to be more effective than texture-based or laboratory-derived calibrations. Although the CEC-based calibration was tested using Hydra probe, it is expected that regardless of the type of soil moisture sensor used, the performance of the CEC-based calibration would be similar to results obtained in this study,

The limited sensing volume of point based sensors as well as the high cost and labour requirements of installing and maintaining a network of soil moisture instruments led to the development various models that can be used to estimate soil moisture. The Versatile Soil Moisture Budget is a model that has been widely used on the Canadian Prairies but has only been validated at ≥ 0.2 m surface layer thickness and limited to cereal crops and pasture lands. Using *in situ* calibrated Hydra probes described in the second study, the third study reported in chapter 4 assessed the accuracy of the VSMB to

131

simulate soil moisture at the shallow surface (top 0.1 m) and expanded the capability of the model to simulate soil moisture in fields planted with corn and soybeans.

The result showed that VSMB was able to simulate the trend of soil moisture at all the sites but did not capture the peaks and nadirs accurately. The highest surface RMSE at coarse and fine textured sites were 0.072 m^3 m^{-3} and 0.101 m^3 m^{-3}, respectively. The entire root zone showed a mean RMSE of 32 mm in 2013 and 53 mm in 2014. The results obtained in this study were comparable to those obtained from other models reported by Sridhar et al. (2008), Gervais et al. (2010) and Mkhabela and Bullock (2012). It was noted that days with significant rainfall occurrence had higher RMSEs and bias compared to the overall data. The representativeness of the observed daily soil moisture at the surface layer obtained from the arithmetic mean of 96, 15-minute readings on days with significant rainfall is questionable, especially at coarse textured sites. An alternative method that may provide a better representative daily soil moisture value is aggregating the moisture values recorded after the rainfall event. This study showed that the VSMB has great prospects for modelling both surface and root-zone soil moisture at an operational level. Data collected from soil moisture instruments can be used for periodical validation, especially on days with significant rainfall.

The last study chapter focused on upscaling from a point measurement, as reported in previous chapters, to a field-scale footprint. The chapter highlighted different methods of upscaling soil moisture and the method used in the chapter, which is consistent with the SMAPVEX project, was the averaging of several point measurements. The representativeness of soil moisture installed at a single location (SM_{TS}) in the field and the VSMB model was compared to the average soil moisture obtained from 48 in-

field sampled points. Although the VSMB is a one dimensional vertical model, it was applied for field spatial assessment. The VSMB overestimated observed field averaged soil moisture at all the fine-textured sites but yielded an impressive RMSE range of 0.037 m^3 m^{-3} – 0.050 m^3 m^{-3} at the coarse textured sites. Overall, the arbitrarily placed soil moisture instrument had better statistical indicators than the VSMB model at both the coarse and fine textured sites.

The last study showed that despite the reasonable estimation of field soil moisture by the VSMB, the installation of a single soil moisture instrument at a single location on the field is a justifiable approach to upscaling. This is important for producers who use single data point from an arbitrary location to assess the field condition. With the exception of visible low areas or in-field slope greater than 2%, the results obtained in this study provide a good estimation of the representativeness that farmers can expect.

6.2   Ongoing and Future Research

The accuracy, adaptability and calibration of soil moisture instruments were the focus of the first two studies. However, there is a need to study the impact of freeze-thaw cycles on the instruments that are deployed over several years. The RISMA network, established in 2012, is in its fifth year of installation but no study has been conducted in this province to determine how the long winters influence the accuracy of the probes. The top soil in most regions of Manitoba is typically frozen from November to March with occasional, short term freeze-thaw cycles occurring in October and April.

The frost depth is usually between 0.6 m to 1 m over the winter. During snowmelt, surface runoff is dominant and this may cause vertically installed probes at the soil surface to lose contact with the soil. It will be a valuable undertaking if the accuracy of the devices used in monitoring soil moisture is tested under these various environmental conditions.

The assessment of vertical soil moisture distribution patterns is another area that could be explored. This would allow for the identification of preferential or lateral soil water movement which often results in "out-of-sequence" soil moisture response, i.e., a soil layer that showed response to precipitation earlier than the layer above it. Models such as the VSMB do not account for such out-of-sequence soil moisture response and this could impact the assessment of the model's performance. The results in chapter 4 considered the accuracy of the VSMB over the duration of the growing season. It would be interesting to compute the RMSE and the MBE for different periods of the year either by climatic season or by the crop growth stage. Such delineation may provide valuable quantitative information on periods of the year or crop growth stage when the VSMB performs better or worse and hence pinpoint specific areas of model sensitivity.

Soil Moisture Active and Passive Validation Experiment 12 (SMAPVEX12) provided a great data set for various scientific research (Rowlandson et al., 2013; Adams et al., 2015; McNairn et al., 2015) including validating the representativeness of single site soil moisture against an in-field average from 48 samples reported in the last study chapter. A similar campaign, SMAPVEX16, was recently concluded in Manitoba within a similar footprint as SMAPVEX12. Based on the importance of calibration highlighted in the results obtained in the second study of this thesis; the experimental design was

modified to include an extra calibration sample collection on each soil sampling day. In addition, tipping bucket rain gauges were placed at many more fields to increase the density of rainfall measurements. The use of rainfall data obtained from the field is important for model validation due to the spatial variability in the intensity of rainfall.

The Province of Manitoba is set to deploy several soil moisture monitoring instruments across the agricultural regions of the province. There is a limit to the number of probes that can be installed across the province as it is impractical to install these instruments on every field. Therefore, it is important to analyze the best method of upscaling the result from the point measurements to accurately represent a specified spatial extent. The study on the field-scale representativeness of point-based soil moisture provides a valuable baseline on the level of bias that may be expected. A synergy between monitored surface soil moisture, remote sensing data and root-zone models can be used to provide a complete spatio-temporal monitoring of soil moisture across the province. Whichever model is selected for this purpose, independent assessment of the various components should be done to ensure that each sub-routine has the capability to handle the various crop, soil and weather variations across the agricultural regions of the province.

6.3   References

Adams, J.R., McNairn, H., Berg, A.A. and Champagne, C. 2015. Evaluation of near-surface soil moisture data from an AAFC monitoring network in Manitoba, Canada: Implications for L-band satellite validation. J. Hydrol. **521**: 582–592.

Aspinall, D., Nicholls, P.B. and May, L.H. 1964. The effects of soil moisture stress on the growth of barley. I. Vegetative development and grain yield. Crop Pasture Sci. **15**: 729–745.

Bellingham, K. 2007. The Stevens Hydra Probe Inorganic Soil Calibrations. Available at http://www.stevenswater.com/catalog/products/soil_sensors/datasheet/The%20Stevens%20Hydra%20Probe%20Inorganic%20Soil%20Calibrations.pdf (verified 19 June 2014)

Denmead, O.T. and Shaw, R.H. 1960. The Effects of Soil Moisture Stress at Different Stages of Growth on the Development and Yield of Corn. Agron. J. **52**: 272-274.

Gervais, M., Bullock, P. R., Mkhabela, M., Finlay, G. and Raddatz, R. 2010. Improvements to the accuracy of modelled soil water content from the Second Generation Prairie Agrometeorological Model. Can. J. Soil Sci. **90**: 523–526.

Hanesiak, J.M., Raddatz, R.L. and Lobban, S. 2004. Local initiation of deep convection on the Canadian prairie provinces. Bound.-Layer Meteorol. **110**: 455–470.

Heapy, L. A., Webster, G. R., Love, H. C., McBeath, D. K., Von Maydell, U. M., and Robertson, J. A. 1976. Development of a barley yield equation for central Alberta. 2. Effects of soil moisture stress. Can. J. Soil Sci. **56**: 249–256.

Logsdon, S.D. 2009. CS616 Calibration: Field versus Laboratory. Soil Sci. Soc. Am. J. **73**: 1-6.

Logsdon, S.D. and Hornbuckle, B.K. 2006. Soil Moisture Probes for a Dispersive Soil. Pages 1-14. *in* Purdue University, West Lafayette, USA.

Manitoba Government. 2013. Manitoba 2011 Flood Review. Available at http://www.gov.mb.ca/asset_library/en/2011flood/flood_review_task_force_report.pdf (verified 10 August 2016)

McNairn, H., Jackson, T.J., Wiseman, G., Béliar, S., Berg, A., Bullock, P., Colliander, A., Cosh, M.H., Kim, S.-B., Magagi, R., Moghaddam, M., Njoku, E.G., Adams, J.R., Homayouni, S., Ojo, E.R., Rowlandson, T., Shang, J., Goïta, K. and Hossein. M. 2015. The Soil Moisture Active Passive Validation Experiment 2012 (SMAPVEX12): Pre-Launch Calibration and Validation of the SMAP Satellite. IEEE Trans. Geosci. Remote Sens. **53**: 2784–2801.

Mkhabela, M.S. and Bullock, P. R. 2012. Performance of the FAO AquaCrop model for wheat grain yield and soil moisture simulation in Western Canada. Agric. Water Manag. **110**: 16–24.

Rowlandson, T.L., Berg, A.A., Bullock, P.R., Ojo, E.R., McNairn, H., Wiseman, G. and Cosh, M.H. 2013. Evaluation of several calibration procedures for a portable soil moisture sensor. J. Hydrol. **498**: 335–344.

Saarenketo, T. 1998. Electrical properties of water in clay and silty soils. J. Appl. Geophys. **40**: 73–88.

Seneviratne, S.I., Corti, T., Davin, E.L., Hirschi, M., Jaeger, E.B., Lehner, I., Orlowsky, B. and Teuling, A.J. 2010. Investigating soil moisture–climate interactions in a changing climate: A review. Earth-Sci. Rev. **99**: 125–161.

Sentek Technologies. 2011. Calibration Manual for Sentek Soil Moisture Sensors. V 2.0. Available at http://www.sentek.com.au/downloads/downloads.asp (verified 25 October 2013).

Sridhar, V., Hubbard, K. G., You, J. and Hunt, E. D. 2008. Development of the Soil Moisture Index to Quantify Agricultural Drought and Its "User Friendliness" in Severity-Area-Duration Assessment. J. Hydrometeorol. **9**: 660–676

Walker, G.K. 1989. Model for operational forecasting of western Canada wheat yield. Agric. For. Meteorol. **44**: 339–351.

Wei, J., and Dirmeyer, P.A. 2012. Dissecting soil moisture-precipitation coupling. Geophys. Res. Lett. **39**: 1–6.

APPENDICES

I The VSMB Input Files

The VSMB has two input files that are linked to the source code: the soil/crop information (Appendix I.1) and the Weather data (Appendix I.2) to generate several output files which include the modelled soil moisture at each pre-defined depth. The definition of major variables is listed on the second page of the VSMB code (Appendix II).

I.1   Soil/Crop Information

```
     READ (1,3003) ISFL,IESG,IFTP,ISTP,SMCOF,NOSNO,KSNO
 1101    401     5      7         0.7        0.7       0 0701
 ISFL   IESG    IFTP   ISTP     SMCOF(1)     (2)    NOSNO KSNO


     READ (1,2070) M9,N9,H9,R9,KNTROL,CN2,DRS2
 Fallow:   1     1    1.0        .50       7 89.0 1.00
 Cropped:  1     1    1.0        .70
           M9    N9    H9         R9    KNTROL CN2 DRS2


     READ(1,502) CAPAC
46.0 94.0 188.0 282.0
CAPAC is the field capacity (mm) and the number of variables depends on
the number of layers (4 layers here)
```

READ(1,502) CONTNT,SNSTR,PESTR,MRST1,IDRN,NDRN

47.0 104.0 208.0 312.0   1   0   0

CONTNT is the available water content (4 variables like CAPAC).   MRST1   IDRN NDRN
Note that **SNSTR** and **PESTR** have been commented out and are not used in this revised version but are left there just in case. Thus, no value is assigned to them in the soil input data.

READ(1,2399) EXCAP,TRP,SSLP,DRN,IFRNT

56.0 112.0 224.0 336.0   0.0 5.0 150.0150.0150.0100.0   3

EXCAP   TRP SSLP DRN   IFRNT
Note that **EXCAP** is the saturated water content (one value for each of the four layers). **DRN** is drainage rate and limit (but the values are no longer used)

READ(1,2388) PRMWLT,OBDPTH

20.0 40.0 80.0 120.0   10.0 30.0 70.0 130.0

PRMWLT   OBDPTH
PRMWLT (mm) is the permanent wilting point values for each layer while the OBDPTH (cm) specifies the bottom depth of each layer.

READ(1,2) ((COEFS(I,J),J=1,6),I=1,5)

```
0.40 0.10 0.02 0.01
0.45 0.10 0.02 0.01
0.45 0.20 0.10 0.02      Growth
0.55 0.20 0.15 0.05      Stages
0.55 0.20 0.20 0.10
```
COEFS   Each Depth ⟶

READ(1,8) ISTGES,NEW,ISYR,NDYR,NSY,SDATE,XLAT

** 5   3   19472005   5 140   58.65**

ISTGES NEW   ISYR NDYR NSY SDATE XLAT

READ(1,37) (IDATES(I),I=1,NODATE)

020430020625020715020815020905041231

IPHEND

I.2   Weather Data

```
READ(17,*,END=25)IYR,MIO,IDIN,JD,TMAX,TMIN,RMIN,RMAX,PCP,WIN
```

2012	5	1	122	16.2	9.2	0	0	9.4	0
2012	5	2	123	15.7	5.6	0	0	2.7	0
2012	5	3	124	13.6	3.3	0	0	1.0	0
2012	5	4	125	12.9	1.0	0	0	1.0	0
2012	5	5	126	20.1	8.4	0	0	0.4	0
2012	5	6	127	20.2	9.4	0	0	5.4	0

II   The VSMB Code

```
    DIMENSION TABLE1(100),TABLE2(100),CONTNT(6),COEFS(5,6),X(6)
    DIMENSION IDATES(165),KDATES(165),IPLOT(6),IPHEND(5)
    DIMENSION COF(6),DELTA(6),CAPAC(6),CONRST(6),PRCNT(6)
    DIMENSION EXCAP(6),EXCSW(6),PRMWLT(6),OBDPTH(6),DPTHZN(6)
    DIMENSION WF(6),DUL(6),SW(6),SAT(6),PLL(6),DRN(4)
    DIMENSION FLOW(6),SWX(6),FLUX(6)
    DIMENSION HEAD(15),SMCOF(2),AQ(4,14),TEPIC(3)
    REAL SUMROF,SUMET,SUMDRN,SUMPCP,CUMDEP,SUMDEL,SUMWAT1,SUMWAT2
    REAL CN,CN1,CN2,CN3,CNPD,CNPW,PB,SMX,DXX,WX
    REAL THET1,THET2,DBAR,SWFLOW,TMEAN,PAX,PIN,TMAX,TMIN
    REAL DEL,XDEL,DRAIN,WLEACH,DRS2,HOBKG,ROFSUM,PI,FAT,GDD
    REAL BCV,TSUM,EPICT1,EPICT2,AVTEP,PHOTO,BMT,XLAT,WINSPD,SUMGDD
    REAL SOLRAD,SUNHRSMAX,SOLARMAX,PLHGT,ELE,RMAX,RMIN,WIN,PCP
    REAL SUFWAT,ACCSNO,SNOWEQ,SNOCF,SNOLOS,SNO,GS,CRPCOF,WATDMD
    REAL FETLO,FETRA,FETSO,CRADSO,PE,PARTONE,PARTWO,PARTHRE,PARTFOR
    REAL WSP,OPE,WEMAX,WEMIN,STMAX,STMIN,SWEMAX,SWEMIN,PMAX
    REAL PMIN,PWEMAX,PWEMIN,PDAYS,SUMPDAYS,SUMCHU,CHU
    INTEGER ISTZ,IZN,IZNS,IFRNT,IZ,IY,DCOUNT,IYR,IYROLD,IDENT
    INTEGER YESDAY,SDATE,IBMTS,DAYHAV,JDAY,JDDAY,MIO,IDIN,FLAG
    INTEGER ISTGES,NSY,NEW,IRTN,NDYR,ISYR,KNTROL,M9,N9,JD,REW,INUM
    INTEGER NP, INT, IP, ISFL,IESG,IFTP,ISTP,KSNO,IST,IDT,IDATE
    INTEGER NODATE,PLANTYP
C   THESE ARE THE CUMULATIVE RUNOFF, EVAPOTRANP,AND LEACHING
C
C   THESE ARE THE CUMULATIVE RUNOFF, EVAPOTRANP,AND LEACHING
C   IE SUMROF, SUMET, SUMDRN
C
    LOGICAL  MOREDAT,MORDAT
    CHARACTER*1 APLOT(6),BLANK,TENTH
```

```
      CHARACTER*1 LPLOT(50)
      CHARACTER*1 KPLOT(50)
      DATA APLOT /'1','2','3','4','5','6'/
      DATA BLANK /' '/
      DATA TENTH /'+'/
      DATA A1,E1,D1,H1,P2,R2,W1,T2/0.0,0.0,0.0,0.0,0.0,0.0,0.0,0.0/
      DATA RUNOFF,RUNOF/0.0,0.0/
      DATA AQ/0.00,0.04,0.20,0.32,0.00,0.00,0.12,0.23,0.00,0.04,0.22,0.3
     19,0.00,0.30,0.62,0.91,0.22,0.67,1.16,1.59,0.42,0.84,1.38,1.88,0.21
     2,0.42,0.69,0.94,0.00,0.00,0.00,0.00,0.00,0.00,0.00,0.00,0.03,0.13,
     30.21,0.32,0.06,0.27,0.42,0.65,0.01,0.18,0.34,0.53,0.00,0.04,0.20,0
     4.32,0.00,0.00,0.12,0.23/
```

```
C     ---------------------------------------------------
C     DEFINE CONTROL COEFFICIENTS
C
C         A1               Melt-water Infiltration to Soil
C         AQ               Snowmelt Rate Table
C         AYE              Total Infiltration
C         BYE(X)           Infiltration Water Allocated to Each Zone
C         CAPAC            Available Water Capacity of Each Zone
C         CN1              Curve Number for Dry Soil
C         CN3              Curve Number for Wet Soil
C         CNPD             Parameter of Curve Number when Soil is Dry
C         CNPW             Parameter of Curve Number when Soil is Wet
C         COEFS            K-Coefficients (Roots)
C         COF              Adjusted K-Coefficients
C         CONTNT           (Redefined) Computed Moisture Content of Each Zone
C         CONTNT (CONRST)  Available Water in Each Zone at Start
C         CUMDEP           Total Depth of All Zones
C         D2               Total Deficit after Melt-water Infiltration
C         DAYSM            Days per Month
C         DD (XX)          Daily Snowmelt
C         DEL              Relative Moisture Content of Each Zone
C         DPTHZN           Actual Depth of Each Zone (mm)
C         DRN              Drainage Rate and Limits
C         E1               Melt-water Drainage out of Snowpack
C         EXCAP            Total Void Space of Each Zone
C         F1               Hobbs-Krogman Multiplier for Over-Winter Storage Pot
C         IDATE            Month/Day
C         IDATES           Crop Stage Dates (Replaced with IPHEND)
C         IDENT            Year
C         IDIN             Day of the Month
C         IDT              Year/Month/Day of Daily Calculations
C         IESG             Ending Date of Winter Budget
C         IFRNT            Number of Zones Wetted First Day after Rain
C         IFTP             Rain/Snow Threshold Temperature- Fall
C         IPHEND           Crop Development Stage Dates
C         IRTN             Number of Years in Rotation
C         ISFL             Beginning Date of Winter (Snow) Budget
C         IST              Crop Development Stage
C         ISTGES           Total Number of Crop Development Stages
C         ISTP             Rain/Snow Threshold Temperature -Spring
```

```
C       ISYR                    Starting Year
C       IYMODA                  Year/Month/Day
C       IYR                     Year
C       IZNS                    Total Number of Zones
C       JDDAY or JD             Julian Day
C       KNTROL                  Zones Using 1st Z-Table
C       KSNO                    Snow Blow Change Date
C       M9, N9, H9, R9          Drying Curve Index Parameters
C       MIO                     Month of the Year
C       MRST1, 2                Moisture Re-Initialize Parameters
C       NDYR                    Last Year of Run
C       NEW                     Crop Stage for K-Adjustment Start
C       NP, INT, IP             I/O Units-Daily Print, weather In, S.M.Plot
C       NSY                     Crop Stages per Year
C       OBDPTH                  Bottom Depth of Each Zone (CMS)
C       PCP                     Precipitation
C       PE/OPE                  Potential Evapotranspiration
C       PRCNT                   Soil Moisture at Each Depth
C       PRMWLT                  Permanent Wilting Point
C       R2                      Snowmelt Surface Runoff
C       RMAX                    Maximum Relative Humidity
C       RMIN                    Minimum Relative Humidity
C       RUNOFF                  Surface Runoff
C       SCL                     Plot Scaling Factor
C       SDATE                   Seeding Date (can be simulated or provided as input)
C       SMCOF                   % Snowfall after wind blowing (snow coefficient)
C       SMX                     S Value from SCS Equation, Transfer to mm Scale
C       SSLP                    Slope/Runoff Coefficient
C       SUMDEL                  Actual Evapotranspiration (AE) Daily
C       T1                      Snowmelt Refrozen in Upper Soil
C       TABLE1                  1st Z-Table (Drying Curve)
C       TABLE2                  2nd Z-Table
C       TMAX                    Maximum Temperature
C       TMIN                    Minimum Temperature
C       TRP                     Surface Water after First Day
C       WIN                     Wind Speed
C       XDEL                    Actual Evaporation for Each Zone
C       XLAT                    Latitude of Site


C    THERE ARE TWO INPUT FILES VWBMOD7.IN CONTAINIG THE SOIL AND CROP
C    PARAMETERS. THE SECOND INPUT FILE IS THE WEATHER FILE CONTAIN THE DAILY
C     WEATHER DATA.

C    OPEN (UNIT=99,FILE='GRAS.OUT',STATUS='UNKNOWN')
C    OPEN (UNIT=26,FILE='PDAY.OUT',STATUS='UNKNOWN')
     OPEN (UNIT=82,FILE='CHU.OUT',STATUS='UNKNOWN')

     OPEN (UNIT=1,FILE='MB31.IN',STATUS='OLD')
     OPEN (UNIT=17,FILE='MB31WEA.IN',STATUS='OLD')
C     OPEN (UNIT=13,FILE='EVAWEAD.IN',STATUS='OLD')
```

```
C     THERE ARE ASLO TWO OUTPUT FILES SNOWTABLE.OUT CONTAINING THE SURFACE
AND
C     WINTER OUTPUT AND DAILYOUT CONTINING SOIL MOISTURE OUTPPUT ON A DAILY
BASIS

      OPEN (UNIT=21,FILE='MODSNO3.OUT',STATUS='UNKNOWN')
CC    OPEN (UNIT=17,FILE='FDEWSOUT.DAT',STATUS='UNKNOWN')
      OPEN (UNIT=18,FILE='MODOUT3.OUT',STATUS='UNKNOWN')
      OPEN (UNIT=19,FILE='MODSOLA3.OUT',STATUS='UNKNOWN')
      OPEN (UNIT=10,FILE='EVAP3.OUT',STATUS='UNKNOWN')

      WRITE(21,*)'DATE  POTEVAP  EVAP  SNOFAL  SNOWEQ GRONDSNO
    # CUMSNO   TOTSNO        MEANT  SOILT'
      WRITE(19,*)' DATE   SOLRAD   SOLARMAX SUNHRSMAX  PHOTO   POTEV
    #  AET'

      WRITE(18,*)' DATE  SOILTEM   PRECIP POTEVAP DUAL   WATR1 WATR2
    $WATR3 WATR4 WATR5 WATR6  IST  IBMTS  IPHEND'
      WRITE(10,*) 'DATE   AET  ZONEVA RELSM DRYCUV  PE  ROOTCOF(I)'
C     WRITE(26,*)'JD   T1    T2  P-days AccP   IST'
      WRITE(82,*)'JD  TMAX   TMIN  CHU  SUMCHU   IST'
C     WRITE(99,*)'JDAY TMAX   TMIN   GDD  SUMGDD IST'


C   SIMULATION CONTROL COEFFICIENTS
C
C   READING TITLE CARD
C

C
      READ(1,987) HEAD
 987 FORMAT(15A4)
C
C   INPUT SNOW BUDGET CONTROLS
C
      READ(1,3003) ISFL,IESG,IFTP,ISTP,SMCOF,NOSNO,KSNO
 3003 FORMAT(4I6,6X,2F10.5,2I5)
      IF((SMCOF(1)+SMCOF(2)).LE.0.0) NOSNO=1
C
C   READING SOIL CHARACTARISTIC TABLES
C

 2070 FORMAT(2I5,2F10.5,I5,F6.1,F5.2)

C   NOTE THAT CN2 IS THE SCS CURVE NUMBER AND
C   DRS2 CONTROLS LEACHING OUT OF THE  BOTTOM LAYER
C   VALUES OF DRS2 BETWEEN 0.75-0.8  WAS FOUND TO SIMULATE
C   THE MOISTURE CONTENT OF THE BOTTOM LAYER OF A LOAM SOIL RESONABLY.
C   IF THIS CONSTANT (DRS2) IS NOT DESIRED THEN SET IT TO '1'
```

```fortran
      READ(1,2070) M9,N9,H9,R9,KNTROL,CN2,DRS2
      IF(KNTROL.LE.0) KNTROL=6
      IF(M9.GT.1) M9=1
       IF(N9.GT.1) N9=1
      IF(M9.GT.0.OR.N9.GT.0) GO TO 2100
      READ(1,9)TABLE1
    9 FORMAT(10F5.2)
      IF (1.EQ.1) GO TO 2090
 2100 CONTINUE
      N=N9
      DO 2080 I=1,100
      X9=I*0.01
      M=M9
      IF(X9.GE.R9) M=0
      IF(X9.GE.R9) N=1
      Z=(((X9/R9)**M)*N/X9)+((((R9-X9)/R9)**N)*M/R9)
      Z=((X9/R9)**(M*N*H9))*Z
      TABLE1(I)=Z
 2080 CONTINUE
 2090 CONTINUE
C
      READ(1,2070) M9,N9,H9,R9
      IF(M9.GT.1) M9=1
      IF(N9.GT.1) N9=1
      IF(M9.GT.0.OR.N9.GT.0) GO TO 2101
      READ(1,9)TABLE2
      IF (1.EQ.1) GO TO 2091
 2101 CONTINUE
      N=N9
      DO 2081 I=1,100
      X9=I*0.01
      M=M9
      IF(X9.GE.R9) M=0
      IF(X9.GE.R9) N=1
      Z=(((X9/R9)**M)*N/X9)+((((R9-X9)/R9)**N)*M/R9)
      Z=((X9/R9)**(M*N*H9))*Z
      TABLE2(I)=Z
 2081 CONTINUE
 2091 CONTINUE
C
C   READING THE ZONAL CONTENTS AND CAPACITIES
C
      READ(1,502) CAPAC
  502 FORMAT(6F5.1,5X,2F5.1,I5,5X,2I5)
      IZNS=6
 1210 CONTINUE
      IF(CAPAC(IZNS).GT.0.0) GO TO 1220
      IF(IZNS.LE.2) GO TO 1220
```

```
      IZNS=IZNS-1
      IF (1.EQ.1) GO TO 1210
 1220 CONTINUE
      READ(1,502) CONTNT,SNSTR,PESTR,MRST1,IDRN,NDRN
      IOUT=0
C
C  READING SATURATION, DRAINAGE FACTORS, PERMANENT WILTING POINT
C     AND ZONE DEPTHS(CMS).
C
      READ(1,2399) EXCAP,TRP,SSLP,DRN,IFRNT
 2399 FORMAT(12F5.1,I5)
      SSLP=SSLP/5.0
      IF(IFRNT.LT.1)   IFRNT=1
      IF(IFRNT.GT.IZNS)IFRNT=IZNS
      READ(1,2388) PRMWLT,OBDPTH
 2388 FORMAT(6F5.1,5X,6F5.1)
C
C    Calculate the actual depth of each zone or soil layer
C    DPTHZN(6) This value is to be used to convert from
C    Volumetric moisture content to detph of water in the zone (mm)
C    Calculate volumetric parameters to be used in SCS runoff
      DO 2385  I = 1,IZNS
      IF (I.EQ.1) THEN
        DPTHZN(I) = OBDPTH(I)*10.
      ELSE
        DPTHZN(I) =10*( OBDPTH(I) - OBDPTH(I-1))
      ENDIF
        DUL(I) = CAPAC(I)/DPTHZN(I)
        SAT(I) = EXCAP(I)/DPTHZN(I)
        PLL(I) =  PRMWLT(I)/DPTHZN(I)
 2385 CONTINUE
      DO 2368 I=1,50
      LPLOT(I)=BLANK
 2368 KPLOT(I)=BLANK
      DO 2366 I=1,5
      LPLOT(I*10)=TENTH
 2366 KPLOT(I*10)=TENTH
C
C  CONVERT FIELD CAPACITY AND WATER CONTENT TO PLANT AVAILABLE WATER
C    AND TOTAL VOID SPACES TO EXCESS PORE SPACES.
C
      DO 2389 I=1,IZNS
      IF(PRMWLT(I).GT.(CAPAC(I)*.95)) PRMWLT(I)=.95*CAPAC(I)
      CAPAC(I)=CAPAC(I)-PRMWLT(I)
      IF(EXCAP(I).LT.CONTNT(I)) EXCAP(I)=CONTNT(I)
      CONTNT(I)=CONTNT(I)-PRMWLT(I)
      EXCAP(I)=EXCAP(I)-(CAPAC(I)+PRMWLT(I))
      IF(EXCAP(I).LT.0.0) EXCAP(I)=0.0
```

```
 2389 CONTINUE
C
C  TOTAL EXCESS (DRAINABLE) PORE SPACES OVER LAYER 1      (EXFRNT)
C                             OVER ALL ROOT ZONES (EXTOTL)
C  THE PARAMETERS BELOW ARE NO LONGER USED IN THIS VERSION.  THEY WERE
C  USED TO HANDLE EXCESS DRAINGE (ABOVE FIELD CAPACITY) IN THE ORIGINAL
C  MODEL.
     EXFRNT=EXCAP(1)
     EXTOTL=EXCAP(1)
     DO 2386 I=2,IZNS
     IF(I.LE.IFRNT) EXFRNT=EXFRNT+EXCAP(I)
     EXTOTL=EXTOTL+EXCAP(I)
 2386 CONTINUE
C
C  DEFAULT EXCESS TO DOUBLE CAPAC TO NOT IMPEDE DRAINAGE
C  AGAIN NO LONGER USED
     IF(EXTOTL.GT.0.0) GO TO 2378
     IFRNT=IZNS
     DO 2377 I=1,IZNS
 2377 EXCAP(I)=CAPAC(I)*2.0
 2378 CONTINUE
C
C  DEFAULT DRAINAGE COEFFICIENTS
C  AGAIN NO NOLGER USED
     IF(DRN(1).LE.0.0) DRN(1)=EXFRNT
     IF(DRN(2).LE.0.0) DRN(2)=DRN(1)
     IF(DRN(3).LE.0.0) DRN(3)=DRN(2)
     DRS=DRN(4)*.01
     IF(DRS.GT.1.0) DRS=1.0
     IF(DRS.LT.0.2) DRS=0.2
     DRN(2)=DRN(2)/DRS
C
C  INITIALIZE STORAGE TERMS
C
     DEFCIT=0.0
     BYE=0.0
     PDL=0.0
     DO 15 I=1,6
     COF(I)=0.0
  15 X(I)=0.
     SNOCF=SMCOF(1)

C
C  READING ZONAL COEFS. FOR THE RUN
C
     READ(1,2) ((COEFS(I,J),J=1,6),I=1,5)
   2 FORMAT(6F5.2)
     DO 3140 I=1,IZNS
 3140 CONRST(I)=CONTNT(I)
```

```
C
C    KSIG=1
C    IDAT1=0531
C    IDAT2=0831
C    PE3RDYR=0.
C    AE3RDYR=0.
C    CALL MONISO (CAPAC,IDAT1,IDAT2,KSIG,AE3RDYR,PE3RDYR)
C
     IN2=31
     DCOUNT = 0
 3190 CONTINUE
C
C   READING OF RUN CHARACTARISTICS
C  SEEDING DATE"SADTE" SHOULD BE READ HERE IF IT IS
C  ADDED TO THE INPUT FILE, OTHEREWISE IT WILL BE
C  SIMULATED. NOTE THAT IT IS IN JULIAN DAY.
C
     READ(1,8) ISTGES,NEW,ISYR,NDYR,NSY,SDATE,XLAT

   8 FORMAT(2I4,8X,4I4,2(2X,F6.2),2I3)
     NODATE=ISTGES+1

     READ(1,7) ELE,PLANTYP
   7 FORMAT(F6.1,4X,2I3)
C  PLANTYP INDICATES THE PLANT GROWTH TO BE SIMULATED. ADDED BY E. ROTIMI

C  1=WHEAT
C  2=CANOLA
C  3=GRASS
C  4=CORN
C  5=SOYBEAN

C  READING THE CONTROL DATES FOR THE RUN
C  NOTE THAT IDATE(1-5)  CAN BE USED FOR ACTUAL PHENELOGY DATES.
C  IN THAT CASE THEY ARE PASSED TO IPHEN(1-5). IDATES(6) IS THE
C  DATE TO END SIMULATION E.G. THE FALL SAMPLING DATE.
     READ(1,37) (IDATES(I),I=1,NODATE)
  37 FORMAT(12I6)

     F1=1.
     T1=0.
     T2=0.
     W1=0.
     S2=0.0
     MRST2=0
     RFAC=1.0
     DO 1230 IZN=1,IZNS
 1230 S2=S2+CAPAC(IZN)
     IF(OBDPTH(IZNS).GT.0)THEN
```

```
      ENDIF
      IRTN=IDATES(NODATE)*.0001
      IS=IDATES(1)*.0001
      IRTN=IRTN-IS
      IS=0
      IF(IDATES(1).GT.1300) GO TO 3160
      DO 3150 I=1,NODATE
      IDATES(I)=IDATES(I)+ISYR*10000
 3150 CONTINUE
 3160 CONTINUE
       DO 3186 I=1,NODATE
 3186   KDATES(I)=IDATES(I)
      IF((IDATES(NODATE)-(IRTN*10000)).LT.IDATES(1)) IRTN=IRTN-1
      IRTN=IRTN+1
C
C    INPUT DAILY DATA
C
C  IDENT        YEAR
C  IDATE        MONTH/DAY
C  PAX(MAX)      MAXIMUM TEMPERATURE
C  PIN(MIN)      MINIMUM TEMPERATURE
C  PCP         PRECIPITATION
C  PE          POTENTIAL EVAPOTRANSPIRATION
C
C    TEST OF BEGINING DATE
C
C  YOU HAVE TO CHANGE XLAT BELOW TO THE LATITUDE OF YOUR SITE
C  IN ORDER FOR THE BIOMETEOROLOGICAL TIME SCALE TO WORK PROPERLY.
C   YOU CAN REMOVE THIS FROM HERE AND READ THE LATITUDE  OFF YOUR INPUT
TABLE
C  IN CASE SEVERAL SITES DIFFERING IN LATITUDE ARE TO BE SIMULATED

CC        XLAT = 49.7


C  INITIALIZE ALL THE  CUMULATIVE VARIABLES
      ROFSUM =0.
      SUMROF = 0.
      SUMET  = 0.
      SUMDRN = 0.
      SUMPCP = 0.
      ACCSNO = 0.
      SUMWAT1 = 0.
      SUMWAT2 = 0.
      TSUM = 0.
      EPICT1=0.
      EPICT2=0.
```

```
C INITIALIZE THE THREE DAY RUNNING MEAN OF SOIL TEMPERATURE TO A DUMMY
NUMBER
C  999.9

          DO J = 1,3
       TEPIC(J) = 999.9
      END DO
C THIS CAN BE USED TO CONTROL YEARLY RUN OTHERWISE RUN CAN
C CONTROLLED BASED ON THE SIZE OF YOUR WEATHER DATA AND .MOREDAT.

CC        DO 111  IYR=ISYR+1900,NDYR+1900
          IYROLD=ISYR
        MOREDAT = .TRUE.

C  INITALIZE SEEDING DATE AND PHENOLOGY PARAMETERS
C  IF SEEDING DATE IS TO BE SIMULATED THEN SDATE MUST BE
C  SET TO ZERO HERE. IF THESE PARAMETER ARE SUPPLIED IN
C  THE INPUT TABLE THEN BY-PASS THE NXT 6 LINES


C         SDATE = 0
C         YESDAY = 0
C      IBMTS  = 1
C      IST = 1
C       BMT = 0.
      DO J = 1,5
      IPHEND(J) = 0
      END DO
      DAYHAV = 366
C  THIS IS THE LOOP THAT READS YOUR INPUT WEATHER DATA
C  NOTE THE ORDER ON THE INPUT WEATHER VARIABLES!!!!!!
C  YEAR, JULIAN DAY, MAX TEMP, MIN TEMP, SOLAR RADIATION
C  RAINFALL (mm) TOTAL PRECIPITAION (mm)
c  IF YOU CHANGE THIS ORDER IN YOUR INPUT FILE THEN YOU HAVE
C  TO CHANGE TO PROGRAM  ACCORDINGLY.

      DO WHILE (MOREDAT)
     READ(17,*,END=25)IYR,MIO,IDIN,JD,TMAX,TMIN,RMIN,RMAX,PCP,WIN
C    #SOLRAD

   WSP=WIN*0.955 !Correction factor for 2m reading (0.955 for
   ! my CS stations at 2.5m & 0.748 for MAFRI stations at 10m)

     IF (TMAX.GT.0.0) THEN
     RAIN = PCP
     ELSE
     RAIN=0.0
     ENDIF
```

```
          CALL  JULIAN(IYR,MIO,IDIN,JDAY,FLAG)
CC        CADATE(IYR,JDAY,MIO,IDIN)

C INITIALIZE CROP GROWTH PARAMETER AT THE START OF EACH YEAR
          IF(IYR.GT.IYROLD) THEN
          IYROLD=IYR
          SDATE = 0
          YESDAY = 0
          IBMTS  = 1
     IST  = 1
          BMT = 0.
          SUMPDAYS=0
           GDD=0
     PDAYS=0
     SUMCHU=0
     SUMGDD=0.
          DO J = 1,5
          IPHEND(J) = 0
          END DO
          DAYHAV = 366
          ENDIF
C CALL THE SUBROUTINE TO CALCULATE THE SOLAR RADIATION (MJM-2DAY-1)
C   CALCULATE MAXIMUM RADIATION AT THE TOP OF THE ATMOSPHERE AND USE
HARGREAVE'S
C  RELATIONSHIP TO CALCULATE SOLAR RADATION (SOLRAD) IN MJ/M2.

C     CALL FAO(PE,SOLARMAX,WSP,ELE,TMAX,TMIN,TMEAN,RMAX,RMIN,XLAT,JD,
C    #SOLRAD,SUNHRSMAX)
C     OPE=PE

          CALL SOLAR (JDAY, XLAT, SUNHRSMAX, SOLARMAX)
          SOLRAD = 0.16*SQRT(TMAX-TMIN)*SOLARMAX

CC CONVERTS SOLAR RADITION TO Megajoules from kilojoules
CC          SOLRAD = SOLRAD/1000.

C   THIS CAN BE USED TO CONTROL THE DAILY LOOP IF DESRIED

CC        DO 112  IREC=IREC0101,IREC1231

C   SNOW EQUIVALENT IS OBTAINED AS THE DIFFERENCE BETWEEN TOTAL PRECIP
C   AND RAINFALL.  SNOCOF = 0.7 READ FROM THE INPUT TABLE, ASSUMING THAT
C   30% OF ALL SNOW IS BLOWN
C   OFF THE FIELD. ON A REGIONAL SCALE IT MAKES SENSE TO SET SNOCOF = 1.

     SNOWEQ = (PCP - RAIN) * SNOCF
      IF (SNOWEQ.LT.0.) SNOWEQ =0.

C   DETERMINE THE ACTUAL DATE, MONTH AND DAY FROM THE JULIAN DAY
```

```
C   IN THE INPUT RECORD


     IDATE=(MIO*100)+IDIN
C
C      IF(PESTR.GT.0) PE=PESTR
C CLCUATE THE SURFACE SOIL TEMPSRATURE

     TMEAN = (TMAX + TMIN) * 0.5
     IF (IYR.GT.1999) THEN
      IDENT=IYR-2000
     ELSE
      IDENT=IYR-1900
     ENDIF


     IDT=IDENT*10000+IDATE
     IYMODA = (10000*IDENT)+IDATE
CC
CC     IF(IDT.LT.IDATES(1)) GO TO 113
CC
C  GO INTO THIS SECTION IF SEEDING DATE HAS NOT BEEN FOUND
C  AND DATE IS BETWEEN APRIL 15 TO JUNE 15 - (NOW CHANGED TO START ON
c  MARCH 1 DUE TO CLIMATE CHANGE AND WARMING)
C  ONLY FIND THE SOWING DATE IF THERE IS A CROP - NOT FOR FALLOW
C  FOR FALLOW NOTE THAT NSY IS SET TO 1  IN THE INPUT TABLE
     IF ((SDATE.EQ.0).AND.(NSY.GT.1)) THEN
     IF((IDATE.GE.301).AND.(IDATE.LT.615)) THEN
     IF(TMEAN.LT.10.0) GO TO 3
     IF(PCP.GT.2.0) GO TO 3
     IF(W1.GE.10.0) GO TO 3
     IF(CONTNT(1).GE.0.9*CAPAC(1)) GO TO 3
     YESDAY=YESDAY+1
     IF(YESDAY.EQ.5) SDATE=JDAY
   3 CONTINUE
     ENDIF

C  IF ON JUNE I5 SEEDING DATE HAS NOT BEEN FOUND THEN
C  JUNE 15 BECOMES THE SEEDING DATE.
     IF((IDATE.EQ.615).AND.(SDATE.EQ.0)) SDATE =JDAY
     ENDIF
C
C   DETERMINE THE CROP PHENOLOGY ONCE THE SEEDING DATE HAS BEEN
C   FOUND. THE CROP GROWTH STAGES FOR SPRING WHEAT ARE
C  1=EMMERGENCE 2=JOINTING 3=HEADING 4=SOFT DOUGH AND 5=RIPENING.
C  THIS IS BASED ON BAIER & ROBERTSON BIOMETEOROLOGICAL TIME SCALE
C INSTEAD OF FINDING IPHEND HERE, YOU CAN SET IT EQUAL TO
C IDATES (1-5) FROM THE INPUT TABLE IF PHENOLOGY IS KNOWN AND SKIP HERE
```

```
C=======================================================================
C MODIFIED BY ROTIMI TO SIMULATE CANOLA P-DAY AND GRASS GROWTH. INPUT
C PLANT TYPE 1,2,3,4 OR 5 FOR WHEAT, CANOLA, GRASS, CORN AND SOYBEAN.

      IF (PLANTYP.EQ.1) GO TO 88
      IF (PLANTYP.EQ.2) GO TO 87
      IF (PLANTYP.EQ.3) GO TO 86
      IF (PLANTYP.EQ.4) GO TO 85
      IF (PLANTYP.EQ.5) GO TO 84

   88 CONTINUE
      IF ((SDATE.GT.0).AND.(JDAY.GT.SDATE)) THEN
       IF (IBMTS.LT.6) THEN

       CALL DAYLET(JDAY,XLAT,PHOTO)
       CALL SBMTS(IBMTS,BMT,PHOTO,TMAX,TMIN)
         IF(BMT.GE.1.0) THEN
         IPHEND(IBMTS) = IDT
          IST=IST+1
         IBMTS = IBMTS + 1
         BMT = 0.0
          ENDIF
        ENDIF
       ENDIF
C     ENDIF
C   4 FORMAT(7X,3I2,2F4.1,8X,F4.1,11X,F4.1)
       GO TO 22

C      IF (PLANTYP.EQ.2) THEN
   87 CONTINUE
      IF ((SDATE.GT.0).AND.(JDAY.GT.SDATE)) THEN

       CALL DAYLET(JDAY,XLAT,PHOTO)
        CALL PDAY(TMAX,TMIN,PDAYS)

        SUMPDAYS=PDAYS+SUMPDAYS
      IF ((SUMPDAYS.LE.140).OR.(SUMPDAYS.GT.836)) THEN
        IST=1
      ELSEIF ((SUMPDAYS.GT.140).AND.(SUMPDAYS.LE.299)) THEN
        IST=2
      ELSEIF ((SUMPDAYS.GT.299).AND.(SUMPDAYS.LE.419)) THEN
        IST=3
      ELSEIF ((SUMPDAYS.GT.419).AND.(SUMPDAYS.LE.529)) THEN
        IST=4
      ELSEIF ((SUMPDAYS.GT.529).AND.(SUMPDAYS.LE.836)) THEN
        IST=5
      ENDIF
      ENDIF
C     ENDIF
```

```
      GO TO 22

C    IF (PLANTYP.EQ.3) THEN
  86 CONTINUE
    IF ((SDATE.GT.0).AND.(JDAY.GT.SDATE)) THEN

      CALL SOLAR (JDAY, XLAT, SUNHRSMAX, SOLARMAX)
       CALL GRASS(TMAX,TMIN,GDD)

      SUMGDD=GDD+SUMGDD
       IF (SUNHRSMAX.LE.10.5) THEN
         IST=1
       ELSEIF (EPICT1.GT.1) THEN
         IST=2
       IF(SUMGDD.GE.240) THEN
         IST=3

       ENDIF
      ENDIF
     ENDIF
CC    ENDIF

      GO TO 22

C    IF (PLANTYP.EQ.4) THEN
C  CHU STAGES 1=EMMERGENCE(VE), 2=LEAF ELONGATION(V1), 3=EAR INITIATION(V6)
C  4=SILKING(R1), 5=DOUGH-MATURITY(R4)

  85 CONTINUE
    IF ((SDATE.GT.0).AND.(JDAY.GT.SDATE)) THEN

      CALL DAYLET(JDAY,XLAT,PHOTO)
       CALL CORNHEAT(TMAX,TMIN,CHU)

      SUMCHU=CHU+SUMCHU
    IF ((SUMCHU.LE.330).OR.(SUMCHU.GT.2600)) THEN
      IST=1
     ELSEIF ((SUMCHU.GT.330).AND.(SUMCHU.LE.780)) THEN
      IST=2
     ELSEIF ((SUMCHU.GT.780).AND.(SUMCHU.LE.1480)) THEN
       IST=3
     ELSEIF ((SUMCHU.GT.1480).AND.(SUMCHU.LE.2165)) THEN
       IST=4
     ELSEIF ((SUMCHU.GT.2165).AND.(SUMCHU.LE.2600)) THEN
       IST=5
     ENDIF
     ENDIF
C    ENDIF
```

```
         GO TO 22


C      IF (PLANTYP.EQ.5) THEN
C  CHU STAGES 1=EMMERGENCE(VE), 2=4TH TRIFOLIOLATE(V4),
C    3=BEGINNING POD(R3), 4= FULL SEED(R6)
C    5=FULL MATURITY(R8)

  84 CONTINUE
     IF ((SDATE.GT.0).AND.(JDAY.GT.SDATE)) THEN

      CALL DAYLET(JDAY,XLAT,PHOTO)
       CALL CORNHEAT(TMAX,TMIN,CHU)

       SUMCHU=CHU+SUMCHU
     IF ((SUMCHU.LE.230).OR.(SUMCHU.GT.2378)) THEN
       IST=1
      ELSEIF ((SUMCHU.GT.230).AND.(SUMCHU.LE.794)) THEN
       IST=2
      ELSEIF ((SUMCHU.GT.794).AND.(SUMCHU.LE.1446)) THEN
       IST=3
      ELSEIF ((SUMCHU.GT.1446).AND.(SUMCHU.LE.2136)) THEN
       IST=4
      ELSEIF ((SUMCHU.GT.2136).AND.(SUMCHU.LE.2378)) THEN
       IST=5
     ENDIF
    ENDIF
C    ENDIF

     GO TO 22



C=======================================================================
  22 CONTINUE
C
    ACCSNO = ACCSNO + SNOWEQ
    W1    = W1 + SNOWEQ
C  THIS IS THE OLD ALGORITHM FOR DISTINGUISHING BETWEEN
C  RAINFALL $ SNOWFALL. THIS IS NO LONGER USED
C    READ(INT,4,END=252)IDENT,MIO,IDIN,PAX,PAN,PCP,PE
C
C    IF(PESTR.GT.0)   PE =PESTR
C    IF(IDATE.EQ.IDRN) RFAC=0.0
C    IF(IDATE.EQ.NDRN) RFAC=1.0
C    PCP=PCP*RFAC
C
    MDT=MDT+1
    MONTH=IDATE/100
    IDAY = IDATE-MONTH*100

                        154
```

```
C
C  IDATES      CROP STAGE DATES (REPLACED WITH IPHEND)
C  IDT         YEAR/MONTH/DAY OF DAILY CALCULATIONS
C  IST         CROP DEVELOPMENT STAGE

 911  INUM=JD-SDATE
C     DO 911 YO=SDATE,DAYHAV

C    INUM GIVES THE SERIAL NUMBER FROM SEEDING DAY TO HAVEST.

 912 CONTINUE


C ===============================================
C  CALCULATE THE DAILY POTENTIAL EVAPORATION
C  USING THE PRIESTLY TAYLOR EQUATION
C  AKINREMI'S MODIFICATION

      CALL POTET(TMEAN,SOLRAD,PE,W1)
      OPE=PE

C  Set harvest date to a week after crop maturity

      IF(IDT.EQ.IPHEND(5))DAYHAV = JDAY + 7
   23 IF(IDT.EQ.IPHEND(IST))IST=IST+1
      IF(IST.GT.NSY) SNOCF = SMCOF(1)
      IF(IST.GT.5) IST = 5
      IF((IST.GT.NSY).OR.(JDAY.GT.DAYHAV))IST=1
      IF(IDATE.EQ.KSNO)SNOCF=SMCOF(2)




C    PREPARING THE BINOMIAL SMOOTHING FOR TEMPERATURE
C
C     MAXSM=(PX1+PX2*2.+PAX*3.)/6.
C
C    TESTING TO DETERMINE IF SNOW BUDGET APLIES

CC     IF(IDATE.GT.ISFL.AND.(IS.EQ.1.OR.MAXSM.LT.IFTP)) GO TO 299
CC     IF(IDATE.LT.IESG)GO TO 300
CC     IF(IDATE.GT.IESG.AND.IDATE.LT.ISFL.AND.ACCSNO.LT.0.01)SMCOFF=1.
CC     IF(MAXSM.LT.IFTP.AND.IDATE.GT.700) GO TO 300
CC     IF(MAXSM.LT.ISTP.AND.IDATE.LT.700) GO TO 300
C     IF(W1.GT.0.) GO TO 300


C
C  Determine the soil surface temperature using an algorithm
C  found in the epic model and adapted for VSMB model by Wole Akinremi
C  USES A 3-DAY RUNNING MEAN TO DESCRIBE THE MEMORY EFFECT OF SOIL TEMP.
```

```
            TEPIC(3) = TMEAN + 0.25*(TMAX-TMIN)
C  FIND THE THREE DAY RUNNING MEAN
      NUMDAY = 0
         DO J = 1,3
         IF(TEPIC(J).NE.999.9)THEN
         TSUM = TSUM + TEPIC(J)
         NUMDAY= NUMDAY + 1
      ENDIF
      END DO
C  CORRECT SOIL TEMPERATURE FOR SNOW
         BCV = 0.
          AVTEP = TSUM/FLOAT(NUMDAY)
      TSUM =  0.
      IF(W1.GT.0.) THEN
       BCV = W1/(W1+EXP(2.303 -0.2197*W1))
      ELSE
       BCV = 0.
      ENDIF
      EPICT2 = EPICT1
      EPICT1 = BCV*EPICT2+(1-BCV)*AVTEP
C  MOVE THE TEMP ACCUMULATOR ONE DAY FORWARD
         TEPIC(3) = EPICT1
      DO J = 1,2
           TEPIC(J) = TEPIC(J+1)
      END DO
C
   F1=1.0
C    IF (1.EQ.1) GO TO 101
C
C   SNOW BUDGET CALCULATIONS
C
C 299 SMCOFF=SNOCF
 300 IS=1
C
C   CALCULATE WATER EQUIVELENT OF SNOW PACK AND HOLDING CAPACITY
C
   D1=S2
   DO 1240 IZN=1,IZNS
 1240 D1=D1-CONTNT(IZN)
   H1 = W1 * 0.15
C
C   CALCULATE APPLICABLE CURVE AND POTENTIAL DAILY MELT
C  THE MCKAY SNOMELT EQUATION IS USED HERE.
C  IS         INDICATOR FOR SNOW BUDGET IN EFFECT
C  ACCSNO(W1)    SNOWPACK AFTER BLOW-OFF
C  D1          TOTAL DEFICIT (ALL ZONES)
C  S2          TOTAL CAPACITY
C  H1          MELTWATER RETAINED IN THE SNOWPACK
```

```
C  XX(P2)        DAILY SNOWMELT
C  R1(T2)        ACCUMULATED SNOWMELT IN THE SNOWPACK
C
   IF(TMAX.GT.8.3)GO TO 310
   IF(TMAX.GT.5.6)GO TO 330
   IF(TMAX.GT.2.8)GO TO 350
   JF=1
   IF (1.EQ.1) GO TO 360
310 JF=4
   IF (1.EQ.1) GO TO 360
330 JF=3
   IF (1.EQ.1) GO TO 360
350 JF=2
360 CONTINUE
C
C  MCKAY SNOWMELT EQUATION
C
   L=JF
   J=MONTH
   DD=AQ(L,J+1)
   IF (IDAY.GT.22) DD=(AQ(L,J+2)+AQ(L,J+1))*.5
   IF (IDAY.LT.8) DD=(AQ(L,J+1)+AQ(L,J))*.5

C  CONVERT SNOMELT IN INCHES TO SNOWMELT IN mm
   P2 = DD * 25.4
   IF(TMAX.LT.0.) THEN
   P2 = 0.0
   H1 = 0.0
   ENDIF
   IF(P2.GE.W1) THEN
    P2 = W1
    H1=0.
    W1=0.
   ELSE
    W1 = W1 - P2
   ENDIF
C
C   CALCULATE RETENSION AND ACTUAL LOSS TO SNOW PACK
C
C  A1        MELTWATER INFILTRATION TO SOIL
C  E1        MELTWATER DRAINAGE OUT OF SNOWPACK
C  R2        SNOWMELT SURFACE RUNOFF
C  T1        SNOWMELT REFROZEN IN UPPER SOIL
C  D2        TOTAL DEFICIT AFTER MELTWATER INFILTRATION
C  F1        HOBBS-KROGMAN MULTIPLIER FOR OVER-WINTER STORAGE POT
C
380  R1 = T2 + P2
   IF(R1.LT.H1) THEN
   H1 = R1
```

```
      E1 = 0.
      ELSE
      E1 = R1 - H1
      ENDIF
      T2 = H1
CC    IF(R1.LE.H1)GO TO 435
  435 IF(E1.LE.0.) E1=0.

C   CALCULATE INFILTRATION,RUNOFF AND SOIL MOISTURE DEFICIT
C
      A1=E1
      F1=1.
      T1=0.
CC    EXFRNT=0.
CC    DO 1260 I=1,IFRNT
CC    T1=T1+EXCSW(I)
CC    EXFRNT=EXFRNT+EXCAP(I)
CC 1260 CONTINUE
CC    T1=T1/EXFRNT
CC    D2=D1-A1
CC    D1=D2
CC   R2=E1-A1
      IF(W1.LE.0.)W1=0.
C    IF(PAX.GT.-7.)GO TO 437
C
C    INFILTRATION RATE ADJUSTMENT DUE TO FREEZING OF SOIL
C
      F1=1.0-T1
C  437 PRECIP=A1
C    IF (1.EQ.1) GO TO 119
C
C  SNOW BUDGET ENDS
C
  101 MONTH=IDATE/100
      AYE   = 0.
      IS    = 0
      T1    = 0.
      F1    = 1.
      SMCOFF= 1.0
      RUNOFF=0.
      RUNOF=0.
C
C  RUNOFF; NON-FROZEN SOIL
C  ORIGINAL RUNOFF EQUATION WAS REPLACED BY Wole Akinremi
C  USING THE SCS EQUTION SHOWN BELOW. THE SCS NUMBER IS SET
C  IN THE INPUT FILE FOR THE SOIL TO BE MODELLED.
C  TOTAL SURFACE WATER IS MELT PLUS RAIN
  119 SUFWAT = RAIN + E1
      IF (SUFWAT.EQ.0.) GO TO 141
```

```
C  USED THE HOB-KROGMAN'S TECHNIQUE TO CALCULATE RUNOFF
C  IF THE SOIL IS FROZEN
C
     IF((EPICT1.LT.0.).AND.(E1.GT.0.)) GO TO 409
C    IF(PCP.GT.10.0) RUNOFF = 0.1*PCP
C    IF(PCP.GT.25.4) RUNOFF = 2.54+((PCP-25.4)*0.5)
C    RUNOFF = RUNOFF * SSLP
C*****************************************************************
C            OCT. 5, 1987
C     CHANGE THE DEPMAX TO 45 CM WHEN CALCULATE WX VALUE
C     ASSUME ONLY THE TOP 45 CM WATER CONTENT AFFECTS RUNOFF
C   *************************************************************
C   ** CALCULATE RUNOFF BY WILLIAMS -SCS CURVE NO. TECHNIQUE ******
C   *************************************************************
C   CALCULATION OF RUNOFF ACCORDING TO SCS CURVE NUMBER
C   CNPW  : PARA. OF CURVE NUMBER WHEN SOIL IS WET
C   CNPD  : PARA. OF CURVE NUMBER WHEN SOIL IS DRY
C   CN1   : CURVE NUMBER FOR DRY SOIL
C   CN3   : CURVE NUMBER FOR WET SOIL
C   SMX   : S VALUE FROM SCS EQUATION, TRANSFER TO mm SCALE
C   *************************************************************
     DXX=0.
     CUMDEP = 0.
     DO 2384 L=1,IZNS
     CUMDEP = CUMDEP + DPTHZN(L)/10.
        WX=1.016*(1.-EXP(-4.16*CUMDEP/45.))
        WF(L)=WX-DXX
        DXX=WX
2384 CONTINUE
     AC2=100.-CN2
     CN3=CN2*EXP(.006729*AC2)
     CN1=AMAX1(.4*CN2,CN2-20.*AC2/(AC2+EXP(2.533-.0636*AC2)))
C    CN1=CN2*(.3067+.00168*CN2)
C    CN3=CN2*(2.4175-.0276*CN2+.00014*CN2**2)
     IF(CN2.GT.96.) CN1=CN2*(.02*CN2-1.)
     IF(CN1.GE.100.) CN1=100.
     IF(CN3.GE.100.) CN3=100.
     CNPW=0.
     CNPD=0.
     DO 701 L=1,IZNS
        SW(L) =(CONTNT(L)+PRMWLT(L))/DPTHZN(L)
        CNPW=CNPW+(SW(L)/DUL(L))*WF(L)
        CNPD=CNPD+((SW(L)-PLL(L))/(DUL(L)-PLL(L)))*WF(L)
701 CONTINUE
     IF(CNPD.GE.1.) THEN
        CN=CN2+(CN3-CN2)*CNPW
     ELSE
        CN=CN1+(CN2-CN1)*CNPD
     ENDIF
```

```
      IF(CN.EQ.0.) CN=.99
      SMX=254.*(100./CN - 1.)
C  REDUCE THE RETENTION FACTOR IF SOIL IS FROZEN
C  FORMULA ADAPTED FROM EPIC MODEL, THIS METHOD WAS
C  FOUND INAPPROPRAITE. AS SUCH, USE THE HOBB-KROGMAN'S
C  TECHNIQUE SHOWN BELOW.
CC     IF((EPICT1.LT.0.).AND.(E1.GT.0.))
CC   #  SMX = SMX*(1-EXP(-0.00292*SMX))
C
      PB=SUFWAT-0.2*SMX
      IF (PB.LE.0.) GO TO 141
      RUNOFF=PB*PB/(SUFWAT+.8*SMX)
      IF(1.EQ.1) GO TO 141
C
C  SECOND METHOD FOR CALCULATING RUNOFF IN A FROZEN SOIL
C  IE USING THE HOBB-KROGMAN'S APPROACH
  409 IF((EPICT1.LT.0.).AND.(E1.GT.0.)) THEN
C     IF(CONTNT(1).GT.18.) GO TO 410
C     IF(CONTNT(1).GT.12.) GO TO 420
C     IF(CONTNT(1).GT.5.) GO TO 430
C     HOBKG =1.0
C     IF (1.EQ.1) GO TO 440
C 410  HOBKG = 0.25
C     IF (1.EQ.1) GO TO 440
C 420  HOBKG = 0.5
C     IF (1.EQ.1) GO TO 440
C INSTEAD OF USING THE ABOVE TECHNIQUE AKINREMI FOUND THAT HOBKG
C CAN BE APROXIMATED AS THE RATIO OF SOIL MOISTURE TO FIELD CAPACITY
C COINCIDENTALLY AN IDENTICAL METHOD WAS USED BY ASH ET AL 1992

  430  HOBKG = CONTNT(1)/CAPAC(1)
  440  RUNOF = SUFWAT*HOBKG
      ENDIF
C************END OF SCS METHOD OF RUNOFF CALC***************
C
C    CALCULATING EFFECT OF PE DEMAND RATE
C
  141 SUMDEL=0.
C
C    COMPUTATION OF THE MOISTURE DEPLETION FROM EACH ZONE
C  AYE         TOTAL INFILTRATION
C  RUNOFF       SURFACE RUNOFF
C  DEL          RELATIVE MOISTURE CONTENT OF EACH ZONE
C  COF          ADJUSTED K-COEFFICIENTS
C
C  ALLOW SUBLIMATION TO GO ON AT MAXIMUM (PE)
C  ONLY IF THERE IS MORE THAN 10 MM OF SNOW.
      SNOLOS = 0.
      IF (W1.GT.10.) THEN
```

```
      IF(W1.GT.PE)THEN
       W1 = W1 - PE
       SNOLOS = PE
       PE=0.
       ELSE
       PE = PE - W1
       SNOLOS = W1
       W1 = 0.
       ENDIF
       ENDIF
     DO 110 I=1,IZNS
     DEL=CONTNT(I)/CAPAC(I)
     IF(DEL.GT.1.0) DEL=1.0
     COF(I)=COEFS(IST,I)
     IF(IST.LT.NEW)GO TO 98
C THE LINE BELOW CAN BE USED TO AVOID USING CROP COEFFICIENT ADJUSTMENT
C    IF(1.EQ.1)GO TO 98
     DO 96 J=2,I
     K=J-1
C
C    ADJUSTING  SOIL MOISTURE COEFICIENT FOR STRESS
C
  96 COF(I)=COF(I)+COF(I)*COF(K)*(1.-CONTNT(K)/CAPAC(K))
  98 IT=DEL*100.
     IF(IT.GT.0)GO TO 102
     WORK=0.
     IF (1.EQ.1) GO TO 108
 102 IF(KNTROL.GT.6) GO TO 103
     IF(I.GT.KNTROL) GO TO 104
     WORK=TABLE1(IT)
     IF (1.EQ.1) GO TO 108
 104 WORK=TABLE2(IT)
     IF (1.EQ.1) GO TO 108
 103 IF(IST.EQ.1) GO TO 106
     WORK=TABLE1(IT)
     IF (1.EQ.1) GO TO 108
 106 WORK=TABLE2(IT)
C
C    COMPUTING OF WATER LOSS FROM EACH ZONE
C
C XDEL        ACTUAL EVAPORATION FOR EACH ZONE
C BYE(X)       INFILTRATION WATER ALLOCATED TO EACH ZONE
C SUMDEL        ACTUAL EVAPORTRANSPIRATION(AE) DAILY
C CONTNT       (REDEFINED) COMPUTED MOISTURE CONTENT OF EACH ZONE
C
 108 CONTINUE
C
     XDEL=DEL*WORK*PE*COF(I)
     WRITE(10,151) IYMODA,SUMDEL,XDEL,DEL,WORK,PE,COF(I)
```

161

```
  151 FORMAT(I6,1X,5(1X,F5.3),2X,1F3.2)


    IF(XDEL.GT.CONTNT(I))XDEL=CONTNT(I)
    DELTA(I)=XDEL
  110 SUMDEL = SUMDEL + DELTA(I)
    SUMDEL = SUMDEL + SNOLOS


C    APPLYING PRECIPITATION AND EVAPORATION TO EACH ZONE
C
    DO 230 I=1,IZNS
    CONTNT(I)=CONTNT(I)-DELTA(I)
    IF(CONTNT(I).LT.0.)CONTNT(I)=0.
  230 CONTINUE
C NOTE THAT THERE ARE TWO TYPES OF "RUNOFF" RUNOF IS FROM SNOW
C WHILE RUNOFF IS FROM RAINFALL
    PINF = SUFWAT - (RUNOFF + RUNOF)
C    **CALCULATE DRAINAGE AND SOIL WATER REDISTRIBUTION************
    FLUX(1)=PINF
    DO 1300 L=1,IZNS
       IF (FLUX(L).EQ.0.) GO TO 1000
       HOLDw= SAT(L)*DPTHZN(L)-(CONTNT(L)+PRMWLT(L))
       IF (FLUX(L).LE.HOLDw) GO TO 1000
       DRAIN=(SAT(L)-DUL(L))*DPTHZN(L)
       CONTNT(L)=SAT(L)*DPTHZN(L)-DRAIN-PRMWLT(L)
       FLUX(L)=FLUX(L)-HOLDw+DRAIN
       GO TO 1200
 1000    CONTNT(L)=CONTNT(L)+FLUX(L)
       DRAIN=((CONTNT(L)+PRMWLT(L))-DUL(L)*DPTHZN(L))
       IF(L.EQ.IZNS)
    #    DRAIN=((CONTNT(L)+PRMWLT(L))-DRS2*DUL(L)*DPTHZN(L))
       IF (DRAIN.LT.0.) DRAIN = 0.
       CONTNT(L)=CONTNT(L)-DRAIN
       FLUX(L)=DRAIN
 1200    IF (L.LT.IZNS) FLUX(L+1)=FLUX(L)
 1300 CONTINUE
    IF (L.GE.IZNS) L=IZNS
    WLEACH=FLUX(L)
    DO 1400 L=1,IZNS
       FLUX(L)=0.0
 1400 CONTINUE


C*********************************************************
C  This is modification adapted from the ceres model to
C  account for moisture redistribution or unsaturated flow.
C  This modifcation was made by wole Akinremi.
c***************************************************************

    DO 405 L=1,IZNS
       FLOW(L)=0.0
```

```fortran
      SWX(L)=(CONTNT(L) + PRMWLT(L))/DPTHZN(L)
  405 CONTINUE
      ISTZ=1
      NIND=IZNS-1
      IF (DPTHZN(1).LE.50.0) ISTZ=2
      DO 407 L=ISTZ,NIND
       MU = L + 1
       THET1=CONTNT(L)/DPTHZN(L)
       THET2=CONTNT(MU)/DPTHZN(MU)
       DBAR=0.88*EXP(35.4*(THET1+THET2)*0.5)
       IF (DBAR.GT.100.) DBAR=100.
       FLOW(L)=10*DBAR*(THET2-THET1)/((DPTHZN(L)+DPTHZN(MU))*0.5)
       SWFLOW=FLOW(L)*10./DPTHZN(L)
       IF(FLOW(L).GT.0.) THEN
         IF(SWX(L)+SWFLOW.GT.SAT(L)) THEN
         FLOW(L)=(SAT(L)-SWX(L))*(DPTHZN(L)/10.)
         ELSE
         IF(SWX(L)+SWFLOW.GT.DUL(L))
    1     FLOW(L)=(DUL(L)-SWX(L))*(DPTHZN(L)/10.)
         ENDIF
       ELSE
         IF(SWX(MU)-SWFLOW.GT.SAT(MU)) THEN
         FLOW(L)=(SWX(MU)-SAT(MU))*(DPTHZN(MU)/10.)
         ELSE
          IF(SWX(MU)-SWFLOW.GT.DUL(MU))
    1     FLOW(L)=(SWX(MU)-DUL(MU))*(DPTHZN(MU)/10.)
         ENDIF
       ENDIF
       SWX(L)=SWX(L)+FLOW(L)/(DPTHZN(L)/10.)
       SWX(MU)=SWX(MU)-FLOW(L)/(DPTHZN(MU)/10.)
       CONTNT(L)=SWX(L)*DPTHZN(L) - PRMWLT(L)
       CONTNT(MU)=SWX(MU)*DPTHZN(MU) - PRMWLT(MU)
  407 CONTINUE
      DO 408 L = 1,MU
      PRCNT(L)=SWX(L)
  408 CONTINUE

  404 CONTINUE


C   DAILYPRINTOUT
C
      WRITE(18,12)IYMODA,EPICT1,PCP,OPE,SUMDEL,PRCNT,IST,IBMTS,
     #IPHEND(IBMTS-1)
      WRITE(19,14)IYMODA,SOLRAD,SOLARMAX,SUNHRSMAX,PHOTO,OPE,SUMDEL

         IF (PLANTYP.EQ.2) THEN
      WRITE(26,4)JDAY,TMAX,TMIN,PDAYS,SUMPDAYS,IST
        ENDIF
```

```fortran
      IF (PLANTYP.EQ.3) THEN
   WRITE(99,4)JDAY,TMAX,TMIN,GDD,SUMGDD,IST
      ENDIF

      IF (PLANTYP.EQ.4) THEN
   WRITE(82,4)IYMODA,TMAX,TMIN,CHU,SUMCHU,IST
      ENDIF

      IF (PLANTYP.EQ.5) THEN
   WRITE(82,4)IYMODA,TMAX,TMIN,CHU,SUMCHU,IST
      ENDIF

    4 FORMAT (I6,4(1X,F7.2),2X,I2,4(1X,F7.2))

    WRITE(21,13)IYMODA,OPE,SUMDEL,SNO,SNOWEQ,GS,W1,ACCSNO
   #,TMEAN,EPICT1
cc    DCOUNT = 0
cc    ENDIF
   12 FORMAT(1X,I6,2(2X,F6.2),2(2X,F5.2),2X,6F6.3,5X,I2,2X,I2,2X,I6)
   13 FORMAT(1X,I6,6(2X,F6.2),2X,F8.2,2(2X,F5.1))
   14 FORMAT(1X,I6,(6(1X,F8.2)))
C  UPDATE THE THREE CUMULATIVE VARIABLES
    ROFSUM = ROFSUM + RUNOF     !SNOWMELT RUNOFF
    SUMROF = SUMROF + RUNOFF    !RAINFALL RUNOFF
    SUMET  = SUMET  + SUMDEL    !TOTAL USE BY PLANTS
    SUMDRN = SUMDRN + WLEACH    !TOTAL DRAINAGE BELOW THE ROOT ZONE
    SUMPCP = SUMPCP + PCP       !TOTAL PRECIPITATION




C  CALCULATE THE PAPRAMETERS NECESSARY FOR WHEAT YIELD PREDICTION FROM
C  SOIL MOISTURE BALANCE ALONE - USING EMPIRICAL RELATIONSHIPS.
     IF(IBMTS.LT.2) THEN
      CRPCOF = 0.3
     ELSEIF(IBMTS.LT.3) THEN
      CRPCOF = 0.3 + 0.5*(IBMTS-2)
     ELSEIF(IBMTS.LT.4) THEN
      CRPCOF = 0.8 + 0.2*(IBMTS-3)
     ELSEIF(IBMTS.LT.5) THEN
      CRPCOF = 1 - 0.2*(IBMTS-4)
     ELSEIF(IBMTS.LT.6) THEN
      CRPCOF = 0.8 - 0.3*(IBMTS-5)
     ELSE
      CRPCOF = 0.3
     ENDIF

     IF ((sdate.GT.0).AND.(IBMTS.LT.6)) THEN
     WATDMD = AMAX1(SUMDEL, CRPCOF* OPE)
```

164

```
      SUMWAT1 = SUMWAT1 + SUMDEL
   SUMWAT2 = SUMWAT2 + WATDMD
    ENDIF


C  CALCULATE WHEAT GRAIN YIELD FROM  ACCUMULATED MOISTURE AT CROP
c  MATURITY- USING CON CAMPBELL AND RADDATZ EMPIRICAL EQUATIONS

   IF(IDT.EQ.IPHEND(5)) THEN
     CAMPB1 = 9.2*(SUMWAT1 - 71.8)
     RADZ1  = 9.8*(SUMWAT1 - 60.7)
     RADZ2  = 26.4*(SUMWAT1/SUMWAT2)*(JDAY-SDATE) - 18.5
     RADZ3  = 10.8*(SUMWAT1/SUMWAT2)*((JDAY-SDATE)**1.2)
   ENDIF
C------------------------------------------------------------
C   OUTPUT THESE THREE VARIBLES AT THE END OF THE RUN
   IF(IDT.EQ.IDATES(NODATE)) THEN
   WRITE(18,*)' PRECP  RAINRUNOF  SNORUNOF     EVAP   DRAIN
  #  CUMSNO   SNOWDPT'
   WRITE(18,232)SUMPCP,SUMROF,ROFSUM,SUMET,SUMDRN,ACCSNO,W1
    write(18,*)
    write(18,*)
    WRITE(18,*)'  SEEDING EMERGENCE JOINTING HEADING SOFT-DOUGH
  #MATURITY'
    WRITE(18,234)SDATE,IPHEND
    write(18,*)
    write(18,*)
    WRITE(18,*)' YEAR  SEED HARV  ETVAP    PEVAP  CAMP1   RADZ1
   # RADZ2  RADZ3'

    WRITE(*,*) XLAT
    WRITE(18,233) IYR,SDATE,DAYHAV,SUMWAT1,SUMWAT2,
   #     CAMPB1,RADZ1,RADZ2,RADZ3
    ENDIF
 232 FORMAT(7(2X,F8.2))
 233 FORMAT(I6,2I5,6(2X,F7.2))
 234 FORMAT(5X,I4,5(3X,I6))


C
C  11 FORMAT(3X,I2,I4,I2,F5.1,2F4.1,8F5.1,2I4,F6.1,2F5.1)
C NOTE THAT FROM HERE TO THE END OF THE PROGRAM NONE OF THE CODE
C IS USED.  THEY WERE LEFT INTACT JUST AS A MATTER OF COURSE.
C **** DONT DELETE THE SUBROUTINES, HOWEVER******


   IF(IDT.EQ.IDATES(NODATE))GO TO 241
   IF(IYR.GT.NDYR) GO TO 3110
 113  CONTINUE
    END DO    ! DO WHILE MORE DATA
```

165

```
   25  MOREDAT = .FALSE.
CC 112  CONTINUE    ! FOR THE DAILY WEATHER READING
CC 111  CONTINUE    ! FOR THE YEAR
C
C     END OF RUN HOUSEKEEPING
C     AND SUMMARY PRINTOUT
C
 241 CONTINUE
     IF(TOPOB.GT.0)THEN
C     WRITE(IP,3095) (J,J=1,5)
 3095 FORMAT(9X,':',5I10)
     ENDIF
C
C   YEARLY RESTART MODULE
C
     IF(IRTN.GT.(NDYR-ISYR)) GO TO 3110
     IF(NDYR.LE.ISYR) GO TO 3110
     DO 3120 I=1,NODATE
 3120 IDATES(I)=IDATES(I)+(10000*IRTN)
     MRST2=1
     IF(MRST1.LT.1) GO TO 3132
     WRITE(*,*)'RE-INITIALIZE SOIL MOISTURE'
     RFAC=1.0
     DO 3130 I=1,IZNS
 3130 CONTNT(I)=CONRST(I)
 3132 CONTINUE
      PRINT*,IDATE,IDATES(NODATE),NDYR
cc     IF(IDATES(NODATE).LT.((NDYR+1)*10000)) GO TO 111
 3110 CONTINUE
C
     TOPOB=0.0
C     WRITE(IP,3086)
 3086 FORMAT(8X,'DWB PERM.WLT.PT.  FLD.CAP.  SATN.')
     DO 3080 I=1,IZNS
     DDIF=(OBDPTH(I)-TOPOB)*10.
     PCN1= PRMWLT(I)/DDIF
     PCN2=(CAPAC(I)/DDIF)+PCN1
     PCN3=(EXCAP(I)/DDIF)+PCN2
     TOPOB=OBDPTH(I)
 3080 CONTINUE
 3085 FORMAT(1X,'ZONE ',I5,3F10.5)
C
C   NEW CONTROL DATA FILE
C
     KSIG=3
     IDAT2=0
     PE3RDYR=0.0
     AE3RDYR=0.0
C     CALL MONISO(CAPAC,IDAT1,IDAT2,KSIG,AE3RDYR,PE3RDYR)
```

```
C
C  NEW WEATHER FILE FILE
C
C
C  NEW STARTING SOIL MOISTURE
C
      RESTART=0.
      READ(1,502,END=251) CONRST
      DO 3198 I=1,IZNS
       RESTART=CRSTART+CONRST(I)
      CONRST(I)=CONRST(I)-PRMWLT(I)
      IF(CONRST(I).GT.CAPAC(I)) CONRST(I)=CAPAC(I)
 3198 CONTINUE
 3196 CONTINUE
      IF(RESTART.GT.0.)THEN
      GRNDW=WTMAX
      DO 3194 I=1,IZNS
 3194 CONTNT(I)=CONRST(I)
      ENDIF
       DO 3188 I=1,NODATE
 3188   IDATES(I)=KDATES(I)
C
  251 CONTINUE
  252 CONTINUE
      CLOSE (UNIT=1,STATUS='KEEP')
      CLOSE (UNIT=10,STATUS='KEEP')
      CLOSE (UNIT=11,STATUS='KEEP')
      CLOSE (UNIT=12,STATUS='KEEP')
      CLOSE (UNIT=13,STATUS='KEEP')
      CLOSE (UNIT=20,STATUS='KEEP')
      CLOSE (UNIT=19,STATUS='KEEP')
      CLOSE (UNIT=18,STATUS='KEEP')
      CLOSE (UNIT=17)
      STOP
      END
      SUBROUTINE MONISO(SM,IY,MD,K,AEDAY,PEDAY)
C
CC  MONITOR SOIL MOISTURE
C
      DIMENSION SM(6)
      DEDAY=PEDAY
      IF (K.NE.1) GO TO 10
      FC=0.0
      R1=0.0
      R2=0.0
      R4=0.0
      R7=0.0
      S=0.0
      DO 20 I=1,6
```

```
   20 FC=FC+SM(I)
      IPRINT=IY
      JPRINT=MD
      IF (1.EQ.1) GO TO 100
   10 CONTINUE
      IF (K.NE.2) GO TO 30
      IF (MD.NE.IPRINT) GO TO 40
      R3=AEDAY
      R6=DEDAY
      DO 50 I=1,6
   50 S=S+SM(I)
      SMRL1=S/FC*100.0
      S=0.0
      R1=R1+SMRL1
      IF (1.EQ.1) GO TO 100
   40 CONTINUE
      R3=R3+AEDAY
      R6=R6+DEDAY
      IF (MD.NE.JPRINT) GO TO 60
      IF (IY.EQ.1.OR.IY.EQ.3.OR.IY.EQ.5)GO TO 60
      DO 70 I=1,6
   70 S=S+SM(I)
      SMRL2=S/FC*100.0
      S=0.0
      R2=R2+SMRL2
      R3=R3+AEDAY
      R6=R6+DEDAY
      R4=R4+R3
      R7=R7+R6
    5 FORMAT (2I5,4F10.5)
   60 CONTINUE
      IF (1.EQ.1) GO TO 100
   30 CONTINUE
      IF (K.NE.3) GO TO 100
C     IF (MD.NE.0) GO TO 100
      R1=R1/3.0
      R2=R2/3.0
      R4=R4/3.0
      R7=R7/3.0
      R1=0.
      R2=0.
      R3=0.
      R6=0.
      R4=AEDAY
      R7=DEDAY
  100 CONTINUE
      RETURN
      END
```

```fortran
      SUBROUTINE POTET(TMEAN,SOLRAD,PE,W1)

C  THIS SUBROUTINE, GIVEN THE APPROPRIATE INPUT DATA, WILL CALCULATE
C  POTENTIAL EVAPORATION FROM THE EQUATION OF PRIESTLY-TAYLOR
C  MODIFIED TO USE SOLAR RADIATION TO ESTIMATE NET RADIATION

      REAL TMEANK, TMEAN
      REAL SOLRAD,PE,W1
      REAL SLOPE2, PSYCH1, PSYCH2, RADNEW, WATLOS
      REAL SATVP, DALYVP


C  start the computation Taylor Pot Evap.
      TMEANK = TMEAN + 273.        !MEAN TEMP oK
C  calculate the saturated vapour pressure
      SATVP=10*(EXP(52.58-(6790.5/TMEANK)-5.03*LOG(TMEANK)))
c
C  calculate the slope of the saturated vapour presuure
C  in pa/oC and convert to mbar.oc
       SLOPE2 = SATVP*(6790.5/TMEANK**2-5.03/TMEANK)

C  calculate the psychrometric constant and convert
         PSYCH1 = 0.06428*TMEAN + 64.5571
         PSYCH2 = PSYCH1/100.


C  calculate net radiation and convert to mm/day of water
         RAD2= 0.63*(SOLRAD*1000*1000/43200) - 40  ! WATT/M2
         IF (RAD2.LT.0.) RAD2 = 0.
         RAD3 = RAD2*43200/(2450*1000)      !MM/DAY
C account for the albedo of snow in winter
         IF(W1.GT.10.) THEN
         RAD2= 0.25*(SOLRAD*1000*1000/43200) - 40  ! WATT/M2
         IF (RAD2.LT.0.) RAD2 = 0.
         RAD3 = RAD2*43200/(2830*1000)      !MM/DAY
         ENDIF
         WATLOS = (SLOPE2*RAD3)/(SLOPE2 + PSYCH2)
         PE = 1.28*WATLOS

      END  ! OF THE SUBROUTINE POTET



      SUBROUTINE CADATE (IYY,JDAY,MONTH,IDAY)

C  This subroutine, given the year and julian date from the
C  the weather file calculates the month and the date for VWB3.2
      INTEGER MON(12),MONL(12),XMONTH(12),JDAY,MONTH,IDAY
      INTEGER IYY
      DATA MON/31,59,90,120,151,181,212,243,273,304,334,365/
      DATA MONL/31,60,91,121,152,182,213,244,274,305,335,366/
```

```
C*****DETERMINE WHICH MONTH OF THE YEAR THE DATA READ FALLS INTO
C
      DO 10 I=1,12
      IF(MOD(IYY,4).EQ.0.) THEN
      XMONTH(I) = MONL(I)
      ELSE
      XMONTH(I) = MON(I)
      ENDIF
      IF ((JDAY.LE.XMONTH(I)).AND.(I.EQ.1)) THEN
      MONTH = I
      IDAY =  JDAY
      IF (1.EQ.1) GO TO 20
      ELSEIF (JDAY.LE.XMONTH(I)) THEN
      MONTH=I
      IDAY = JDAY-XMONTH(I-1)
      IF (1.EQ.1) GO TO 20
      END IF
   10 CONTINUE
   20 CONTINUE
      END     ! THE END OF SUBROUTINE CADATE

      SUBROUTINE SBMTS(IBMTS,BMT,PHOTO,TMAX,TMIN)
C  THIS SUBROUTINE WAS ORIGINALLY WRITTEN FOR WHEAT AND BARLEY
C  IT WAS MODIFIED BY WOLE AKINREMI FOR WHEAT ONLY.  THE NECESSARY
C  PARAMETERS OF BARLEY WERE REMOVED USING BRACKETS JUST IN CASE
C  THEY ARE NEEDED LATER.

      INTEGER IBMTS
      REAL PA0(5),PA1(5),PA2(5),PB0(5),PB1(5),PB2(5),
     # PB3(5),PB4(5),BMT,PHOTO,TMAX,TMIN,CDT,TMAX1,TMIN1
      DATA PA0/0.,8.413,10.93,10.94,24.38/
C  PA0 BARLEY( /1.0E19,6.136,11.,2.061,-0.697/)
      DATA PA1/0.,1.005,0.9256,1.389,-1.14/
C  PA1 BARLEY (/-9.89E-20,1.297,0.1841,0.3229,0.08793/)
      DATA PA2/0.,0.,-0.06025,-0.08191,0./
C  PA2 BARLEY (/0.,0.,-0.01334,0.,0./)
      DATA PB0/44.37,23.64,42.65,42.18,37.67/
C  PB0 BARLEY (/4.34,10.09,-1.361,15.91, 4.144/)
      DATA PB1/0.01086,-0.003512,2.958E-4,2.458E-4,6.733E-5/
C  PB1 BARLEY (/0.01664,1.128E-3,4.423E-3,2.927E-3,0./)
      DATA PB2/-0.000223,5.026E-5,0.,0.,0./
C  PB2 BARLEY (/-5.417E-4,-5.725E-5,-8.797E-5,-1.638E-4,0./)
      DATA PB3/0.009732,3.666E-4,3.943E-4,3.109E-5,3.442E-4/
C  PB3 BARLEY (/0.01416,7.619E-4,0.002052,0.02282,0.01687/)
      DATA PB4/-2.267E-4,-4.282E-6,0.,0.,0./
C  PB4 BARLEY (/-4.805E-4,-1.854E-5,-9.571E-6,-0.004666,-7.821E-4/)
C
C   INITIALIZE BMTS AT THE SEEDING DATE
```

```fortran
C
C    JDAY=JDAY-2
C    JDAY=JDAY+1
C     DO 4  I=1,2
C    1=WHEAT    2=BARLEY
C
C     IF(IBMTS.EQ.6) GO TO 4
C IF(IDATE(3).EQ.1215.AND.PHEND(5).EQ.0) GO TO 900
C THE TEMPERATURE FOR WHEAT MUST BE CONVERTED TO DEGREE FARENHEIT
C THAT OF BARLEY MUST BE IN DEGREE CELCIUS.
C
   TMAX1=(TMAX*9./5.) + 32.
   TMIN1=(TMIN*9./5.) + 32.
   FUN1=(PA1(IBMTS)*(PHOTO-PA0(IBMTS)))+
  # (PA2(IBMTS)*((PHOTO-PA0(IBMTS))**2))
   IF(FUN1.LT.0.0) FUN1=0.0
   IF(IBMTS.EQ.1) FUN1=1.0
   FUN2=(PB1(IBMTS)*(TMAX1-PB0(IBMTS)))+
  # (PB2(IBMTS)*((TMAX1-PB0(IBMTS))**2))
   IF(FUN2.LT.0.) FUN2=0.0
   FUN3=(PB3(IBMTS)*(TMIN1-PB0(IBMTS)))+
  # (PB4(IBMTS)*((TMIN1-PB0(IBMTS))**2))
   IF(FUN3.LT.0.0) FUN3=0.0
   CDT = FUN1*(FUN2+FUN3)
   BMT = BMT + CDT
   RETURN
   END



    SUBROUTINE GRASS(TMAX,TMIN,GDD)
   REAL TMAX,TMIN,GDD,TMEAN
   TMEAN=(TMAX+TMIN)*0.5
   GDD=TMEAN-5
   IF (GDD.LT.0.) GDD=0.0
   RETURN
   END   !SUBROUTINE GDD



    SUBROUTINE PDAY(TMAX,TMIN,PDAYS)
C THIS SUBROUTINE CALCULATE P-DAY ACCUMULATION for CANOLA USING
C      DAILY MAX and MIN TEMP from Shaykewich, C.F. 2001. Included in VSMB
C      by E. RoTimi Ojo

   REAL TMAX,TMIN,WEMAX,WEMIN,STMAX,STMIN,SWEMAX,SWEMIN,PMAX
   REAL PMIN,PWEMAX,PWEMIN,PDAYS,SUMPDAYS
C    INTEGER JD,IST
C    LOGICAL MODATA
```

```fortran
C     SUMPDAYS=0
C     OPEN (UNIT=25,FILE='TARYN.IN',STATUS='OLD')
C     OPEN (UNIT=26,FILE='PDAYTEST.OUT',STATUS='UNKNOWN')

C     MODATA=.TRUE.

C     DO WHILE (MODATA)
C     READ(25,*,END=7)JD,TMAX,TMIN

      WEMAX=((2*TMAX)+TMIN)/3
      WEMIN=(TMAX+(2*TMIN))/3

      STMAX=TMAX-17
      STMIN=TMIN-17
      SWEMAX=WEMAX-17
      SWEMIN=WEMIN-17

      IF ((TMAX.LE.5).OR.(TMAX.GE.30)) PMAX=0
      IF ((TMAX.GT.5).AND.(TMAX.LT.17)) THEN
       PMAX=10*(1-(STMAX*STMAX/144))
       END IF
      IF ((TMAX.GE.17).AND.(TMAX.LT.30)) THEN
       PMAX=10*(1-(STMAX*STMAX/169))
       END IF

      IF ((TMIN.LE.5).OR.(TMIN.GE.30)) PMIN=0
      IF ((TMIN.GT.5).AND.(TMIN.LT.17)) THEN
       PMIN=10*(1-(STMIN*STMIN/144))
       END IF
      IF ((TMIN.GE.17).AND.(TMIN.LT.30)) THEN
       PMIN=10*(1-(STMIN*STMIN/169))
       END IF

      IF ((WEMAX.LE.5).OR.(WEMAX.GE.30)) PWEMAX=0
      IF ((WEMAX.GT.5).AND.(WEMAX.LT.17)) THEN
       PWEMAX=10*(1-(SWEMAX*SWEMAX/144))
       END IF
      IF ((WEMAX.GE.17).AND.(WEMAX.LT.30)) THEN
       PWEMAX=10*(1-(SWEMAX*SWEMAX/169))
       END IF

      IF ((WEMIN.LE.5).OR.(WEMIN.GE.30)) PWEMIN=0
      IF ((WEMIN.GT.5).AND.(WEMIN.LT.17)) THEN
       PWEMIN=10*(1-(SWEMIN*SWEMIN/144))
       END IF
      IF ((WEMIN.GE.17).AND.(WEMIN.LT.30)) THEN
       PWEMIN=10*(1-(SWEMIN*SWEMIN/169))
       END IF
```

```
        PDAYS=((3*PMAX)+(5*PMIN)+(8*PWEMAX)+(8*PWEMIN))/24

C     SUMPDAYS=PDAYS+SUMPDAYS

C     IF ((SUMPDAYS.LE.140).OR.(SUMPDAYS.GT.836)) IST=1
C     IF ((SUMPDAYS.GT.140).AND.(SUMPDAYS.LE.360)) IST=2
C     IF ((SUMPDAYS.GT.360).AND.(SUMPDAYS.LE.529)) IST=3
C     IF ((SUMPDAYS.GT.529).AND.(SUMPDAYS.LE.700)) IST=4
C     IF ((SUMPDAYS.GT.700).AND.(SUMPDAYS.LE.836)) IST=5

C     END DO
C   7 MODATA= .FALSE.

      CLOSE (UNIT=82,STATUS='KEEP')
C     CLOSE (UNIT=26,STATUS='KEEP')
C     CLOSE (UNIT=25,STATUS='KEEP')

      RETURN
      END   !SUBROUTINE P-DAY


      SUBROUTINE DAYLET (DAY,XLAT,PHOTO)
      REAL PHOTO
      INTEGER DAY

      REAL*4    XLAT,XLON,TH
C   Convert the Latitude to radians (note that latitude in
C     Southern hemisphere is preceeded with a minus sign (-)
      Dlat=XLAT*.01745
C     xlon=112.783
C     th is simply 2 x 3.1416 i.e. pie
      th=6.2832*day/365

C /* equation of time
C     et=0.0172+0.4281*cos(th) - 7.3515*sin(th)
C    #   -3.3495*cos(2*th) - 9.3619*sin(2*th)

C /* solar declination  (deg)
      dec=0.39637 - 22.91326*cos(th) + 4.02543*sin(th)
    #      -0.38720*cos(2*th) + 0.05197*sin(2*th)
    #      -0.15453*cos(3*th) + 0.08479*sin(3*th)

C /* solar declination (rad)
      decd=dec*.01745

C /* half day length (hours)
C     tempo1=(sin(lat))/(cos(lat)
C     tempo2=(sin(decd))/cos(decd)
      PHOTO = 7.6394*acos(-1.0*(tan(dlat))*tan(decd))
```

```
C /* local time of solar noon (hours)
C  ltsn = 12 -(105 -xlon)/15 - ET/60
C /* sun up and sun down times (hours) */
C  sunup=ltsn-hdaylen
C  sundown=ltsn+hdaylen
   END   !end of subroutine daylet


!  ===================================================================
   SUBROUTINE SOLAR (JDAY, XLAT, SUNHRSMAX, SOLARMAX)
!  ===================================================================
!  SUBROUTINE SOLAR estimates (1) day length (SunHrsMax)
!  and (2) maximum, daily, solar radiation MAXIMUM (SOLARMAX).
!  ===================================================================
!  All angles are in radians.
!  ===================================================================

   INTEGER JDAY
   REAL*4 XLAT,SUNHRSMAX,SOLARMAX
   REAL*4 PI,A0,C1,C2,C3,S1,S2,S3
   REAL*4 LAT,RS_SC,DA,WS,E0

!   Assign constants.
   PI=3.141593
   A0=.006917
   C1=-0.399912
   C2=-0.006758
   C3=-0.002697
   S1=0.070257
   S2=0.000907
   S3=0.00148
   RS_SC=1367.*3600./1000000. ! Solar constant (MJ.m-2.d-1).

!   Calculate the day angle (DA).
   DA=(JDAY-1.)*2.*PI/365.

!   Calculate the solar declination.
   DEC=A0+C1*COS(DA*1.)+S1*SIN(DA*1.)
  1    +C2*COS(DA*2.)+S2*SIN(DA*2.)
  2    +C3*COS(DA*3.)+S3*SIN(DA*3.)

!   Calculate the eccentricity correction factor E0.
   E0=1.+.033*COS(2.*PI*JDAY/365.)

!   Calculate the sunrise hour angle (WS), day length (h)
!   and the maximum, daily, solar radiation (MJ.m-2.d-1).
   LAT=XLAT*PI/180.
   COSWS=-TAN(DEC)*TAN(LAT)
   IF (COSWS.GT.1.0) THEN ! dark all day e.g. north pole, winter.
     WS=0.
```

```fortran
      SUNHRSMAX=0.
   RSMAXMJ=0.

    ELSE IF (COSWS.LT.-1.0) THEN ! bright all day e.g. north pole, summer.
      WS=PI
      SUNHRSMAX=24.
      RSMAXMJ=24./PI*RS_SC*E0*SIN(LAT)*SIN(DEC)*(WS-TAN(WS))
    ELSE
      WS=ACOS(COSWS)
      SUNHRSMAX=WS*24./PI
    SOLARMAX=24./PI*RS_SC*E0*SIN(LAT)*SIN(DEC)*(WS-TAN(WS))

   END IF
   END ! SUBROUTINE SOLAR

! =============================================================
   SUBROUTINE JULIAN(IYR,IMO,IDY,IJLN,FLAG)
! Julian converts from calendar day to julian day.
! =============================================================
! A flag (FLAG) is turned high if the YrMoDy inputs are valid.
! =============================================================
! LEAP is set to 1 in a leap year, 0 in a non-leap year.
! =============================================================

   INTEGER LEAP,FLAG,IMO,IDY,IYR,IJLN

   IF ((IDY.LT.1).OR.(IMO.LT.1).OR.(IMO.GT.12).OR.(IYR.LT.1)) THEN
        FLAG=0
    IJLN=999
    RETURN
   END IF

   FLAG=1
   LEAP=0
   IF (MOD(IYR,4).EQ.0) LEAP=1

   IF (IMO.EQ.1) THEN
     IJLN=IDY
    ELSEIF (IMO.EQ.2) THEN
     IJLN=31+IDY
        IF ((IDY.GT.28).AND.(LEAP.EQ.0)) FLAG=0
        IF ((IDY.GT.29).AND.(LEAP.EQ.1)) FLAG=0
    ELSEIF (IMO.EQ.3) THEN
     IJLN=59+IDY
    ELSEIF (IMO.EQ.4) THEN
     IJLN=90+IDY
     IF (IDY.GT.30) FLAG=0
    ELSEIF (IMO.EQ.5) THEN
     IJLN=120+IDY
```

```
        ELSEIF (IMO.EQ.6) THEN
          IJLN=151+IDY
          IF (IDY.GT.30) FLAG=0
        ELSEIF (IMO.EQ.7) THEN
          IJLN=181+IDY
        ELSEIF (IMO.EQ.8) THEN
          IJLN=212+IDY
        ELSEIF (IMO.EQ.9) THEN
          IJLN=243+IDY
          IF (IDY.GT.30) FLAG=0
        ELSEIF (IMO.EQ.10) THEN
          IJLN=273+IDY
        ELSEIF (IMO.EQ.11) THEN
          IJLN=304+IDY
          IF (IDY.GT.30) FLAG=0
        ELSEIF (IMO.EQ.12) THEN
          IJLN=334+IDY
        END IF

        IF ((LEAP.EQ.1).AND.(IMO.GT.2)) IJLN=IJLN+1
        IF (FLAG.EQ.0) IJLN=999

        RETURN
        END ! SUBROUTINE JULIAN

        SUBROUTINE FAO(PE,SOLARMAX,WSP,ELE,TMAX,TMIN,TMEAN,RMAX,RMIN,
       #XLAT,JD,SOLRAD,SUNHRSMAX)


!   THIS SUBROUTINE CALCULATES POTENTIAL (REFERENCE) EVAPO-
!   TRANSPIRATION (IN MM/DAY) FROM THE FAO-56 PENMAN MONTEITH included
!    by E. RoTimi Ojo (2010)

        INTEGER INUM,MIO,IDIN,JD
        REAL DADA,FKE,TIMI,FIYI,BUKI,PI,XLAT,FAT,WSP,ELE
        REAL SOLARMAX,SUNHRSMAX,DELE,PLHGT,FAMA,PEJU,YEMI,TMAX,TMIN
        REAL FAXA,FINA,FENA,RMAX,RMIN,BADA,SOPE,TMEAN,STB,TMAXK,TMINK
        REAL FETLO,FETRA,FETSO,SOLRAD,CRADSO,PE,PARTONE,PARTWO,PARTHRE
        REAL PARTFOR

        TMEAN = (TMAX + TMIN) * 0.5
C ===
C      CALCULATING THE AERODYNAMIC RESISTANCE (Ra)
        DELE=208/WSP !This gives the Ra (s/m)

C    WSP is the windspeed in m/s measured at 2m. If measured at
C    a different height (z), the FAO-Penman Montieth conversion factor is
C      CF=4.87/ln((67.2*z)-5.42)
```

```
C ===
C    CALCULATING THE SURFACE RESISTANCE (Rs)
C    This assumes that active LAI = 0.5LAI and that LAI=24h where h
C     is the plant height (h=0.12 for hypothetical grass reference)

     FAMA=69.44 ! Rs unt is s/m

C ===
C    CALCULATING THE ATMOSPHERIC PRESSURE (P) IN kPa
     PEJU=101.3*(((293-(0.0065*ELE))/293)**5.26)
C    ELE is site elevation above sea levels in meters

C ===
C    CALCULATING THE PSYCHOMETRIC CONSTANT (Y) IN KPa/C
     YEMI=0.000665*PEJU

C ===
C    CALCULATING THE SATURATION VAPOR PRESSURE (Es). This is needed
C     for both Tmax and Tmin. The mean Es (MENA) is then calculated
     FAXA=0.611*EXP((17.27*TMAX)/(TMAX+237.3))
     FINA=0.611*EXP((17.27*TMIN)/(TMIN+237.3))
     FENA=(FAXA+FINA)*0.5

C ===
C    CALCULATING THE SLOPE OF THE SATURATION VAPOR PRESSURE
     SOPE=(4098*(0.611*EXP((17.27*TMEAN)/(TMEAN+237.3))))/
    # ((TMEAN+237.3)**2)

C ===
C    CALCULATING THE ACTUAL VAPOR PRESSURE (Ea)
     BADA=((0.01*FINA*RMAX)+(0.01*FAXA*RMIN))/2


     PI=3.142
     STB=4.903*0.000000001 !Stefan-Boltzmann Constant

     FAT=XLAT*PI/180 !Converts latitude to radians

     FKE=(2*PI*JD/365)
     TIMI=1+(0.033*COS(FKE)) !Inverse relative distance of earth-sun
     FIYI=0.409*SIN(FKE-1.39) !Solar Declination Angle
     BUKI=ACOS(-1*TAN(FAT)*TAN(FIYI)) !Sunset Hour Angle
     SOLARMAX=(37.586*TIMI)*((BUKI*SIN(FAT)*SIN(FIYI))+
    $   (1*COS(FAT)*COS(FIYI)*SIN(BUKI)))

     SUNHRSMAX=24*BUKI/PI !Daylight hours i.e Max Sunshine Duration (N)

C  CALCULATING SOLAR RADIATION (Rs) MJ/m2/DAY if not provided in data
```

```
C   This is based on the Hargreaves' radiation formular using Tmax
C    and Tmin.

C     SOLRAD=0.16*SOLARMAX*(SQRT(TMAX-TMIN))


C   Clear Sky Solar Rad (Rso) is based on the site elevation (ELE)
      CRADSO=(0.75+(0.00002*ELE))*SOLARMAX

C   Net Solar Rad (Rns)
      FETSO=0.77*SOLRAD !Based on albedo of 0.23

C   Net Longwave Rad (Rnl)

      TMAXK=TMAX+273.16
      TMINK=TMIN+273.16

      FETLO=STB*(((TMAXK**4)+(TMINK**4))/2)*(0.34-(0.14*SQRT(BADA)))
     # *((1.35*SOLRAD/CRADSO)-0.35)

C    NET RADIATION (Rn) MJ/m2/day
      FETRA=FETSO-FETLO

C ===
C    The Penman Monteith ETo is thus:

      PARTONE=0.408*SOPE*FETRA
      PARTWO=(YEMI*(185396.2/(TMEAN+273)))
      PARTHRE=(FENA-BADA)/DELE
      PARTFOR=(SOPE+(YEMI*(1+(FAMA/DELE))))

      PE=(PARTONE+(PARTWO*PARTHRE))/PARTFOR


      RETURN
      END  !SUBROUTINE MONTIETH

C ********************************

      SUBROUTINE CORNHEAT(TMAX,TMIN,CHU)


!  THIS SUBROUTINE CALCULATES CORN HEAT UNITS ADAPTED BY
!  E. ROTIMI OJO (2014)


      REAL TMAX,TMIN,YMAX,YMIN,CHU
```

```
IF (TMIN.LE.4.4) THEN
YMIN=0
ELSE
YMIN=(1.8*(TMIN-4.4))

ENDIF

IF (TMAX.LE.10) THEN
YMAX=0
ELSE
YMAX=(3.33*(TMAX-10))-(0.084*(TMAX-10)*(TMAX-10))

ENDIF

CHU=(YMIN+YMAX)*0.5

RETURN
END  !SUBROUTINE CORNHEAT
```